Calibrating S&P 500 Index Options Under Alternative Formulations of the Heston (1993) Model

João Frederico Freitas Silva

Master in Financial Mathematics

Supervisor:
PhD, José Carlos Gonçalves Dias, Full Professor,
ISCTE-IUL

October, 2024

Finance Department
Mathematics Department

Calibrating S&P 500 Index Options Under Alternative Formulations of the Heston (1993) Model

João Frederico Freitas Silva

Master in Financial Mathematics

Supervisor:
PhD, José Carlos Gonçalves Dias, Full Professor,
ISCTE-IUL

October, 2024

"I have no special talent. I am only passionately curious." – Albert Einstein

Acknowledgment

I would like to thank my supervisor, Professor Doutor José Carlos Gonçalves Dias, for generously offering his time and availability whenever I needed guidance.

I am also grateful to ISCTE for the invaluable academic environment and support I have received over the past two years.

Finally, I want to thank my family for their constant support, especially my mother, who, despite having gone through difficult times in her life, always found a way to be there for me. I am thankful to my girlfriend for her love, patience, and understanding throughout my most challenging days, and to my friends for being the true definition of friendship.

Resumo

O modelo de Heston, conhecido por incorporar volatilidade estocástica, é crucial para a determinação do preço de derivativos financeiros. No entanto, a sua calibração apresenta desafios significativos, particularmente em termos de eficiência computacional e estabilidade numérica. A complexidade inerente do modelo surge do uso de equações diferenciais estocásticas para descrever tanto o preço do ativo quanto a sua volatilidade, exigindo técnicas numéricas sofisticadas para a estimação dos parâmetros. Assegurar a estabilidade numérica mantendo a precisão é um feito complicado.

O objetivo desta tese é calibrar de forma eficiente as opções do índice S&P 500 utilizando várias técnicas de calibração sob formulações alternativas do modelo de Heston (1993). As técnicas de calibração incluem: Mean error sum of squares (MSE); Relative mean error sum of squares (RMSE); e Christoffersen (2009) (IVRMSE). As formulações examinadas incluem: o modelo de Heston original, onde abordamos a "little Heston trap"; formulação consolidada de integral único; representação de Attari (2004); transformada rápida de Fourier (FFT) de Carr e Madan (1999); e a transformada rápida fracional de Fourier (FRFT) de Chourdakis (2005).

Palavras-chave: Modelo de Heston (1993), Volatilidade Estocástica, Avaliação de Opções.

Abstract

The Heston model, renowned for incorporating stochastic volatility, is crucial for accurate pricing of financial derivatives. However, its calibration poses significant challenges, particularly in computational efficiency and numerical stability. The model's inherent complexity arises from its use of stochastic differential equations to describe both the stock price and its volatility, requiring sophisticated numerical techniques for parameter estimation. Ensuring numerical stability while maintaining accuracy is a delicate balance.

The purpose of this thesis is to efficiently calibrate S&P 500 index options using various calibration techniques under alternative formulations of the Heston (1993) model. The calibration techniques examined include: Mean Squared Error (MSE); Relative Mean Squared Error (RMSE); and Christoffersen (2009) (IVRMSE). The formulations examined include: the original Heston model where we address the "little Heston trap"; consolidated single integral formulation; Attari (2004) representation; fast Fourier transform (FFT) formulation by Carr and Madan (1999); and, Chourdakis (2005) fractional fast Fourier transform (FRFT).

Keywords: Heston (1993) Model, Stochastic Volatility, Option Pricing.

Contents

Acknowledgment iii

Resumo v

Abstract vii

List of Figures xi

List of Tables xv

Chapter 1. Introduction 1

1.1. Context and motivation ... 1

1.2. Aims, objectives and thesis methodology ... 1

1.3. Core questions ... 2

1.4. Importance ... 2

1.5. Thesis structure ... 2

Chapter 2. Literature review 3

2.1. Heston model ... 4

2.2. Model assumptions and limitations ... 4

2.3. Heston model dynamics ... 5

2.4. Variance process distribution and properties ... 9

2.5. The European call price ... 11

2.6. Heston PDE ... 12

2.7. PDE for P_1 and P_2 ... 15

2.8. Characteristic functions ... 16

2.9. Fourier analysis ... 19

2.10. Gil-Pelaez (1951) inversion formula ... 20

2.10.1. The little Heston trap ... 21

2.11. Heston model formulations ... 22

2.11.1. Original version ... 23

2.11.2. Consolidated integrals ... 23

2.11.3. Attari (2004) ... 23

2.11.4. Carr and Madan (1999) fast Fourier transform 24
2.11.5. Chourdakis (2005) fractional fast Fourier transform 27
2.12. Numerical integration schemes 28
2.12.1. Composite trapezoidal rule 28
2.12.2. Gauss-Laguerre quadrature 29
Chapter 3. Data and methodology 31
3.1. Data 31
3.2. Procedures 33
3.3. Bias detection using a one-sample t-test 34
3.4. Matlab program 35
Chapter 4. Results 37
4.1. MSE loss function 38
4.2. RMSE loss function 41
4.3. IVRMSE loss function 44
Chapter 5. Conclusions 47
Appendix A. Additional results 49
A.1. MSE loss function 50
A.2. RMSE loss function 55
A.3. IVRMSE loss function 60
Appendix B. Evolution plots 65
B.1. Evolution plots of κ 66
B.2. Evolution plots of θ 69
B.3. Evolution plots of σ 72
B.4. Evolution plots of v_0 75
B.5. Evolution plots of ρ 78
References 81

List of Figures

B.1.1 MSE Heston original ... 66
B.1.2 MSE Heston single integrand ... 66
B.1.3 MSE Attari ... 66
B.1.4 MSE FFT ... 66
B.1.5 MSE FRFT ... 66
B.1.6 RMSE Heston original ... 66
B.1.7 RMSE Heston single integrand ... 67
B.1.8 RMSE Attari ... 67
B.1.9 RMSE FFT ... 67
B.1.10 RMSE FRFT ... 67
B.1.11 IVRMSE Heston original ... 67
B.1.12 IVRMSE Heston single integrand ... 67
B.1.13 IVRMSE Attari ... 68
B.1.14 IVRMSE FFT ... 68
B.1.15 IVRMSE FRFT ... 68
B.2.1 MSE Heston original ... 69
B.2.2 MSE Heston single integrand ... 69
B.2.3 MSE Attari ... 69
B.2.4 MSE FFT ... 69
B.2.5 MSE FRFT ... 69
B.2.6 RMSE Heston original ... 69
B.2.7 RMSE Heston single integrand ... 70
B.2.8 RMSE Attari ... 70
B.2.9 RMSE FFT ... 70
B.2.10 RMSE FRFT ... 70
B.2.11 IVRMSE Heston original ... 70
B.2.12 IVRMSE Heston single integrand ... 70
B.2.13 IVRMSE Attari ... 71
B.2.14 IVRMSE FFT ... 71
B.2.15 IVRMSE FRFT ... 71
B.3.1 MSE Heston original ... 72
B.3.2 MSE Heston single integrand ... 72
B.3.3 MSE Attari ... 72
B.3.4 MSE FFT ... 72

B.3.5 MSE FRFT 72
B.3.6 RMSE Heston original 72
B.3.7 RMSE Heston single integrand 73
B.3.8 RMSE Attari 73
B.3.9 RMSE FFT 73
B.3.10 RMSE FRFT 73
B.3.11 IVRMSE Heston original 73
B.3.12 IVRMSE Heston single integrand 73
B.3.13 IVRMSE Attari 74
B.3.14 IVRMSE FFT 74
B.3.15 IVRMSE FRFT 74
B.4.1 MSE Heston original 75
B.4.2 MSE Heston single integrand 75
B.4.3 MSE Attari 75
B.4.4 MSE FFT 75
B.4.5 MSE FRFT 75
B.4.6 RMSE Heston original 75
B.4.7 RMSE Heston single integrand 76
B.4.8 RMSE Attari 76
B.4.9 RMSE FFT 76
B.4.10 RMSE FRFT 76
B.4.11 IVRMSE Heston original 76
B.4.12 IVRMSE Heston single integrand 76
B.4.13 IVRMSE Attari 77
B.4.14 IVRMSE FFT 77
B.4.15 IVRMSE FRFT 77
B.5.1 MSE Heston original 78
B.5.2 MSE Heston single integrand 78
B.5.3 MSE Attari 78
B.5.4 MSE FFT 78
B.5.5 MSE FRFT 78
B.5.6 RMSE Heston original 78
B.5.7 RMSE Heston single integrand 79
B.5.8 RMSE Attari 79
B.5.9 RMSE FFT 79
B.5.10 RMSE FRFT 79
B.5.11 IVRMSE Heston original 79
B.5.12 IVRMSE Heston single integrand 79
B.5.13 IVRMSE Attari 80
B.5.14 IVRMSE FFT 80

B.5.15 IVRMSE FRFT 80

List of Tables

3.1.1 Sample properties of the S&P 500 index options 31
3.1.2 Market implied volatilities 32

4.1.1 MSE Heston original - implied volatility percentage errors 38
4.1.2 MSE Attari - implied volatility percentage errors 39
4.1.3 MSE Heston original - calls (puts) statistical analysis 40
4.1.4 MSE Attari - calls (puts) statistical analysis 40
4.2.1 RMSE Heston original - implied volatility percentage errors 41
4.2.2 RMSE Attari - implied volatility percentage errors 42
4.2.3 RMSE Heston original - calls (puts) statistical analysis 43
4.2.4 RMSE Attari - calls (puts) statistical analysis 43
4.3.1 IVRMSE Heston original - implied volatility percentage errors 44
4.3.2 IVRMSE Attari - implied volatility percentage errors 45
4.3.3 IVRMSE Heston original - calls (puts) statistical analysis 46
4.3.4 IVRMSE Attari - calls (puts) statistical analysis 46

A.1.1 MSE Heston single integrand - implied volatility percentage errors 50
A.1.2 MSE FFT - implied volatility percentage errors 51
A.1.3 MSE FRFT - implied volatility percentage errors 52
A.1.4 MSE Heston single integrand - calls (puts) statistical analysis 53
A.1.5 MSE FFT - calls (puts) statistical analysis 53
A.1.6 MSE FRFT - calls (puts) statistical analysis 53
A.2.1 RMSE Heston single integrand - implied volatility percentage errors 55
A.2.2 RMSE FFT - implied volatility percentage errors 56
A.2.3 RMSE FRFT - implied volatility percentage errors 57
A.2.4 RMSE Heston single integrand - calls (puts) statistical analysis 58
A.2.5 RMSE FFT - calls (puts) statistical analysis 58
A.2.6 RMSE FRFT - calls (puts) statistical analysis 58
A.3.1 IVRMSE Heston single integrand - implied volatility percentage errors . 60
A.3.2 IVRMSE FFT - implied volatility percentage errors 61
A.3.3 IVRMSE FRFT - implied volatility percentage errors 62
A.3.4 IVRMSE Heston single integrand - calls (puts) statistical analysis 63
A.3.5 IVRMSE FFT - calls (puts) statistical analysis 63
A.3.6 IVRMSE FRFT - calls (puts) statistical analysis 63

CHAPTER 1

Introduction

1.1. Context and motivation

The 1987 stock market crash exposed significant limitations in classical option pricing models like Black and Scholes (1973) and Merton (1973), particularly the assumption of constant volatility. Empirical studies following the crash revealed that stock returns exhibit skewness and fat tails, with volatility varying over time and often inversely related to stock prices. This highlighted the need for a more flexible approach to option pricing that could capture these observed market behaviors.

Heston (1993) introduced a groundbreaking framework that allows volatility to evolve as a stochastic process, addressing the limitations of earlier models. By modeling key empirical features of stock returns, such as skewness, fat tails, and accounting for volatility smiles or skews in implied volatilities, coupled with an analytical representation for pricing European call options, the Heston model has become a cornerstone in both academic research and practical financial modeling. This thesis examines the model's significance, its applications in modern finance, and its lasting impact on the understanding of volatility and option pricing.

1.2. Aims, objectives and thesis methodology

The aim of this thesis is to effectively calibrate S&P 500 index options using alternative formulations of the Heston (1993) model. The calibration will be done using three different loss functions, including:

- Mean error sum of squares (MSE);
- Relative mean error sum of squares (RMSE);
- Christoffersen (2009) (IVRMSE).

The formulations investigated include:

- Original Heston model;
- Consolidated single integral;
- Attari (2004) representation;
- Carr and Madan (1999) fast Fourier transform;
- Chourdakis (2005) fractional fast Fourier transform.

The objective is to assess the computational efficiency and calibration accuracy of various calibration techniques for the investigated formulations, thereby improving their practical use in financial markets. Empirical data from S&P 500 index options will be utilized to evaluate the performance of the study. This will involve implementing each calibration technique for every formulation, measuring the accuracy of the implied volatility surface generated, and comparing their computational speed and efficiency. The results will provide insights into the trade-offs between computational efficiency and calibration accuracy.

1.3. Core questions

This thesis will answer two core questions:

- Is there anything we can implement to mitigate the numerical instabilities associated with the Heston (1993) model?
- Across each calibration technique, which formulation provides the best balance between computational efficiency and calibration accuracy?

1.4. Importance

Traditional calibration techniques for the Heston model are often computationally intensive and prone to numerical instabilities, leading to significant pricing errors. These challenges are particularly problematic in real-time trading and risk management scenarios, where both speed and accuracy are crucial. Addressing these issues is essential for enhancing the practical applicability of the Heston model.

1.5. Thesis structure

This thesis is structured into five chapters, each addressing a specific aspect of the research:

- The Introduction chapter provides the context, motivation, aims, objectives of the study, thesis methodology, core questions and its importance.
- The Literature review chapter reviews existing literature on the Heston model, its alternative formulations and the numerical integration schemes that will be used.
- The Data and methodology chapter describes the data, calibration techniques procedures, calibration bias detection procedures and a brief explanation about the Matlab code behind the thesis.
- The Results chapter presents the formulations that got the best results for each calibration technique.
- The Conclusions chapter summarizes the findings.

We present two appendices, the first one with the results that were not presented in the Results chapter and the second one dedicated to Heston (1993) model parameters evolution plots. Finally, the thesis ends with its references.

CHAPTER 2

Literature review

This chapter provides a solid review of the literature behind the Heston (1993) model. By delving into the Heston model's comprehensive literature, we aim to present an extensive understanding of its foundational principles, its development over time, and the various enhancements proposed by different researchers. This review not only solidifies the theoretical foundations of the Heston model but also provides a critical analysis of its practical applications and limitations.

The chapter begins by introducing a brief history behind the Heston model, so the reader can better understand its value and its importance in financial modeling. The historical context of the model's development is crucial as it highlights the limitations of previous models and the innovative steps taken by Heston to address them. By understanding this history, readers can appreciate the model's significance and its impact on the field of quantitative finance.

Next, we talk about the model assumptions and limitations. These assumptions, while simplifying the complex reality of financial markets, enables the derivation of mathematical solutions. However, they also introduce limitations that need to be carefully considered when applying the model to real-world data.

We discuss the model dynamics along with a complete derivation of the original Heston model. We introduce the reader to some basic Fourier analysis concepts and, additionally, we address the "Little Heston Trap". It is presented the various Heston model formulations used to price options in this thesis, briefly describing each one of them and we finish with the numerical integration schemes that will be used.

2.1. Heston model

Since its introduction in 1993, the Heston model has become one of the most important models in stochastic volatility pricing, a revolutionary approach to option pricing. Its rise is tied to the 1987 stock market crash, which exposed limitations in the Black-Scholes-Merton model of Black and Scholes (1973) and Merton (1973), particularly the assumption of normally distributed stock returns with constant volatility. Empirical studies since the crash have shown that returns exhibit skewness and kurtosis, and that volatility is time-varying, often inversely related to price.

A widely used method for modeling time-varying volatility involves allowing volatility to be driven by its own stochastic process. This approach is employed in stochastic volatility models, such as the Heston (1993) model. Some of the pioneering models in this area were proposed by Hull and White (1987), Scott (1987), Wiggins (1987), Chesney and Scott (1989), and Stein and Stein (1991).

The parameters of the Heston model can generate skewness and kurtosis, leading to a smile or skew in implied volatilities derived from option prices produced by the model. It intuitively captures the inverse relationship between stock price levels and volatility, making it straightforward and easy to comprehend. Furthermore, the Heston model provides a closed-form solution for call option prices, which includes a numerically evaluated integral, enhancing both its flexibility and practicality. For these reasons, the Heston model has become the most widely used stochastic volatility model for pricing equity options.

A key innovation of the Heston model is its use of characteristic functions for option pricing, eliminating the need to know the terminal price density. This insight led to a new approach in option pricing, known as pricing by characteristic functions.

2.2. Model assumptions and limitations

Heston assumes that the underlying stock price, S_t, follows a stochastic process close to the geometric Brownian motion and that the variance, v_t, is also stochastic, following a Cox-Ingersol-Ross (1985) process that incorporates mean reversion.

Heston assumes a correlation between the Wiener processes under the underlying stock price and the variance dynamics where this correlation is typically negative in real-world data. This can be explained by the leverage effect.

Heston assumes that the underlying does not pay dividends during the option's life. This limitation can lead to mispricing of options on dividend-paying stocks.

Under the risk-neutral measure, the Heston model assumes a constant rate of interest throughout the option's life. This limitates the reality of stochastic interest rates.

A drawback of the Heston model is that it requires multiple parameters to be calibrated simultaneously, which can be complex and time-consuming. Additionally, the parameters calibrated to historical data may not remain stable for extended periods, necessitating frequent recalibration to ensure accuracy.

The model also fails to account for sudden jumps in prices, leading to an underestimation of the probability of large price movements and, finally, due to its mean-reverting nature, the Heston model tends to underestimate the implied volatility skew, particularly for short maturities.

2.3. Heston model dynamics

The Heston Model, under the physical measure $\mathbb{P}$, is represented by the following bivariate system of stochastic differential equations

$$\begin{aligned} dS_t &= \mu S_t \, dt + \sqrt{v_t} S_t \, dW_{1,t}^{\mathbb{P}} \\ dv_t &= \kappa(\theta - v_t) \; dt + \sigma \sqrt{v_t} dW_{2,t}^{\mathbb{P}} \end{aligned} \tag{2.1}$$

where $\mathbb{E}^{\mathbb{P}}[dW_{1,t}^{\mathbb{P}} dW_{2,t}^{\mathbb{P}}] = \rho dt$.

μ is the drift of the stock price process. The κ parameter controls the speed of mean reversion of the variance process. It represents the velocity at which the process will revert to its mean. θ is the long-term mean of the variance. When the distance to the mean, $(\theta - v_t)$, is high, the strength of mean reversion, $\kappa(\theta - v_t)$, will be high as well with a strong opposite force pushing the trajectory back to its mean. The higher the κ or the distance to the mean, the stronger the mean reversion force. The volatility of the variance σ, controls the amplitude of the possible fluctuations around the mean. The randomness of the stock price and its variance are controlled by two correlated Wiener processes. The correlation ρ controls the relationship between the dynamic of the underlying stock price and its volatility. So, in addition to the drift of the stock price process, the Heston model has five unknown parameters: v_0, the initial level of the variance; κ, the speed of reversion of the variance process; θ, the long-term mean of the variance; σ, the volatility of the variance; and ρ, the correlation between the stock price and its variance.

If $2\kappa\theta > \sigma^2$, the drift is sufficiently large to make the origin unreachable for v_t. This is known as the Feller condition. If the Feller (1951) condition is violated, v_t will visit the origin, almost surely, but will not stay at zero, that is, the origin boundary is strongly reflecting. When calibrating the Heston model, it is fairly common for the model's parameters to violate the Feller condition. While this is not catastrophic, since v_t only briefly touches zero, it is still concerning. This is because the model may frequently produce extremely low volatility levels (e.g., below 0.01), which is not a typical market behavior. In practice, this suggests that users should exercise caution when interpreting the results of the model, especially in cases where the Feller condition is violated.

In the Heston model, the distribution of the log stock price at maturity, $\ln S_T$, can display skewness and excess kurtosis based on the chosen parameter values. The correlation parameter ρ plays a key role in controlling the skewness of the distribution for both $\ln S_T$ and the continuously compounded return $\ln(S_T/S_0)$ over the time interval $[0, T]$. When ρ is positive, the probability distributions exhibit positive skewness, while a negative ρ

results in negatively skewed distributions; this will be the typical case as we explained before. The volatility of variance parameter σ influences the kurtosis of the distribution. A high σ leads to greater dispersion in the variance process, causing the return distribution to exhibit higher kurtosis and fatter tails. In contrast, when σ is low, the distribution tends to have less pronounced tails.

Another characteristic of the Heston model is that the implied volatilities derived from option prices generated by the model will display a volatility smile or skew. The shape of this skew depends on the parameter values. Specifically, the correlation parameter ρ influences the direction of the skew: when $\rho > 0$, the skew will have a positive slope, and when $\rho < 0$, the skew will exhibit a negative slope, this will be the typical case. Increasing values of the volatility of variance σ means that the variance fluctuates more than usual; this will lead to a steeper smile. Low values of the volatility of the variance σ means that the variance does not fluctuate as much; this will lead to a flatter smile. Finally, the parameters κ, θ and v_0 control the level of the smile. The mean reversion speed κ also controls the curvature. A high κ makes the volatility revert faster, flattening the volatility smile because volatility spikes will be short-lived; a low κ means slow reversion, leading to a steeper volatility smile, as volatility deviations from θ can last longer.

As we know, equations (2.1) represent the Heston model under the physical measure $\mathbb{P}$, but, for pricing purposes, we need the processes for (S_t,v_t) under the risk-neutral measure $\mathbb{Q}$. It is also more convenient to work with a model that is expressed in terms of independent Brownian motions. If we let $Z^{\mathbb{P}}_{1,t}$ and $Z^{\mathbb{P}}_{2,t}$ for $t \geq 0$ be two independent Brownian motions under the real measure $\mathbb{P}$, we can rewrite $dW^{\mathbb{P}}_{1,t}$ and $dW^{\mathbb{P}}_{2,t}$ as

$$\begin{aligned} dW^{\mathbb{P}}_{1,t} &= \sqrt{1-\rho^2}dZ^{\mathbb{P}}_{1,t} + \rho dZ^{\mathbb{P}}_{2,t} \\ dW^{\mathbb{P}}_{2,t} &= dZ^{\mathbb{P}}_{2,t} \end{aligned} \tag{2.2}$$

where $\mathbb{E}^{\mathbb{P}}[dZ^{\mathbb{P}}_{1,t}dZ^{\mathbb{P}}_{2,t}] = 0$. Substituting the equations of (2.2) in the bivariate system of SDEs in (2.1) give us

$$\begin{aligned} dS_t &= \mu S_t dt + \sqrt{v_t}S_t\sqrt{1-\rho^2}dZ^{\mathbb{P}}_{1,t} + \sqrt{v_t}S_t\rho dZ^{\mathbb{P}}_{2,t} \\ dv_t &= \kappa(\theta - v_t)dt + \sigma\sqrt{v_t}dZ^{\mathbb{P}}_{2,t} \end{aligned} \tag{2.3}$$

To change the measure we need to introduce the two-dimensional Girsanov theorem which includes the idea behind the Radon-Nikodym derivative. Note that we rewrote the original bivariate system of SDEs (2.1) in terms of independent Brownian motions because in the two-dimensional Girsanov theorem that we will present, we make use of the independence concept. Nevertheless, independence is not necessary, since every derivation in this thesis that uses independence between Brownians can be reformulated for correlated Brownians.

We will now introduce the reader to some well-known results that are mandatory here in this subject. The following definition and theorems can be found in [**26**].

DEFINITION 2.3.1. *Let $(\Omega, \mathscr{F}, \mathbb{P})$ be a probability space, let $\tilde{\mathbb{P}}$ be another probability measure on $(\Omega, \mathscr{F})$ that is equivalent to $\mathbb{P}$, and let Z be an almost surely positive random variable with $\mathbb{E}[Z] = 1$ that relates $\mathbb{P}$ and $\tilde{\mathbb{P}}$ via*

$$\tilde{\mathbb{P}}(A) = \int_A Z(\omega) d\mathbb{P}(\omega) \quad \text{for every } A \in \mathscr{F}. \tag{2.4}$$

Then Z is called the Radon-Nikodym derivative of $\tilde{\mathbb{P}}$ with respect to $\mathbb{P}$, and we write

$$Z = \frac{d\tilde{\mathbb{P}}}{d\mathbb{P}}.$$

THEOREM 2.3.2. *(Lévy, Two-dimensions) Let $M_1(t), M_2(t)$ for $t \geq 0$, be martingales relative to a filtration $\mathcal{F}(t)$, $t \geq 0$. Assume that for $i, j = 1, 2$, we have $M_i(0) = 0$, $M_i(t)$ has continuous paths, and $[M_i, M_j](t) = t\delta_{ij}$ for all $t \geq 0$. Then $M_1(t), M_2(t)$ are independent Brownian motions.*

PROOF. See [[**26**], p. 159]. □

In the above theorem, δ_{ij} is called the Kronecker delta and is defined as

$$\delta_{ij} = \begin{cases} 1, & \text{if } i = j \\ 0, & \text{if } i \neq j \end{cases},$$

for $i, j = 1, 2$.

THEOREM 2.3.3. *(Two-dimensional Girsanov) Let $W(t) = (W_1(t), W_2(t))$, $0 \leq t \leq T$, be a two-dimensional Brownian motion (i.e., a vector of two independent, one-dimensional Brownian motions) on a probability space $(\Omega, \mathscr{F}, \mathbb{P})$, and let $\mathscr{F}(t)$, $0 \leq t \leq T$, be a filtration for this two-dimensional Brownian motion. Let $\theta(t) = (\theta_1(t), \theta_2(t))$ be a two-dimensional adapted process. Define*

$$\begin{aligned} Z(t) &= exp\left(-\sum_{j=1}^{2} \int_0^t \theta_j(u) dW_j(u) - \frac{1}{2} \int_0^t \sum_{j=1}^{2} \theta_j^2(u) du\right), \\ \tilde{W}_j(t) &= W_j(t) + \int_0^t \theta_j(u) du \qquad \text{for} \qquad j = 1, 2, \end{aligned} \tag{2.5}$$

and assume that

$$\mathbb{E}\left[\int_0^T \sum_{j=1}^{2} \theta_j^2(u) Z^2(u) du < \infty\right]. \tag{2.6}$$

Set $Z = Z(t)$. Then $E[Z] = 1$, and under the probability measure $\tilde{\mathbb{P}}$ given by the equation (2.4), the process $\tilde{W}(t)$ is a two-dimensional Brownian motion.

PROOF. By Lévy, two-dimensions Theorem, it suffices to show that $\tilde{W}_i(t)$ is an $\mathcal{F}_t$-martingale under $\tilde{\mathbb{P}}$ and $[\tilde{W}_i, \tilde{W}_j](t) = t\delta_{ij}$ $(i, j = 1, 2)$. Indeed, for $i = 1, 2$, $\tilde{W}_i(t)$ is an $\mathcal{F}_t$-martingale under $\tilde{\mathbb{P}}$ if and only if $\tilde{W}_i(t) Z_t$ is an $\mathcal{F}_t$-martingale under $\mathbb{P}$, since

$$\tilde{\mathbb{E}}[\tilde{W}_i(t) | \mathcal{F}_s] = \mathbb{E}\left[\frac{\tilde{W}_i(t) Z_t}{Z_s} | \mathcal{F}_s\right] = \frac{\tilde{W}_i(s) Z_s}{Z_s} = \tilde{W}_i(s),$$

with $0 \leq s \leq t \leq T$. Applying Itô´s lemma to $f(X(t)) = e^{X(t)}$ where $X(t)$ is the term inside the exponential of $Z(t)$, we get

$$\begin{aligned}
dZ(t) &= \frac{\partial f(X(t))}{\partial X_t} dX(t) + \frac{1}{2}\frac{\partial^2 f(X(t))}{\partial X^2(t)}(dX(t))^2 \\
&= e^{X(t)} \left(-\sum_{j=1}^{2} \theta_j(t) dW_j(t) - \frac{1}{2}\sum_{j=1}^{2} \theta_j^2(t) dt \right) + e^{X(t)} \frac{1}{2} \sum_{j=1}^{2} \theta_j^2(t) dt \\
&= (-Z(t)) \sum_{j=1}^{2} \theta_j(t) dW_j(t)
\end{aligned}$$

Integrating both sides produces the following

$$Z(t) = Z(0) - \int_0^t (-Z(u)) \sum_{j=1}^{2} \theta_j(u) dW_j(u) \tag{2.7}$$

To ensure that the above integral is well defined and is a martingale, the expected value of this integral squared needs to be finite. We will end up exactly with condition (2.6) of the theorem and therefore $Z(t)$ is a martingale with $\mathbb{E}[Z] = \mathbb{E}[Z(T)] = Z(0) = 1$. Now that we know the form of $Z(t)$ and using $\tilde{W}_j(t)$ from the theorem above, by Itô's product formula we have

$$\begin{aligned}
d\left(\tilde{W}_i(t) Z_t\right) &= \tilde{W}_i(t) dZ_t + Z_t d\tilde{W}_i(t) + dZ_t d\tilde{W}_i(t) \\
&= \tilde{W}_i(t) \left(-Z_t\right) \sum_{j=1}^{2} \Theta_j(t) dW_j(t) + Z_t dW_i(t)
\end{aligned}$$

Use the fact that $[M_i, M_j](t) = t\delta_{ij}$, which we write informally as $dW_i(t)dW_j(t) = dt\delta_{i,j}$. The expression above has no dt term, therefore this shows that $\tilde{W}_i(t)Z(t)$ is an $\mathcal{F}_t$-martingale under $\mathbb{P}$. So $\tilde{W}_i(t)$ is an $\mathcal{F}_t$-martingale under $\tilde{\mathbb{P}}$, Moreover,

$$[\tilde{W}_i, \tilde{W}_j](t) = \left[W_i + \int_0^{\cdot} \theta_i(u) du, W_j + \int_0^{\cdot} \theta_j(u) du \right](t) = [W_i, W_j](t) = t\delta_{i,j}.$$

□

We can now derive the processes for (S_t, v_t) under the risk-neutral measure $\mathbb{Q}$. This is done by applying the two-dimensional Girsanov theorem. Consequently, the risk-neutral version of the bivariate system of SDEs in (2.3) is

$$\begin{aligned}
dS_t &= (r-q) S_t dt + \sqrt{v_t} S_t \sqrt{1-\rho^2} d\tilde{Z}_{1,t}^{\mathbb{Q}_\lambda} + \sqrt{v_t} S_t \rho d\tilde{Z}_{2,t}^{\mathbb{Q}_\lambda} \\
dv_t &= [\kappa(\theta - v_t) - \lambda] dt + \sigma \sqrt{v_t} d\tilde{Z}_{2,t}^{\mathbb{Q}_\lambda}
\end{aligned} \tag{2.8}$$

where

$$\begin{aligned}
\tilde{Z}_{1,t}^{\mathbb{Q}_\lambda} &= Z_{1,t}^{\mathbb{P}} + \frac{\mu - (r-q) - \lambda\rho/\sigma}{\sqrt{1-\rho^2}\sqrt{v_t}} t, \\
\tilde{Z}_{2,t}^{\mathbb{Q}_\lambda} &= Z_{2,t}^{\mathbb{P}} + \frac{\lambda}{\sigma\sqrt{v_t}} t,
\end{aligned}$$

where $\mathbb{E}^{\mathbb{Q}_\lambda}[d\tilde{Z}_{1,t}^{\mathbb{Q}_\lambda} d\tilde{Z}_{2,t}^{\mathbb{Q}_\lambda}] = 0$, with $\lambda = \lambda(S_t, v_t, t)$ for simplification.

Note that we introduced a function λ in the drift term of the risk-neutral variance process in (2.8). This alternative form is used when markets are not complete or when the assets are not traded which is the case for our variance process. As volatility is not a traded asset here, this function is not unique, so this is why we represent the risk-neutral measure $\mathbb{Q}$ with λ, so in a sense we are saying that our measure $\mathbb{Q}$ depends on λ and correspondingly for each λ there is an equivalent martingale measure.

This function is known as the volatility risk premium. According to Heston (1993), Breeden's (1979) consumption model indicates that this premium is proportional to the variance, leading to $\lambda(S_t, v_t, t) = \lambda v_t$, where λ is a constant. The introduction of this function will not complete the market but will better replicate the market implied volatility surface.

By setting $\lambda = 0$, we ensure that the SDE for the variance process under the risk-neutral measure $\mathbb{Q}$ will be the same as the one under the physical measure $\mathbb{P}$. For simplification, in this thesis we set $\lambda = 0$, but this is not always needed. For further details on the estimation of λ, refer to Bollerslev et al. (2011). All derivations in this thesis will include the volatility risk premium $\lambda(S_t, v_t, t) = \lambda v_t$, where λ is a constant for a more complete model analysis. For simplification, for now on, we will drop the time index on the variance and use $\lambda(S_t, v_t, t) = \lambda v$.

As we seen before, Heston (1993) assumed that the underlying stock does not pay dividends, consequently, every Heston model derivation in this thesis for now on, will be under this assumption. At the end of each derivation we show how to include dividends. The dividends that we will be included in the formulas will always be seen as continuous over the option's life and not stochastic.

In this section we included dividends in the SDE of the stock price in (2.8), by including q in the equation of $\tilde{Z}_{1,t}^{\mathbb{Q}_\lambda}$.

2.4. Variance process distribution and properties

Cox, Ingersoll, and Ross (1985) described the distribution and properties of the variance process. The distribution of future values of the variance process, v_t, can be computed in closed form as

$$v_t = \frac{Y}{2c_t}, \tag{2.9}$$

here we have that $Y = 2c_t v_t$. Conditional on a realized value of v_s, this random variable, Y, (for $t > s$) follows a non-central chi-square distribution with $d = \frac{4\kappa\theta}{\sigma^2}$ degrees of freedom and non-centrality parameter $2c_t v_s e^{-\kappa(t-s)}$, where

$$c_t = \frac{2\kappa}{\sigma^2\big(1 - e^{-\kappa(t-s)}\big)}, \tag{2.10}$$

and with $t > s$. Therefore, the probability density function of the variance process, v_t, at time t, conditional on its value at the current time, s, is given as

$$f(v_t; v_s, \kappa, \theta, \sigma) = ce^{-u-v}\left(\frac{v}{u}\right)^{\frac{q}{2}} I_q(2\sqrt{uv}), \tag{2.11}$$

where $u = c_t v_s e^{-\kappa(t-s)}$, $v = c_t v_t$, $q = \frac{2\kappa\theta}{\sigma^2} - 1$ and $I_q(2\sqrt{uv})$ is a modified Bessel function of the first kind of order q. Finally, the mean and variance of the variance process, v_t, conditional on the value v_s are respectively the following

$$\begin{aligned} m &= \mathrm{E}[v_t|v_s] = \theta + (v_s - \theta)e^{-\kappa(t-s)}, \\ v &= \mathrm{Var}[v_t|v_s] = v_s\frac{\sigma^2}{\kappa}(e^{-\kappa(t-s)} - e^{-2\kappa(t-s)}) + \frac{\theta\sigma^2}{2\kappa}(1 - e^{-\kappa(t-s)})^2. \end{aligned} \tag{2.12}$$

When κ becomes too large, the variance process quickly reverts to its long-term mean, θ. Consequently the mean m will approach θ as $\kappa \to \infty$. A high value of κ will make v_t have little variation around θ where this little variation is considered negligible. Consequently, the variance v will approach 0 as $\kappa \to \infty$.

As $\kappa \to 0$, the mean-reversion effect is almost negligible. The mean m in this regime will approach its current level, reflecting the fact that v_t will not revert quickly to θ and will instead fluctuate around its current value. Hence, the mean m will approach v_s as $\kappa \to 0$. To retrieve the value of v as $\kappa \to 0$ we will rewrite the v expression in (2.12) as

$$\frac{\sigma^2(2v_s + \theta(e^{(2t-s)\kappa} - 2e^{t\kappa} + e^{s\kappa}))}{2e^{2t\kappa}} e^{s\kappa}\left(\frac{e^{(t-s)\kappa} - 1}{\kappa}\right).$$

We can now easily calculate the value of v as $\kappa \to 0$ by taking the product of limits

$$\lim_{\kappa\to 0}\frac{\sigma^2(2v_s + \theta(e^{(2t-s)\kappa} - 2e^{t\kappa} + e^{s\kappa}))}{2e^{2t\kappa}} \lim_{\kappa\to 0} e^{s\kappa} \lim_{\kappa\to 0}\left(\frac{e^{(t-s)\kappa} - 1}{\kappa}\right).$$

The first term of the above expression is expressed as $\sigma^2 v_S$, the second one as 1 and the third one as $(t-s)$. Consequently, the variance v will approach $\sigma^2 v_s(t-s)$ as $\kappa \to 0$. This concludes the properties of the future distribution.

If the variance process does display mean reversion ($\kappa, \theta > 0$), then as time t becomes large, the asymptotic distribution of v_∞ will approach a gamma distribution with the following probability density function

$$f(v_\infty; \kappa, \theta, \sigma) = \frac{\beta^\alpha}{\Gamma(\alpha)} v_\infty^{\alpha-1} e^{-\beta v_\infty}, \tag{2.13}$$

where $\beta = \frac{2\kappa}{\sigma^2}$ and $\alpha = \frac{2\kappa\theta}{\sigma^2}$. The expression in (2.13) can also be named as the steady state function. We will now determine the mean and variance of the steady state function. We will begin by determining the mean. The mean of (2.13) is given by its expected value

$$\mathbb{E}[v] = \int_0^\infty v f(v) dv = \int_0^\infty v\frac{\beta^\alpha}{\Gamma(\alpha)} v^{\alpha-1} e^{-\beta v} dv = \frac{\beta^\alpha}{\Gamma(\alpha)}\int_0^\infty v^\alpha e^{-\beta v} dv.$$

This integral is a well-known form, which is related to the Gamma function. Specifically

$$\int_0^\infty v^\alpha e^{-\beta v} dv = \frac{\Gamma(\alpha+1)}{\beta^{\alpha+1}},$$

thus, the mean is

$$\mathbb{E}[v] = \frac{\beta^\alpha}{\Gamma(\alpha)}\frac{\Gamma(\alpha+1)}{\beta^{\alpha+1}} = \theta.$$

We will now determine the variance. The variance of (2.13) is given as

$$\mathrm{Var}[v] = \mathbb{E}[v^2] - (\mathbb{E}[v])^2 = \int_0^\infty v^2 f(v)dv - \theta^2 = \frac{\beta^\alpha}{\Gamma(\alpha)}\int_0^\infty v^{\alpha+1}e^{-\beta v}dv - \theta^2.$$

Using the Gamma function for the above integral give us

$$\int_0^\infty v^{\alpha+1}e^{-\beta v}dv = \frac{\Gamma(\alpha+2)}{\beta^{\alpha+2}},$$

thus, the variance is

$$\mathrm{Var}[v] = \frac{\beta^\alpha}{\Gamma(\alpha)}\frac{\Gamma(\alpha+2)}{\beta^{\alpha+2}} - \theta^2 = \frac{\sigma^2\theta}{2\kappa}.$$

In all of the above expressions we abreviated v_∞ as v. These findings are consistent with the conclusions presented by [**12**].

2.5. The European call price

Let $C(K)$ denote the price of a European call on a non-dividend paying stock with spot price S_t, strike K and time to maturity $\tau = T - t$. The time-t price of $C(K)$ is the discounted expected value of the payoff under the risk-neutral measure $\mathbb{Q}$ and is expressed as

$$\begin{aligned} C(K) &= e^{-r\tau}\mathbb{E}^{\mathbb{Q}}[(S_T - K)^+] \\ &= e^{-r\tau}\mathbb{E}^{\mathbb{Q}}[(S_T - K)\mathbb{1}_{S_T>K}] \\ &= e^{-r\tau}\mathbb{E}^{\mathbb{Q}}[S_T\mathbb{1}_{S_T>K}] - Ke^{-r\tau}\mathbb{E}^{\mathbb{Q}}[\mathbb{1}_{S_T>K}], \end{aligned} \tag{2.14}$$

where $\mathbb{1}$ is the indicator function. The probabilities above will be obtained under different probability measures. $\mathbb{E}^{\mathbb{Q}}[\mathbb{1}_{S_T>K}]$ is the probability of the call expiring in-the-money under the measure $\mathbb{Q}$, which can be computed as

$$\mathbb{E}^{\mathbb{Q}}[\mathbb{1}_{S_T>K}] = \mathbb{Q}(S_T > K) = \mathbb{Q}(\ln S_T > \ln K). \tag{2.15}$$

To evaluate $e^{-r\tau}\mathbb{E}^{\mathbb{Q}}[S_T\mathbb{1}_{S_T>K}]$, we need to change the probability measure from $\mathbb{Q}$ to another measure which we will denote as $\mathbb{Q}^S$. To do this, we can utilize the Radon-Nikodym derivative which relates the two measures, $\mathbb{Q}$ and $\mathbb{Q}^{\mathbb{S}}$. Now, consider the following Radon-Nikodym derivative

$$\frac{d\mathbb{Q}}{d\mathbb{Q}^{\mathbb{S}}} = \frac{B_T/B_t}{S_T/S_t} = \frac{e^{rT}/e^{rt}}{S_T/S_t} = \frac{S_t e^{r(T-t)}}{S_T} = \frac{\mathbb{E}^{\mathbb{Q}}[e^{x_T}]}{e^{x_T}}. \tag{2.16}$$

Here we will define B_t as the value of a bank account at time $t \geq 0$. For the initial condition we assume that $B(0) = 1$ and that the bank account grows at a constant risk-free rate r over time. Hence, $B(t)$ follows the following differential equation

$$dB(t) = rB(t)dt,$$

Consequently,

$$B_t = \exp\left(\int_0^t r du\right) = e^{rt}. \tag{2.17}$$

In (2.16), we have written $S_t e^{r(T-t)} = \mathbb{E}^{\mathbb{Q}}[e^{x_T}]$, since under the measure $\mathbb{Q}$, the stock grows at the risk-free rate r, also here we define S_T as e^{x_T} where $x_T = \ln S_T$. We will now evaluate the first expectation in the last line of (2.14).

$$\begin{aligned} e^{-r\tau}\mathbb{E}^{\mathbb{Q}}[S_T \mathbb{1}_{S_T>K}] &= e^{-r(T-t)}S_t\mathbb{E}^{\mathbb{Q}}\left[S_T/S_t \mathbb{1}_{S_T>K}\right] = B_t/B_T S_t \mathbb{E}^{\mathbb{Q}}\left[S_T/S_t \mathbb{1}_{S_T>K}\right] \\ &= S_t\mathbb{E}^{\mathbb{Q}}\left[\frac{S_T/S_t}{B_T/B_t}\mathbb{1}_{S_T>K}\right] = S_t\mathbb{E}^{\mathbb{Q}^{\mathbb{S}}}\left[\frac{S_T/S_t}{B_T/B_t}\mathbb{1}_{S_T>K}\frac{d\mathbb{Q}}{d\mathbb{Q}^{\mathbb{S}}}\right] \\ &= S_t\mathbb{E}^{\mathbb{Q}^{\mathbb{S}}}\left[\mathbb{1}_{S_T>K}\right] = S_t\mathbb{Q}^{\mathbb{S}}(S_T > K) = S_t\mathbb{Q}^{\mathbb{S}}(\ln S_T > \ln K). \end{aligned} \tag{2.18}$$

Consequently, the European call price of equation (2.14) can now be written in terms of both measures, $\mathbb{Q}$ and $\mathbb{Q}^{\mathbb{S}}$ as

$$C(K) = S_t\mathbb{Q}^{\mathbb{S}}(\ln S_T > \ln K) - Ke^{-r\tau}\mathbb{Q}(\ln S_T > \ln K). \tag{2.19}$$

We will denote the probability under the measure $\mathbb{Q}^{\mathbb{S}}$ by P_1 and the probability under the measure $\mathbb{Q}$ by P_2. Therefore, (2.19) can be rewritten as

$$C(K) = S_t P_1 - Ke^{-r\tau}P_2. \tag{2.20}$$

P_1 and P_2 represent the probability of the call expiring in-the-money (under different measures), conditional on the value of the stock $S_t = e^{x_t}$, where $x_t = \ln S_t$ and on the value v_t of the volatility at time t. Then the expression (2.20), using the fact that $x_t = \ln S_t$, can be written as

$$C(K) = e^{x_t}P_1 - Ke^{-r\tau}P_2. \tag{2.21}$$

The measure $\mathbb{Q}$ uses the bank account B_t as numeraire and the measure $\mathbb{Q}^{\mathbb{S}}$ uses the stock price S_t. If we assume a value of $q \neq 0$ then, in equation (2.20) and (2.21) we multiply the first term by $e^{-q\tau}$, as explained by Whaley (2006).
To obtain the price $P(K)$ of a European put, we first obtain the price $C(K)$ of a European call and then we find the value of $P(K)$ by using the put-call parity

$$P(K) = C(K) + Ke^{-r\tau} - S_t e^{-q\tau}. \tag{2.22}$$

Here, we also assumed the presence of a continuous dividend yield q.

2.6. Heston PDE

In the Heston model we need to hedge both stock and volatility which are our two sources of randomness. Therefore, we form a portfolio consisting of one option $V = V(S, v, t)$, Δ units of the stock, and φ units of another option $U(S, v, t)$ for the volatility hedge. Under these conditions, the portfolio is valued as

$$\Pi = V + \Delta S + \varphi U. \tag{2.23}$$

Assuming that the portfolio is self-financing, the change in portfolio value is

$$d\Pi = dV + \Delta dS + \varphi dU. \tag{2.24}$$

The hedging portfolio strategy will go as follows. We will apply Itô's lemma to obtain the processes for V and U. After having both processes we can then derive the Π process. To derive the Heston PDE, we need to find the values of Δ and φ that makes the portfolio riskless. Applying Itô's lemma for V and U will return the same expression, one in terms of V and the other in terms of U, so to avoid repeatedness we will ilustrate the Itô's lemma for V

$$dV = V_t dt + V_S dS + \frac{1}{2} V_{SS}(dS)^2 + V_v dv + \frac{1}{2} V_{vv}(dv)^2 + V_{vS} dv dS. \tag{2.25}$$

Now, using the fact that $(dS)^2 = vS^2 dt$, $(dv)^2 = \sigma^2 v dt$, and $dvdS = \sigma\rho v S dt$, using the SDEs in (2.8), where $d\tilde{Z}_{1,t}^{\mathbb{Q}_\lambda} dt = d\tilde{Z}_{2,t}^{\mathbb{Q}_\lambda} dt = d\tilde{Z}_{1,t}^{\mathbb{Q}_\lambda} d\tilde{Z}_{2,t}^{\mathbb{Q}_\lambda} = (dt)^2 = 0$ and $(d\tilde{Z}_{1,t}^{\mathbb{Q}_\lambda})^2 = (d\tilde{Z}_{2,t}^{\mathbb{Q}_\lambda})^2 = dt$, (2.25) is now represented as

$$dV = V_t dt + V_S dS + \frac{1}{2} v S^2 V_{SS} dt + V_v dv + \frac{1}{2}\sigma^2 v V_{vv} dt + \sigma\rho v S V_{vS} dt. \tag{2.26}$$

Now, to save some space we will use the following operator

$$L_1 = ()_t + \frac{1}{2} v S^2 ()_{SS} + \frac{1}{2}\sigma^2 v ()_{vv} + \sigma\rho v S ()_{vS}.$$

Making use of L_1, (2.26) is now represented as

$$dV = (L_1 V)(S, v, t)dt + V_S dS + V_v dv. \tag{2.27}$$

Note that the operator for U will be the same as the operator for V. The difference is that one is in terms of U and the other is in terms of V. Now, substituting the operator L_1 in (2.24) lead us to

$$d\Pi = (L_1 V)(S, v, t)dt + \varphi(L_1 U)(S, v, t)dt + [V_S + \varphi U_S + \Delta]\, dS + [V_v + \varphi U_v]\, dv. \tag{2.28}$$

In the above expression, the last two terms must be zero if we want to hedge the portfolio against movements in both the stock and volatility. Consequently, we must have

$$\varphi = -\frac{V_v}{U_v}, \quad \Delta = -\varphi U_S - V_S. \tag{2.29}$$

We can now substitute the new values of φ and Δ in (2.28) and obtain

$$d\Pi = (L_1 V)(S, v, t)dt + \varphi(L_1 U)(S, v, t)dt. \tag{2.30}$$

Assuming that the portfolio grows at a constant risk-free rate, r, our change in portfolio value is now

$$d\Pi = r\Pi dt = r(V + \Delta S + \varphi U)dt. \tag{2.31}$$

Now, if we substitute the values of φ and Δ in (2.31), make this expression equal to (2.30) and drop the dt terms, we get the following equality

$$\frac{(L_1 V)(S,v,t) - rV + rSV_S}{V_v} = \frac{(L_1 U)(S,v,t) - rU + rSU_S}{U_v}. \tag{2.32}$$

When looking to the equality in (2.32) we see that the left side is a function of V and the right side a function of U. Therefore, each side can be written as a function $f(S,v,t)$. Since we are mainly interested in the option that is used to hedge the volatility, our main focus is therefore the option $U(S,v,t)$. This lead us to the following equality

$$\frac{(L_1 U)(S,v,t) - rU + rSU_S}{U_v} = -f(S,v,t). \tag{2.33}$$

We write the minus sign before the function $f(S,v,t)$ for reasons that will become clearer in a bit. We can rewrite the equality above as

$$(L_1 U)(S,v,t) - rU = -rSU_S - f(S,v,t)U_v. \tag{2.34}$$

Remember, rS is the drift of the stock price SDE. Hence, the function $f(S,v,t)$ must be some sort of drift of the variance SDE. Therefore, using this idea, makes sense why Heston (1993) specifies this function as

$$f(S,v,t) = \kappa(\theta - v) - \lambda(S,v,t), \tag{2.35}$$

where the function $f(S,v,t)$ is the drift of the variance SDE represented in the expression (2.8). The function $\lambda(S,v,t)$ represents the volatility risk premium that we already discussed when deriving the risk-neutral process for the variance process v_t. Substituting (2.35) in (2.34) and rearranging the terms, we produce the Heston PDE in terms of the stock price S as

$$(L_1 U)(S,v,t) - rU + rSU_S + [\kappa(\theta - v) - \lambda v]U_v = 0. \tag{2.36}$$

A European call option with strike price K and maturity at time T satisfies the PDE (2.36) subject to the following boundary conditions

$$\begin{gathered} U(S,v,T) = (S-K)^+, \quad U(0,v,t) = 0, \quad U_S(\infty,v,t) = 1, \quad U(S,\infty,t) = S, \\ rSU_S(S,0,t) + \kappa\theta U_v(S,0,t) - rU(S,0,t) + U_t(S,0,t) = 0. \end{gathered} \tag{2.37}$$

To simplify the PDE in (2.36) which is expressed in terms of (S,v,t) we can define it in terms of the log price $x = \ln S$ and express it in terms of (x,v,t). To do this, we calculate the following derivatives

$$U_S = U_x \frac{1}{S}, \quad U_{vS} = \frac{1}{S} U_{vx}, \quad U_{SS} = -\frac{1}{S^2} U_x + \frac{1}{S^2} U_{xx}.$$

We can now substitute these expressions into the Heston PDE in (2.36) and obtain the Heston PDE in terms of the log price $x = \ln S$. Before doing this, let us use the following operator

$$L_2 = ()_t + \frac{1}{2}v()_{xx} + \frac{1}{2}\sigma^2 v()_{vv} + \sigma\rho v()_{vx}.$$

Making use of L_2, the Heston PDE in terms of the log price $x = \ln S$ is represented as

$$(L_2U)(x, v, t) - rU + \left(r - \frac{1}{2}v\right) U_x + [\kappa(\theta - v) - \lambda v]U_v = 0. \tag{2.38}$$

This completes the derivation of the Heston PDE. If we assume a value of $q \neq 0$ then, in equation (2.36) and (2.37) we replace the term rS by $(r - q)S$, in (2.37), $U(S, \infty, t) = S$ by $U(S, \infty, t) = Se^{-q\tau}$ and finally, in equation (2.38) the term $(r - \frac{1}{2}v)$ by $(r - q - \frac{1}{2}v)$. Note that the boundary conditions in (2.37) is only for call options. One could use the put-call parity and easily obtain the boundary conditions for put options.

2.7. PDE for P_1 and P_2

Since the European call $C(K)$ expressed in (2.21) is a financial derivative, it must also satisfy the Heston PDE (2.38) which consequently we write as

$$(L_2C)(x, v, t) - rC + \left(r - \frac{1}{2}v\right) C_x + [\kappa(\theta - v) - \lambda v]C_v = 0. \tag{2.39}$$

Now, we are interested in the Heston PDE for the in-the-money probabilities P_1 and P_2. Since (2.21) is a linear combination of two terms and we know that it satisfies the above PDE as a whole, this implies that each term will also satisfy the above PDE. Consequently, $e^{x_t}P_1$ and $-Ke^{-r\tau}P_2$ will satisfy the PDE in (2.39). We will use these facts to derive the PDE for P_1 and P_2. To do this, we need to find the required derivatives of these two terms.

$$C_t = e^x P_{1_t}\delta_{i1} - Ke^{-r\tau}\left[rP_2 + P_{2_t}\right]\delta_{i2}, \tag{2.40}$$

$$C_x = e^x\left[P_1 + P_{1_x}\right]\delta_{i1} - Ke^{-r\tau}P_{2_x}\delta_{i2}, \tag{2.41}$$

$$C_{xx} = e^x\left[P_1 + 2P_{1_x} + P_{1_{xx}}\right]\delta_{i1} - Ke^{-r\tau}P_{2_{xx}}\delta_{i2}, \tag{2.42}$$

$$C_v = e^x P_{1_v}\delta_{i1} - Ke^{-r\tau}P_{2_v}\delta_{i2}, \tag{2.43}$$

$$C_{vv} = e^x P_{1_{vv}}\delta_{i1} - Ke^{-r\tau}P_{2_{vv}}\delta_{i2}, \tag{2.44}$$

$$C_{vx} = e^x\left[P_{1_v} + P_{1_{vx}}\right]\delta_{i1} - Ke^{-r\tau}P_{2_{vx}}\delta_{i2}. \tag{2.45}$$

We used the Kronecker delta, δ_{ij}, to ilustrate how each equation is expressed when calculating individually the required derivatives for the terms, $e^{x_t}P_1$ and $-Ke^{-r\tau}P_2$.
To derive the PDE for P_1, in equations (2.40) through (2.45), we use $i = 1$ to only use the terms containing P_1. We substitute these equations into the PDE in (2.39), we drop the e^x terms and making use of the L_2 operator, we get

$$(L_2P_1)(x,v,t) + \left(r + \frac{1}{2}v\right) P_{1_x} + [\rho\sigma v + \kappa(\theta - v) - \lambda v]P_{1_v} = 0. \tag{2.46}$$

Similarly, to derive the PDE for P_2, in equations (2.40) through (2.45), we use $i = 2$ to only use the terms containing P_2. We substitute these equations into the PDE in (2.39), we drop the $-Ke^{-r\tau}$ terms and making use of the L_2 operator we get

$$(L_2P_2)(x,v,t) + \left(r - \frac{1}{2}v\right) P_{2_x} + [\kappa(\theta - v) - \lambda v]P_{2_v} = 0. \tag{2.47}$$

By combining equations (2.46) and (2.47) we get

$$(L_2P_j)(x,v,t) + (r + u_j v)P_{j_x} + (a - b_j v)P_{j_v} = 0, \tag{2.48}$$

for $j = 1, 2$, where $u_1 = \frac{1}{2}$, $u_2 = -\frac{1}{2}$, $a = \kappa\theta$, $b_1 = \kappa + \lambda - \rho\sigma$, and $b_2 = \kappa + \lambda$.
For the option price to satisfy the terminal condition of (2.38), the combined PDEs in (2.48) are subjected to the following terminal condition

$$P_j(x,v,T;\ln K) = \mathbb{1}_{x \geq \ln K} \qquad \text{for all } x \in \mathbb{R}, v \geq 0. \tag{2.49}$$

If we assume a value of $q \neq 0$ then, in equation (2.39) and (2.47) we replace the term $\left(r - \frac{1}{2}v\right)$ by $\left(r - q - \frac{1}{2}v\right)$, in equation (2.46) the term $\left(r + \frac{1}{2}v\right)$ by $\left(r - q + \frac{1}{2}v\right)$ and finally, in equation (2.48) the term $(r + u_j v)$ by $(r - q + u_j v)$. The derivatives from (2.40) to (2.45) would also change because the term $e^{x_t}P_1$ in the equation (2.21) would be replaced with $e^{x_t - q\tau}P_1$.

2.8. Characteristic functions

We could solve (2.48) numerically, but we prefer an analytical solution. One could try separation of variables, but that does not work here, and when one does not know an obvious way to solve a PDE, we try to guess a solution and then perfect it via trial and error. Since we are dealing with probabilities, we naturally switch to their representation in terms of the generally applicable characteristic functions. Each in-the-money probabilities P_j will be recovered from its characteristic function f_j via the Gil-Pelaez (1951) inversion formula. This formula will be introduced but not on this section.
Heston (1993) assumed that the characteristic functions of the terminal stock price, $x_T = \ln S_T$, are of the log linear form

$$f_j(\phi; x_t, v_t) = \exp(C_j(\tau,\phi) + D_j(\tau,\phi)v_t + i\phi x_t), \tag{2.50}$$

where i is the imaginary unit, C_j and D_j are coefficients, $\tau = T - t$ is the time to maturity and ϕ some dummy variable.
Before deriving the PDE for the characteristic functions f_j, we will introduce the 2-dimensional Feynman-Kac theorem. We will use this theorem to show that the PDE for the characteristic functions f_j will follow the same PDE as the one for the in-the-money

probabilities P_j in the equation (2.48). The following theorem can be found in Shreve (2004).

Theorem 2.8.1. *(2-dimensional Feynman-Kac Theorem) Let $W(t) = (W_1(t), W_2(t))$ be a two-dimensional Brownian motion (i.e., a vector of two independent, one-dimensional Brownian motions). Consider the stochastic differential equations*

$$\begin{aligned} dX_1(u) &= \beta_1(u, X(u))\, du + \gamma_{11}(u, X(u))\, dW_1(u) + \gamma_{12}(u, X(u))\, dW_2(u), \\ dX_2(u) &= \beta_2(u, X(u))\, du + \gamma_{21}(u, X(u))\, dW_1(u) + \gamma_{22}(u, X(u))\, dW_2(u), \end{aligned} \tag{2.51}$$

where $X(u) = (X_1(u), X_2(u))$.
The solution to this pair of stochastic differential equations, starting at $X_1(t) = x_1$ and $X_2(t) = x_2$, depends on the specified initial time t and the initial positions x_1 and x_2.
Let a Borel-measurable function $g(y_1, y_2)$ be given. Corresponding to the initial condition t, x_1, x_2, where $0 \leq t \leq T$, we define

$$f(t, x_1, x_2) = \mathbb{E}[g(X_1(T), X_2(T))|\mathcal{F}_t]. \tag{2.52}$$

Here we assume that $\mathbb{E}[g(X_1(T), X_2(T))|\mathcal{F}_t] < \infty$, for all t and x_1, x_2. Then

$$f_t+\beta_1 f_{x_1}+\beta_2 f_{x_2}+\frac{1}{2}(\gamma_{11}^2+\gamma_{12}^2)f_{x_1x_1}+(\gamma_{11}\gamma_{21}+\gamma_{12}\gamma_{22})f_{x_1x_2}+\frac{1}{2}(\gamma_{21}^2+\gamma_{22}^2)f_{x_2x_2} = 0, \tag{2.53}$$

with the terminal condition

$$f(T, x_1, x_2) = g(x_1, x_2) \quad \textit{for all } x_1 \textit{ and } x_2.$$

Proof. Let $0 \leq s \leq t \leq T$ be given. Hence, for the initial condition s we have

$$f(s, x_1, x_2) = \mathbb{E}[g(X_1(T), X_2(T))|\mathcal{F}_s]. \tag{2.54}$$

Using conditional expectations relative to the filtration $\mathcal{F}_s$ in both sides of (2.52) leave us with

$$\begin{aligned} \mathbb{E}[f(t, x_1, x_2)|\mathcal{F}_s] &= \mathbb{E}[\mathbb{E}[[g(X_1(T), X_2(T))|\mathcal{F}_t]]\mathcal{F}_s] \\ &= \mathbb{E}[g(X_1(T), X_2(T))|\mathcal{F}_s] \\ &= f(s, x_1, x_2). \end{aligned}$$

For the second equality we used the iterated conditioning principle and for the last equality we used the equation (2.54). This proves that the function $f(t, x_1, x_2)$ is a martingale.
Let us now assume that $f(t, x_1, x_2)$ is some twice-differentiable function. Itô's lemma shows that

$$\begin{aligned} df &= f_t dt + f_{x_1} dx_1 + f_{x_2} dx_2 + \frac{1}{2} f_{x_1x_1}(dx_1)^2 + f_{x_1x_2} dx_1 dx_2 + \frac{1}{2} f_{x_2x_2}(dx_2)^2 \\ &= \left(f_t + \beta_1 f_{x_1} + \beta_2 f_{x_2} + \frac{1}{2}(\gamma_{11}^2 + \gamma_{12}^2) f_{x_1x_1} + (\gamma_{11}\gamma_{21} + \gamma_{12}\gamma_{22}) f_{x_1x_2} + \frac{1}{2}(\gamma_{21}^2 + \gamma_{22}^2) f_{x_2x_2} \right) dt \\ &\quad + \gamma_{11} f_{x_1} dW_1 + \gamma_{12} f_{x_1} dW_2 + \gamma_{21} f_{x_2} dW_1 + \gamma_{22} f_{x_2} dW_2. \end{aligned}$$

Since the function $f(t, x_1, x_2)$ is a martingale, the dt term must be zero. When taking the differentials, one uses the fact that W_1 and W_2 are independent. That is, $f(t, x_1, x_2)$ satisfies the PDE (2.53), where the equation (2.52) imposes the following terminal condition

$$f(T, x_1, x_2) = g(x_1, x_2) \quad \text{for all } x_1 \text{ and } x_2.$$

□

Let us now suppose a pair of processes (x_t, v_t) that is governed by the following SDEs

$$\begin{aligned} dx_t &= (r + u_j v)dt + \sqrt{v_t}\sqrt{1-\rho^2}dZ^{\mathbb{Q}}_{1,t} + \sqrt{v_t}\rho dZ^{\mathbb{Q}}_{2,t} \\ dv_t &= (a - b_j v)dt + \sqrt{v_t}dZ^{\mathbb{Q}}_{2,t} \end{aligned} \tag{2.55}$$

where $\mathbb{E}^{\mathbb{Q}}[dZ^{\mathbb{Q}}_{1,t}dZ^{\mathbb{Q}}_{2,t}] = 0$. If we define the equation (2.52) as

$$f(t, x, v) = \mathbb{E}^{\mathbb{Q}}[\mathbb{1}_{x_T \geq \ln K}|\mathcal{F}_t],$$

with $x_T = \ln S_T$, then, by an application of the 2-dimensional Feynman-Kac theorem, $f(t, x, v)$ satisfies the PDE in equation (2.48) subjected to the terminal condition defined in the equation (2.49). Now, if we define the equation (2.52) as

$$f(t, x, v) = \mathbb{E}^{\mathbb{Q}}[e^{i\phi x_T}|\mathcal{F}_t],$$

which is the characteristic function for $x_T = \ln S_T$. Then, by an application of the 2-dimensional Feynman-Kac theorem, $f(t, x, v)$, will also satisfy the PDE in equation (2.48) but now subjected to the terminal condition

$$f(T, x, v) = g(x, v) = e^{i\phi x} \qquad \text{for all } x \in \mathbb{R}, v \geq 0.$$

Therefore, following the equation in (2.48), the PDE for the characteristic function f_j is represented as

$$(L_2 f_j)(x, v, t) + (r + u_j v)f_{j_x} + (a - b_j v)f_{j_v} = 0. \tag{2.56}$$

with u_j, a and b_j defined in the last section.

Before continuing, one should note that the modern approach to obtain all of the PDEs that we derived so far is by an application of the two-dimensional Feynman-Kac theorem. In this thesis we used a version of the theorem that makes use of independent Brownians and as we said before, we can rewrite all of the theorems and definitions such that we make use of correlated Brownians. The general principle of the usage of this theorem to derive the PDEs goes as follows. We correctly define the bivariate system of SDEs and the function in the equation (2.52). After that, we find the martingale, apply the Itô's lemma, set the dt term equal to zero and retrieve the PDE.
To evaluate (2.56) we need the following derivatives

$$\begin{gathered} f_{jt} = -\left(C_{j_\tau} + D_{j_\tau} v\right) f_j, \;\; f_{j_x} = i\phi f_j, \;\; f_{j_v} = D_j f_j, \\ f_{j_{xx}} = -\phi^2 f_j, \;\; f_{j_{vv}} = D_j^2 f_j, \;\; f_{j_{vx}} = i\phi D_j f_j. \end{gathered} \tag{2.57}$$

Now, we substitute these derivatives in the PDE (2.56) and drop the f_j terms to obtain

$$v\left(-D_{j_\tau}+\rho\sigma i\phi D_j-\frac{1}{2}\phi^2+\frac{1}{2}\sigma^2 D_j^2+\mu_j i\phi-b_jD_j\right)-C_{j_\tau}+ri\phi+aD_j=0. \tag{2.58}$$

Consequently, this produces two differential equations

$$\begin{aligned}D_{j_\tau}&=\rho\sigma i\phi D_j-\frac{1}{2}\phi^2+\frac{1}{2}\sigma^2 D_j^2+\mu_j i\phi-b_jD_j\\ C_{j_\tau}&=ri\phi+aD_j\end{aligned} \tag{2.59}$$

subjected to the following zero initial conditions:

$$D_j(0,\phi)=C_j(0,\phi)=0. \tag{2.60}$$

The first equation in (2.59) is a Ricatti equation in D_j while the second one is an ordinary differential equation in C_j that can be solved using integration once we obtain D_j. The step by step derivation of the coefficients C_j and D_j can be found in Rouah (2013). After solving the Ricatti equation, the solution D_j can be written as

$$D_j(\tau,\phi)=\frac{b_j-\rho\sigma i\phi+d_j}{\sigma^2}\left(\frac{1-e^{d_j\tau}}{1-g_je^{d_j\tau}}\right). \tag{2.61}$$

Now that we know the solution of the coeficient D_j we substitute its value in the second equation of (2.59) and use integration to obtain C_j. Doing this gets us the following solution for C_j

$$C_j(\tau,\phi)=ri\phi\tau+\frac{a}{\sigma^2}\left[(b_j-\rho\sigma i\phi+d_j)\tau-2\ln\left(\frac{1-g_je^{d_j\tau}}{1-g_j}\right)\right], \tag{2.62}$$

where the coefficients d_j and g_j are as follows:

$$d_j=\sqrt{(\rho\sigma i\phi-b_j)^2-\sigma^2(2u_ji\phi-\phi^2)}\quad,\quad g_j=\frac{b_j-\rho\sigma i\phi+d_j}{b_j-\rho\sigma i\phi-d_j}. \tag{2.63}$$

When we compute the characteristic function, we use v_t as the unobserved initial variance, v_0, and x_t as the log spot price of the underlying stock. This concludes the derivation of the characteristic functions f_j. If we assume a value of $q\neq 0$ then, in the equation (2.56) we substitute the term $(r+u_jv)$ by $(r-q+u_jv)$ and in the equations (2.58), (2.59) and (2.62) we substitute the term r by $r-q$.
In the next section we present some useful results of Fourier analysis and after that, the Gil-Pelaez inversion formula will be presented.

2.9. Fourier analysis

Let us consider a measurable function $f:\mathbb{R}\to\mathbb{C}$. If the Lebesgue integral of the absolute value of f is finite then this function is called Lebesgue integrable and satisfies the following condition

$$||f||_1 = \int_{-\infty}^{\infty} |f(x)|\, dx < \infty, \tag{2.64}$$

Under these conditions we say that $f \in L^1(\mathbb{R})$ and, consequently, the Fourier transform and its inverse exists. There are several definitions of the Fourier transform $\hat{f}$ of a function f. The one that is usually encountered in the mathematical finance literature is

$$(\mathcal{F}f)(u) = \hat{f}(u) \equiv \int_{-\infty}^{\infty} e^{iux} f(x)\, dx, \tag{2.65}$$

with $\hat{f} : \mathbb{R} \to \mathbb{C}$. The original f can be recovered by the inverse Fourier transform of $\hat{f}$ as

$$\mathcal{F}^{-1}(\mathcal{F}f)(x) = f(x) \equiv \frac{1}{2\pi} \int_{-\infty}^{\infty} e^{-iux} \hat{f}(u)\, du. \tag{2.66}$$

Characteristic functions are closely related to Fourier transforms. Let X be a random variable defined on some probability space $(\Omega, \mathcal{F}, \mathbb{P})$. Consider $\varphi_X : \mathbb{R} \to \mathbb{C}$ the characteristic function, F_X the cumulative distribution function of X and f_X the corresponding probability density function. Then, the characteristic function is defined as the Fourier transform of the probability density function f_X

$$(\mathcal{F}f_X)(u) = \varphi_X(u) \equiv \int_{-\infty}^{\infty} e^{iux} dF_X(x) = \int_{-\infty}^{\infty} e^{iux} f_X(x) dx = \mathbb{E}[e^{iuX}]. \tag{2.67}$$

The probability density function f_X can be obtained by the inverse Fourier transform of the characteristic function φ_X

$$\mathcal{F}^{-1}(\mathcal{F}f_X)(x) = f_X(x) \equiv \frac{1}{2\pi} \int_{-\infty}^{\infty} e^{-iux} \varphi_X(u) du. \tag{2.68}$$

2.10. Gil-Pelaez (1951) inversion formula

In 1951, Gil-Pelaez published his famous inversion formula. This formula will help us to recover each in-the-money probabilities P_j from its characteristic functions f_j. After knowing the analytical form of P_j, we substitute its values in the equation (2.20) and, consequently, we finally complete the original derivation of the Heston model. We will begin by introducing the Gil-Pelaez inversion formula.

Proposition 2.10.1. *(Gil-Palaez Inversion Formula) Let $F_X(x)$ be the cumulative distribution function of some random variable X defined on some probability space $(\Omega, \mathcal{F}, \mathbb{P})$. Furthermore, let*

$$\varphi_X(u) \equiv \int_{-\infty}^{\infty} e^{iux} dF_X(x)$$

be the associated characteristic function. Then we have

$$\frac{1}{2}\left[F_X(x) + F_X(x-)\right] = \frac{1}{2} + \int_{-\infty}^{\infty} \frac{e^{iux}\varphi(-u) - e^{-iux}\varphi(u)}{2\pi i u}\, du$$

Proof. See [[**21**], p. 18]. □

To express the option price of a European call in terms of the inverse Fourier transforms, we need to introduce the following lemma.

LEMMA 2.10.2. *We have the equality*

$$\frac{e^{iux}\varphi(-u) - e^{-iux}\varphi(u)}{2\pi iu} = -\frac{1}{\pi}\Re\left(\frac{\varphi(u)e^{-iux}}{iu}\right).$$

Therefore, assuming that $F_X(x)$ is continuous, Gil-Palaez inversion formula simplifies to

$$F_X(x) = \frac{1}{2} - \frac{1}{\pi}\int_0^\infty \Re\left(\frac{\varphi(u)e^{-iux}}{iu}\right) du. \tag{2.69}$$

PROOF. See [[**21**], p. 19]. □

As we saw before, in the Heston model, there are two characteristic functions f_1 and f_2 associated to each in-the-money probabilities P_1 and P_2. This is because each P_j is obtained under different measures. It also seems that only a single characteristic function need to exist, because there is only one underlying stock price in the model. Bakshi and Madan (2000) explain this idea where consequently we define, for now on, $f_2(\phi) = \varphi(\phi)$ and $f_1(\phi) = \varphi(\phi - i)/\varphi(-i)$ where ϕ is a dummy variable.
We can finally determine analytically the form of the in-the-money probabilities P_j. Before we apply the Gil-Pelaez inversion formula one should note that

$$F_X(x) = \mathbb{P}(X \leq x) = 1 - \mathbb{P}(X > x) \Leftrightarrow \mathbb{P}(X > x) = 1 - F_X(x).$$

This implies that

$$\mathbb{P}(X > x) = 1 - \left(\frac{1}{2} - \frac{1}{\pi}\int_0^\infty \Re\left(\frac{\varphi(u)e^{-iux}}{iu}\right) du\right) = \frac{1}{2} + \frac{1}{\pi}\int_0^\infty \Re\left(\frac{\varphi(u)e^{-iux}}{iu}\right) du. \tag{2.70}$$

Now, using the expressions of P_1 and P_2 expressed in the equation (2.20), and using (2.70) we get

$$\begin{aligned} \mathbb{Q}^{\mathbb{S}}(x_T > \ln K) = P_1 &= \frac{1}{2} + \frac{1}{\pi}\int_0^\infty \Re\left(\frac{\varphi(u-i)e^{-iu\ln K}}{\varphi(-i)iu}\right) du \\ \mathbb{Q}(x_T > \ln K) = P_2 &= \frac{1}{2} + \frac{1}{\pi}\int_0^\infty \Re\left(\frac{\varphi(u)e^{-iu\ln K}}{iu}\right) du \end{aligned} \tag{2.71}$$

where we substituted the dummy variable ϕ by u and x_T represents the logarithm of the terminal stock price S_T.
In the next section we will discuss potencial problems on both integrands of equations in (2.71).

2.10.1. The little Heston trap

The integrands of (2.71) are often well-behaved, avoiding numerical issues. However, there are cases where the integrands behavior complicates numerical integration. The first challenge is that the integrands are undefined at $u = 0$, even though the integration range is $[0, \infty)$, necessitating integration starting close to zero. To minimize inaccuracies from excluding the origin, the integrands must not be overly steep near zero. Another issue is that the integrands may exhibit discontinuities. A further complication is integrands that oscillate significantly, typically linked to short-maturity options. Albrecher et al.

(2007) highlighted two formulations of the Heston characteristic function in academic literature: Heston (1993) formulation and a slightly altered version, "Little trap". Though equivalent, the second formulation, as demonstrated by Albrecher et al. (2007), results in a characteristic function that is more suitable for numerical integration. The original formulation of the Heston characteristic function was covered in section 2.8. To derive the second formulation, multiply the numerator and denominator of the coefficient D_j with $e^{-d_j\tau}$, which leads to the equivalent form:

$$D_j(\tau,\phi) = \frac{b_j - \rho\sigma i\phi - d_j}{\sigma^2}\left(\frac{1-e^{d_j\tau}}{1-c_je^{d_j\tau}}\right) \quad , \quad c_j = \frac{1}{g_j} = \frac{b_j - \rho\sigma i\phi - d_j}{b_j - \rho\sigma i\phi + d_j}. \tag{2.72}$$

One part of the solution C_j in (2.62) can be rewritten as:

$$d_j\tau - 2\ln\left(\frac{1-g_je^{d_j\tau}}{1-g_j}\right) = -d_j\tau - 2\ln\left(\frac{1-c_je^{-d_j\tau}}{1-c_j}\right). \tag{2.73}$$

This equality holds by putting $e^{d_j\tau}$ in evidence inside the logarithm in the left expression of (2.73). This implies that C_j can be written in the equivalent form:

$$C_j(\tau,\phi) = ri\phi\tau + \frac{a}{\sigma^2}\left[(b_j - \rho\sigma i\phi - d_j)\tau - 2\ln\left(\frac{1-c_je^{-d_j\tau}}{1-c_j}\right)\right]. \tag{2.74}$$

If we assume a value of $q \neq 0$ then, in (2.74) we substitute the term r by $(r-q)$. Albrecher et al. (2007) assert that while their formulation and Heston's original formulation are fundamentally the same, their approach significantly reduces numerical issues during model implementation. They note that alternative algorithms can be employed to address the discontinuities inherent in the original Heston model. However, the "Little Trap" formulation consistently avoids these problems, making these alternative algorithms almost unnecessary. This makes their formulation a reliable choice for practical applications in numerical modeling.

2.11. Heston model formulations

In this section we present all of the Heston model formulations used to price options in this thesis. We include the Heston original, the consolidated integrals version, the Attari (2004) approach, the fast Fourier transform formulation of Carr and Madan (1999) and the fractional fast Fourier transform of Chourdakis (2005). These formulations offer different approaches to the problem, each bringing unique advantages and practical applications, which will be thoroughly examined in the following subsections. As you can tell by now, we did a complete derivation of the original Heston model and we will see next that the consolidated integral version is a consequence of the original one. For the remaining three formulations we will follow Rouah (2013) but we will only present the formulas, not the complete derivations. We will also consider the little Heston trap for every formulations since its characteristic functions are more suitable for numerical integration. Finally, every Heston model formulation that we will present will include a continuous dividend yield, q.

2.11.1. Original version

As we have seen before, with the Gil-Pelaez inversion formula, we determined an analytical solution for both in-the-money probabilities P_1 and P_2 expressed in the equations (2.71). Now that we have the analytical solution for both P_1 and P_2, we substitute its values in the equation (2.20) and finally obtain the European call price for the original Heston model.

2.11.2. Consolidated integrals

By combining the integrals for the probabilities P_j into a single integral, the numerical integration required for calculating call prices is simplified. This consolidation reduces to one numerical integration instead of two, theoretically cutting the computation which in a sense is more pratical. We obtain the European call price for this formulation by manipulating the original version formula

$$C(K) = \frac{1}{2}S_t e^{-q\tau} - \frac{1}{2}Ke^{-r\tau} + \frac{1}{\pi}\int_0^\infty \Re\left[\frac{e^{-iu\ln K}}{iu}\left(S_t e^{-q\tau}\frac{\varphi(u-i)}{\varphi(-i)} - Ke^{-r\tau}\varphi(u)\right)\right]du. \tag{2.75}$$

2.11.3. Attari (2004)

Attari (2004) presents an alternative formula for the Heston call price. Attari (2004) writes the terminal stock price as $S_T = S_t e^{r\tau + x(t,T)}$, where $x = x(t,T)$ now denotes the stochastic component of the stock price process. Attari's (2004) formula for the call price is presented as

$$C(K) = S_t e^{-q\tau} - \frac{1}{2}Ke^{-r\tau} - \frac{Ke^{-r\tau}}{\pi}\int_0^\infty A(u)du, \tag{2.76}$$

where

$$A(u) = \frac{\left(R(u) + \frac{I(u)}{u}\right)\cos(ul) + \left(I(u) - \frac{R(u)}{u}\right)\sin(ul)}{1+u^2}, \tag{2.77}$$

with

$$\xi(u) = R(u) + iI(u). \tag{2.78}$$

$R(u)$ and $I(u)$ are the real and imaginary parts of $\xi(u)$ and $l = \ln\frac{Ke^{-r\tau}}{S_t}$. $\xi(u)$ here represents the Attari (2004) characteristic function. The logarithm of the terminal stock price is $\ln S_T = \ln S_t + r\tau + x(t,T)$ where the characteristic function $\xi(u)$ is for $x(t,T)$ and not for $\ln S_T$. Consequently, if we want to express the integrand in equation (2.77) in terms of the Heston (1993) characteristic function for $\ln S_T$, we use the following

$$\mathbb{E}^{\mathbb{Q}}[e^{iux(t,T)}] = \mathbb{E}^{\mathbb{Q}}[e^{iu\ln S_T}]e^{-iu(\ln S_t + r\tau)}.$$

Therefore, we set the following

$$\xi(u) = \varphi(u)e^{-iu(\ln S_t + r\tau)} = \exp(C_2(\tau, u) + D_2(\tau, u)v_t - iur\tau), \tag{2.79}$$

where, $\varphi(u) = f_2(u)$ with $f_2(u)$ represented in the equation (2.50). When we compute the characteristic function ξ, we use v_t as the unobserved initial variance, v_0. The primary benefit of Attari's method is that it requires only a single numerical integration to calculate the call option price. Additionally, the presence of the u^2 factor in the denominator of $A(u)$ causes the integrand to dampen rapidly. As a result, when the upper limit of the integral is truncated during numerical integration, the precision loss is minimized. The Attari integrand decreases significantly faster than the Heston integrand, but it is much steeper at the origin. As a result, there is a possibility of encountering difficulties in numerical integration in that region.

2.11.4. Carr and Madan (1999) fast Fourier transform

Before introducing the Carr and Madan (1999) FFT we need to first explain the Carr and Madan (1999) representation. Carr and Madan (1999) derive the call option price using the Fourier transform. Their approach involves adjusting the call price by introducing a damping factor, which goes as follows

$$c(k) = e^{\alpha k} C(K). \tag{2.80}$$

Here we define $k = \ln K$. Carr and Madan introduces this damping factor because the call price $C(K)$ represented in the equation (2.14) is not Lebesgue integrable and consequently its Fourier transform will not exist. Introducing this damping factor makes the adjusted call price $c(k)$ an integrable function and, consequently, it is possible to determine its Fourier transform.

The idea now is to find the Fourier transform $\hat{c}(u)$ of $c(k)$ and then we apply the inverse fourier transform. This will yield us back $c(k)$. We now remove the damping factor and consequently retrieve $C(k)$. Hence, Carr and Madan (1999) formula for the call price is presented as

$$\begin{aligned} C(K) &= e^{-\alpha k} c(k) \\ &= \frac{e^{-\alpha k}}{2\pi} \int_{-\infty}^{\infty} e^{-iuk} \hat{c}(u) du \\ &= \frac{e^{-\alpha k}}{\pi} \int_{0}^{\infty} \Re[e^{-iuk} \hat{c}(u) du], \end{aligned} \tag{2.81}$$

where

$$\hat{c}(u) = \frac{e^{-r\tau}\varphi(u - (\alpha+1)i)}{\alpha^2 + \alpha - u^2 + iu(2\alpha+1)}. \tag{2.82}$$

The last equality in (2.81) holds, because the integrand is a complex number, and since the call price $C(K)$ represents a real number, we evaluate only the real part of the complex number which is even-valued.

Carr and Madan (1999) shows that a sufficient condition for $c(k)$ to be integrable is that $\hat{c}(0)$ is finite. Therefore, this is the same as saying that the numerator $\varphi(-(\alpha+1)i)$ needs to be finite when $u = 0$. Finally, this is the same as existing the $(\alpha+1)$-st moment of S_T, namely $\mathbb{E}[S_T^{\alpha+1}] < \infty$, since $\varphi(u) = \mathbb{E}[e^{iu \ln S_T}] = \mathbb{E}[S_T^{iu}]$.

According to Lord and Kahl (2007), using this particular representation offers several advantages. First, it simplifies the process by requiring only a single numerical integration. Additionally, because the denominator in equation (2.82) is a quadratic function of the integration variable u, the integrand in the Carr and Madan method decays much faster than in the original Heston formulation. This faster decay means that truncating the integration domain in equation (2.81) is less problematic. Lastly, the representation can also enhance computational accuracy, provided the damping factor α is chosen appropriately.

Carr and Madan (1999) also developed a version of their representation for OTM options. They highlight that, as maturity approaches expiration, the call option's value converges to its intrinsic value $(S_T - K)^+$, which leads to increased oscillations in the integrand of the Fourier inversion in equation (2.81), making the integration process significantly more difficult. In this thesis, however, an alternative approach is presented by algorithmically selecting the damping factor α, we later explain how we determined this value. As a result, we will not present Carr and Madan's OTM option pricing formula, instead, we will only use the equation in (2.81) to produce results across a wide range of maturities, including very short and long expirations, for OTM, ATM and ITM options.

Now that we introduced the Carr and Madan (1999) representation, we can now finally introduce the fast Fourier Transform version.

Carr and Madan (1999) applied the FFT to speed up the computation of option prices. The discrete Fourier transform maps a vector of points $\mathbf{x} = (x_1, \ldots, x_N)$ to another vector of points $\hat{\mathbf{x}} = (\hat{x}_1, \ldots, \hat{x}_N)$ via the relation

$$\hat{x}_k = \sum_{j=1}^{N} e^{-i\frac{2\pi}{N}(j-1)(k-1)} x_j, \quad \text{for } k = 1, \ldots, N. \tag{2.83}$$

In the discrete Fourier transform (DFT), these sums are computed independently from one another, resulting in a number of arithmetic operations of order N^2, i.e. $O(N^2)$. The FFT computes these sums simultaneously with $O(N \log_2 N)$ arithmetic operations. The objective of the FFT is to discretize the expression for the call price $C(K)$ in Equation (2.81) and express it in terms of (2.83).

Evaluation of the call price in Equation (2.81) requires the discretization of the range of strikes and of the integration domain. We can approximate the call price by the trapezoidal rule over the truncated integration domain $[0, b]$ for u, using N equidistant points

$$u_j = (j-1)\eta, \quad \text{for } j = 1, \ldots, N.$$

where η is the increment. The trapezoidal rule approximates the call price $C(k)$ as

$$C(k) \approx \frac{\eta e^{-\alpha k}}{\pi} \sum_{j=1}^{N} \Re\left[e^{-iu_j k}\hat{c}(u_j)\right] w_j, \tag{2.84}$$

where the weights are $w_1 = w_N = \frac{1}{2}$ and $w_j = 1$ for $j = 2, \ldots, N-1$. The analytical form of these weights will be explained in the next section.

We focus on strikes near the money, so the discretization of the strike range is centered about the log spot price $\log S_t$. The strike range, therefore, is discretized using N equally spaced points as

$$k_v = -b + (v-1)\lambda + \log S_t, \quad \text{for } v = 1, \ldots, N,$$

where λ is the increment and $b = \frac{N\lambda}{2}$. This results in log strikes over the range $[\log S_t - b, \log S_t + b - \lambda]$. For a log strike value k_v on the grid, we can now express equation (2.84) for the price of the call as

$$C(k_v) \approx \frac{\eta e^{-\alpha k_v}}{\pi} \sum_{j=1}^{N} \Re \left[e^{-iu_j k_v} \hat{c}(u_j) \right] w_j. \tag{2.85}$$

Substituting for u_j and k_v, we get

$$C(k_v) \approx \frac{\eta e^{-\alpha k_v}}{\pi} \sum_{j=1}^{N} \Re \left[e^{-i\lambda\eta(j-1)(v-1)} e^{i(b-\log S_v)u_j} \hat{c}(u_j) \right] w_j. \tag{2.86}$$

We express equation (2.86) in terms of the discrete FFT in (2.83) if we have $x_j = e^{i(b-\log S_v)u_j} \hat{c}(u_j) w_j$ and if the increments η and λ satisfy the constraint

$$\lambda\eta = \frac{2\pi}{N}.$$

This is a key limitation of the FFT method, as it introduces a trade-off between grid sizes. With a fixed N, selecting a fine grid for the integration range inevitably produces a coarser grid for the log strike range, and vice-versa. Increasing the granularity for both grids requires raising N, which increases the computation time. In this thesis we considered $N = 128$ and the increment η value was obtained by following Carr and Madan (1999) idea where we define the upper limit for the integration in equation (2.81) as $\phi_{\max} = N\eta$, with $\phi_{\max} = 1000$. This resulted in $\eta = 7.8125$ and consequently in a log strike increment $\lambda = 0.00628$. For this fixed value of N, we selected this value for $\phi_{\max}$ because a bigger value would generate a log strike range that would not cover the original strike range and a smaller value would generate a log strike range too big when compared to the original strike range. When using these values for N, $\phi_{\max}$, η and λ, our log-strike range k_v covers the original strike range for every calibrated day. Finally, we use the built-in Matlab function LinearInterpolate to apply linear interpolation to obtain the call prices at the desired strikes. One should note that a slight change in one of the values can generate different results. Note that to implement a continuous dividend yield, q, following Whaley (2006), we replace the spot price S by $Se^{-q\tau}$ before passing the price to the function.

2.11.5. Choourdakis (2005) fractional fast Fourier transform

The fractional fast Fourier transform (FRFT) is an extension of the standard FFT, offering more flexibility. It was utilized in option pricing by Chourdakis (2005). The FRFT generalizes the FFT by removing the constraint $\lambda\eta = \frac{2\pi}{N}$ that the FFT imposes on the grid size parameters. Instead of using a strict $1/N$ in the exponent, the FRFT introduces a more general parameter β. Consequently, equation (2.86) can be modified to

$$\hat{x}_v = \frac{\eta e^{-\alpha k_v}}{\pi} \sum_{j=1}^{N} \Re\left[e^{-i2\pi\beta(j-1)(v-1)} x_j\right], \quad \text{for } v = 1, \dots, N.$$

In this approach, the grid size parameters λ and η satisfy $\lambda\eta = 2\pi\beta$. This allows λ and η to be chosen freely while setting

$$\beta = \frac{\lambda\eta}{2\pi}.$$

A special case of the FRFT is when $\beta = 1/N$, which coincides with the FFT. To implement the FRFT for a sequence $x_1, \dots, x_N$, construct the vectors y and z, each having a dimension of $2N$

$$y = \left(\left\{e^{-i\pi(j-1)^2\beta_j} x_j\right\}_{j=1}^{N}, \quad \{0\}_{j=1}^{N}\right),$$

$$z = \left(\left\{e^{i\pi(j-1)^2\beta_j}\right\}_{j=1}^{N}, \quad \left\{e^{i\pi(N-j+1)^2\beta}\right\}_{j=1}^{N}\right).$$

The next step involves taking the FFT of both y and z to obtain $\hat{y} = D(y)$ and $\hat{z} = D(z)$. Then, compute their product element by element, resulting in a new vector $\hat{h}$ of dimension $2N$

$$\hat{h} = \hat{y} \odot \hat{z} = \{y_j z_j\}_{j=1}^{2N}.$$

Before continuing, we need to introduce the inverse of the DFT defined in the equation (2.83). This will be defined as

$$x_k = \frac{1}{N} \sum_{j=1}^{N} e^{i\frac{2\pi}{N}(j-1)(k-1)} \hat{x}_j, \quad \text{for } k = 1, \dots, N. \tag{2.87}$$

This will map a vector of points $\hat{\mathbf{x}} = (\hat{x}_1, \dots, \hat{x}_N)$ to another vector of points $\mathbf{x} = (x_1, \dots, x_N)$, where $\hat{\mathbf{x}} = D(\mathbf{x})$ and $\mathbf{x} = D^{-1}(\hat{\mathbf{x}})$. Next, apply the inverse FFT to $\hat{h}$, yielding a vector $h = D^{-1}(\hat{h})$ with dimension $2N$. Then, perform another product element by element with the vector e defined as

$$e = \left(\left\{e^{-i\pi(j-1)^2\beta}\right\}_{j=1}^{N}, \quad \{0\}_{j=1}^{N}\right).$$

The fractional FFT can thus be expressed as:

$$\begin{aligned} \hat{x} &= e \odot D^{-1}(\hat{h}) = e \odot D^{-1}(\hat{y} \odot \hat{z}) \\ &= e \odot D^{-1}\left(D(y) \odot D(z)\right). \end{aligned}$$

The first N components of $\hat{x}$ are kept, while the remaining N components are omitted, as they are zeros. Like the FFT, the FRFT transforms the N-dimensional vector x into an N-dimensional vector $\hat{x}$. However, the FRFT involves intermediate $2N$-dimensional vectors y and z, necessitating the computation of two FFTs during the intermediate steps. Despite the extra computational effort, this is generally compensated for by the enhanced accuracy obtained from the flexibility to select the integration and strike grids independently and as arbitrarily small as desired.

To carry out the FRFT, we start by selecting an arbitrary number of points, N, an integration increment η, and a log-strike increment λ. We then define $\beta = \lambda\eta/2\pi$ and proceed with the process as outlined in this section. The FRFT is faster than the FFT for the same number of points and another advantage of the FRFT is that we can restrict the range of strikes on which the algorithm is applied.

In this thesis, just like in the FFT, we selected $N = 128$ and the increment η value was also obtained like in the FFT, the difference is that, we considered $\phi_{\max} = [K^-, K^+]$ where the lower and upper bound of this interval depends on the value of the underlying stock price S. This will be explained in more detail in the next chapter. Since N is fixed and $\phi_{\max}$ is determined in this way, we can retrieve the value for the increment η by using the expression we used in the FFT as $\phi_{\max} = N\eta$. The value for the log-strike increment λ can now be freely chosen: we defined $\lambda = \log(K^+/K^-)/N$. When using these values for N, $\phi_{\max}$, η and λ, our log-strike range k_v restricts the range of strikes on which the algorithm is applied for every calibrated day. We could also apply this value of λ in the FFT but since the increments η and λ satisfy the constraint that we saw in the FFT, η would result in a bigger value, and consequently generate a coarser integration grid.

Finally, just like in the FFT, we use the built-in Matlab function LinearInterpolate to apply linear interpolation to obtain the call prices at the desired strikes. And again, a slight change in one of the values can generate different results. To implement a continuous dividend yield q we follow Whaley (2006) and proceed like explained in the FFT.

2.12. Numerical integration schemes

We will begin by introducing two numerical integration schemes that will be used to approximate the integrals presented in the last section for the various Heston model formulations. We will first introduce the composite trapezoidal rule and finish with the Gauss-Laguerre Quadrature. The first one will be used to approximate the integrals for the FFT and FRFT and the second one will be used to approximate the integrals for the remaining formulations. The following numerical integration schemes can be found in Rouah (2013).

2.12.1. Composite trapezoidal rule

The composite trapezoidal rule belongs to the Newton-Cotes quadrature class which are the simplest integration rules, but also the ones that require the most computing power because we assume equally spaced abcissas meaning that many abcissas are required in order for the approximation of a given integral to be accurate, especially if there are regions in the integration domain where the function is steep or highly oscillatory. In the Heston model, we usually require an integral evaluated over the integration domain $(0, \infty)$. This means that when using the composite trapezoidal rule, we must select the domain as $[\phi_{\min}, \phi_{\max}]$, where $\phi_{\min}$ is a very small number and $\phi_{\max}$ is a large number. We saw how the Heston integrand can be oscillatory, hence the selection of $\phi_{\max}$ must be large enough so that the integrand is sufficiently damped to not cause a loss of accuracy in the approximation of

$$\int_a^b f(x)dx \approx \sum_{j=1}^{N} w_i f(x_j), \tag{2.88}$$

where the points $(x_1,...,x_N)$ are called the abcissas and $(w_1,...,w_N)$ are called the weights associated with the abcissas. The Heston integrand is not defined at $\phi = 0$. Therefore, we use $\phi_{\min}$ as the lower limit of the integration domain.

The composite trapezoidal rule approximates the integral in (2.88) as the sum of trapezoids, each with equal width $x_{j+1} - x_j$ and with the height being defined as the value of $f(x)$ at each of the endpoints. We define the abcissas $x_j = a + (j-1)b$ for $j = 1, ..., N$, where $h = (b-a)/(N-1)$ such that $x_1 = a$ and $x_N = b$. By joining the line segments at $f(x_j)$ and $f(x_{j+1})$ the trapezoids are built. This rule uses the weights $w_1 = w_N = \frac{h}{2}$ and $w_j = h$ for $j = 2, ..., N-1$. Therefore, the approximation in (2.87) is defined as

$$\int_a^b f(x)dx \approx \frac{h}{2}f(x_1) + h\sum_{j=2}^{N-1} f(x_j) + \frac{h}{2}f(x_N). \tag{2.89}$$

In the FFT and FRFT, we used N equidistant points over the truncated integration domain, where this explains why we defined $h = 1$ in the equation (2.84). This is because the ratio of N with $N-1$ is approximately 1.

2.12.2. Gauss-Laguerre quadrature

Gauss-Laguerre Quadrature comes from the Gaussian quadrature class which is more accurate than Newton-Cotes quadrature and requires far fewer abscissas, and it uses unequally spaced abscissas. The abscissas are specified for us in advance so we do not need to worry about the upper and lower limits $\phi_{\min}$ and $\phi_{\max}$ for the integration range $(0, \infty)$. We will approximate an integral of the form of (2.88) just like the composite trapezoidal rule. Just like we saw in the composite trapezoidal rule, the Gauss-Laguerre quadrature requires also a set of abcissas $(x_1,...,x_N)$ along with associated set of weights $(w_1,...,w_N)$ whose values will depende on the choice of N.

Gauss-Laguerre quadrature is particularly useful for evaluating integrals over the semi-infinite interval $(0, \infty)$. This is highly relevant in financial mathematics, especially for the Heston model, which requires such integrations. The abcissas $(x_1,...,x_N)$ will be defined as the roots of the Laguerre polynomial $L_N(x)$ of order N defined as:

$$L_N(x) = \sum_{k=0}^{N} \frac{(-1)^k}{k!} \binom{N}{k} x^k. \tag{2.90}$$

The weights (w_1,...,w_N) are obtained with the derivative of (2.89) evaluated at each of the N abcissas:

$$L'_N(x_j) = \sum_{k=1}^{N} \frac{(-1)^k}{(k-1)!} \binom{N}{k} x_j^{k-1}, \quad \text{for } j = 1, ..., N. \tag{2.91}$$

Then, we can finally define the weights as:

$$w_j = \frac{e^{x_j}}{x_j [L'_N(x_j)]^2}, \quad \text{for } j = 1, ..., N. \tag{2.92}$$

Note that (2.90) has $N+1$ terms but its derivative (2.91) has N terms, which is the correct number of terms required for the approximation in (2.88). In this thesis we considered the quadrature with 32 points.

CHAPTER 3

Data and methodology

3.1. Data

The S&P 500 index options were obtained from the Refinitiv database with the sample period extending from January 2nd, 2018 through May 31st, 2022. We excluded options with less than 21 days to maturity, options with more than 270 days to maturity, options that are very deep OTM and options that are very deep ITM due to low liquidity.

We considered a very deep ITM (OTM) call (put) option as an option where its moneyness is greater or equal than 1.12 and very deep OTM if its moneyness is less than 0.88. We define the option moneyness as the ratio between the underlying stock price S, and the strike price, K, given as S/K.

By using this idea, a call option is said to be OTM if its $S/K \in [0.88, 0.97)$; ATM if its $S/K \in [0.97, 1.03)$; ITM if its $S/K \in [1.03, 1.12)$; and, finally, a put option is said to be OTM if its $S/K \in [1.03, 1.12)$; ATM is its $S/K \in [0.97, 1.03)$; ITM if its $S/K \in [0.88, 0.97)$.

Table 3.1.1. present the sample properties of the S&P 500 index used in this thesis. The reported numbers are respectively the average option mid prices in $ and the total number of observations for each moneyness maturity category. As seen before, the sample period extends from January 2nd, 2018 through May 31st, 2022 for a total of 246,194 calls and 230,935 puts. The summary statistics are derived using daily data from the last quote of each option contract at 3:45 p.m. GMT-4.

S/K	Call (Put) options					Subtotal
	Time-to-maturity					
	21-70	71-120	121-170	171-220	221-270	
[0.88,0.94)	4.78 (339.43)	15.91 (356.03)	32.43 (386.40)	51.26 (415.07)	67.03 (432.91)	
	15,974 (12,196)	15,885 (12,357)	14,248 (11,271)	11,010 (8,532)	9,989 (7,774)	67,106 (52,130)
[0.94,0.97)	18.81 (188.26)	47.47 (219.19)	78.95 (258.22)	109.49 (295.88)	132.31 (320.43)	
	7,944 (7,872)	7,869 (7,802)	7,076 (7,036)	5,572 (5,524)	5,109 (5,053)	33,570 (33,287)
[0.97,1.00)	53.23 (110.46)	95.14 (154.32)	134.07 (197.98)	169.81 (237.80)	194.03 (263.01)	
	7,595 (7,595)	7,522 (7,522)	6,746 (6,746)	5,270 (5,270)	4,900 (4,900)	32,033 (32,033)
[1.00,1.03)	116.26 (67.67)	160.52 (113.92)	201.39 (156.81)	238.57 (195.27)	262.97 (220.41)	
	7,213 (7,213)	7,115 (7,115)	6,393 (6,393)	4,964 (4,964)	4,624 (4,624)	30,309 (30,309)
[1.03,1.06)	193.19 (45.61)	233.16 (87.64)	273.46 (127.54)	311.17 (163.49)	334.63 (187.63)	
	6,947 (6,947)	6,840 (6,840)	6,204 (6,204)	4,737 (4,737)	4,445 (4,445)	29,173 (29,173)
[1.06,1.12)	312.20 (27.93)	344.67 (62.25)	382.85 (97.03)	420.31 (128.49)	442.44 (150.67)	
	12,911 (12,911)	12,655 (12,655)	11,520 (11,520)	8,774 (8,774)	8,143 (8,143)	54,003 (54,003)
Subtotal	58,584 (54,734)	57,886 (54,291)	52,187 (49,170)	40,327 (37,801)	37,210 (34,939)	246,194 (230,935)

TABLE 3.1.1. Sample properties of the S&P 500 index options

Table 3.1.2. present in percentage, the averaged market implied volatilities of individual contracts within each moneyness maturity category across the sample periods used.

Sample period	S/K	Call (Put) options				
		Time-to-maturity				
		21–70	**71–120**	**121–170**	**171–220**	**221–270**
Jan 2018 – May 2022	[0.88,0.94)	14.81 (15.27)	14.27 (14.94)	14.89 (15.63)	15.52 (16.34)	15.47 (16.18)
	[0.94,0.97)	14.09 (14.08)	15.08 (15.09)	16.18 (16.17)	17.01 (17.00)	17.02 (17.02)
	[0.97,1.00)	15.77 (15.76)	16.87 (16.86)	17.88 (17.87)	18.60 (18.59)	18.45 (18.43)
	[1.00,1.03)	18.60 (18.61)	19.09 (19.10)	19.76 (19.77)	20.25 (20.25)	19.96 (19.97)
	[1.03,1.06)	21.45 (21.47)	21.21 (21.23)	21.58 (21.61)	21.81 (21.84)	21.38 (21.41)
	[1.06,1.12)	25.06 (25.13)	23.91 (23.97)	23.91 (23.97)	23.82 (23.89)	23.19 (23.26)
Jan 2018 – Dec 2018	[0.88,0.94)	12.91 (12.84)	11.20 (11.32)	10.31 (10.45)	11.15 (11.52)	11.40 (11.76)
	[0.94,0.97)	11.26 (11.20)	11.42 (11.40)	11.15 (11.12)	12.52 (12.49)	12.94 (12.92)
	[0.97,1.00)	12.15 (12.15)	12.94 (12.93)	12.64 (12.63)	14.06 (14.06)	14.18 (14.17)
	[1.00,1.03)	14.51 (14.52)	14.95 (14.96)	14.36 (14.38)	15.54 (15.56)	15.51 (15.53)
	[1.03,1.06)	17.12 (17.15)	16.86 (16.90)	16.04 (16.09)	16.91 (16.95)	16.79 (16.83)
	[1.06,1.12)	20.88 (20.99)	19.50 (19.59)	18.27 (18.36)	18.82 (18.91)	18.44 (18.53)
Jan 2019 – Dec 2019	[0.88,0.94)	11.80 (11.41)	10.95 (10.85)	11.03 (11.03)	11.17 (11.24)	11.65 (11.77)
	[0.94,0.97)	10.56 (10.50)	11.50 (11.48)	12.21 (12.19)	12.58 (12.56)	13.22 (13.19)
	[0.97,1.00)	12.03 (12.02)	13.23 (13.22)	13.86 (13.86)	14.13 (14.12)	14.62 (14.61)
	[1.00,1.03)	14.65 (14.66)	15.28 (15.28)	15.62 (15.63)	15.69 (15.70)	15.98 (15.98)
	[1.03,1.06)	17.16 (17.17)	17.12 (17.15)	17.19 (17.21)	17.08 (17.10)	17.24 (17.26)
	[1.06,1.12)	20.37 (20.45)	19.50 (19.55)	19.22 (19.28)	18.91 (18.96)	18.85 (18.90)
Jan 2020 – Dec 2020	[0.88,0.94)	19.65 (20.12)	19.28 (19.73)	19.50 (19.95)	20.82 (21.03)	19.87 (20.63)
	[0.94,0.97)	20.46 (20.51)	21.04 (21.07)	21.38 (21.38)	23.09 (23.10)	21.59 (21.64)
	[0.97,1.00)	22.65 (22.63)	23.03 (23.02)	23.16 (23.15)	24.78 (24.76)	23.02 (23.00)
	[1.00,1.03)	25.32 (25.32)	25.17 (25.18)	25.00 (25.00)	26.35 (26.36)	24.54 (24.54)
	[1.03,1.06)	27.82 (27.84)	27.12 (27.14)	26.65 (26.68)	27.86 (27.88)	25.81 (25.83)
	[1.06,1.12)	31.05 (31.10)	29.66 (29.70)	28.85 (28.90)	29.67 (29.72)	27.54 (27.60)
Jan 2021 – Dec 2021	[0.88,0.94)	13.17 (12.93)	13.29 (13.47)	14.04 (14.27)	14.37 (14.60)	14.64 (14.85)
	[0.94,0.97)	12.13 (12.11)	14.00 (14.00)	15.26 (15.23)	15.75 (15.74)	16.10 (16.08)
	[0.97,1.00)	13.73 (13.72)	15.79 (15.78)	16.92 (16.91)	17.28 (17.27)	17.55 (17.53)
	[1.00,1.03)	16.85 (16.86)	18.09 (18.09)	18.82 (18.83)	18.96 (18.97)	19.09 (19.10)
	[1.03,1.06)	20.02 (20.04)	20.32 (20.35)	20.64 (20.67)	20.59 (20.62)	20.56 (20.59)
	[1.06,1.12)	24.04 (24.10)	23.32 (23.38)	23.13 (23.20)	22.78 (22.85)	22.55 (22.62)
Jan 2022 – Dec 2022	[0.88,0.94)	16.38 (16.28)	16.30 (16.40)	16.49 (16.64)	17.22 (17.34)	17.66 (17.78)
	[0.94,0.97)	17.55 (17.53)	18.21 (18.19)	18.65 (18.63)	19.43 (19.41)	19.77 (19.74)
	[0.97,1.00)	20.17 (20.17)	20.38 (20.37)	20.57 (20.57)	21.16 (21.16)	21.34 (21.33)
	[1.00,1.03)	22.99 (22.99)	22.58 (22.58)	22.43 (22.43)	22.76 (22.77)	22.77 (22.78)
	[1.03,1.06)	25.54 (25.55)	24.58 (24.59)	24.13 (24.16)	24.21 (24.23)	24.08 (24.11)
	[1.06,1.12)	28.70 (28.73)	27.10 (27.14)	26.28 (26.32)	26.07 (26.12)	25.77 (25.82)

TABLE 3.1.2. Market implied volatilities

In Table 3.1.2., the market implied volatilities of call options within either the ITM or OTM category often closely align with the market implied volatilities of put options in the corresponding opposite category. This generally persists across different sample periods and time-to-maturity categories. For a given time-to-maturity, both calls and puts imply similar U-shaped volatility patterns across different strike prices. The primary factor behind this consistent pricing relationship between calls and puts is due to put-call parity. For this reason, calls and puts exhibit similar levels of mispricing. This will be confirmed later in the results chapter.

3.2. Procedures

We estimated the parameters of the Heston model using loss functions. The methods that we will discuss use the error between quoted market prices and model prices, or between market and model implied volatilities. We obtain the parameter estimates Θ by minimizing the value of the loss functions, so that the model prices or implied volatilities are as close as possible to their market counterparts. A constrained minimization algorithm must be used so that the constraints on the parameters

$$\kappa > 0, \;\; \theta > 0, \;\; \sigma > 0, \;\; v_0 > 0, \;\; \rho \in [-1, 1] \tag{3.1}$$

are respected. Since loss functions use market option prices or implied volatility derived from those prices as inputs, they produce estimates of the risk-neutral parameters of the Heston model.

Consider a set of N_T maturities τ_t (for $t = 1, \ldots, N_T$) and a set of N_K strikes K_k (for $k = 1, \ldots, N_K$). For each maturity-strike pair (τ_t, K_k), we observe a market price $C(\tau_t, K_k) = C_{tk}$ and a corresponding model price $C(\tau_t, K_k; \Theta) = C_{tk}^{\Theta}$, calculated under some Heston model formulation. In this thesis, we focus on two categories of loss functions: those that minimize the error between market and model prices, and those that minimize the error between quoted and model-implied volatilities. Now we introduce two loss functions that fall into the first category.

The first is the mean error sum of squares (MSE) loss function, where the parameter estimates are found by minimizing

$$\frac{1}{N} \sum_{t,k} (C_{tk} - C_{tk}^{\Theta})^2, \tag{3.2}$$

with respect to Θ. The second is the relative mean error sum of squares (RMSE) loss function, which obtains the parameter estimates by minimizing

$$\frac{1}{N} \sum_{t,k} \frac{(C_{tk} - C_{tk}^{\Theta})^2}{C_{tk}}, \tag{3.3}$$

again with respect to Θ.

Next, we move on to the second category of loss functions. By using the implied volatility mean error sum of squares (IVMSE), we estimate the parameters by minimizing

$$\frac{1}{N} \sum_{t,k} (IV_{tk} - IV_{tk}^{\Theta})^2, \tag{3.4}$$

where $IV_{tk} = IV(\tau_t, K_k)$ and $IV^{\Theta}_{tk} = IV(\tau_t, K_k; \Theta)$, respectively, represent the market and model-implied volatilities. However, a drawback of Equation (3.4) is its computational complexity. For each optimization iteration, the Heston price C^{Θ}_{tk} must be computed first, followed by a root-finding procedure to derive the implied volatility IV^{Θ}_{tk} from C^{Θ}_{tk}.

An alternative approach, suggested by Christoffersen et al. (2009), is to approximate Equation (3.4) using the implied volatility relative mean squared error (IVRMSE) loss function. This approach eliminates the need for the root-finding procedure altogether. In this case, the parameter estimates are obtained by minimizing

$$\frac{1}{N} \sum_{t,k} \frac{(C_{tk} - C^{\Theta}_{tk})^2}{\text{BSVega}^2_{tk}}, \tag{3.5}$$

where BSVega_{tk} is the Black-Scholes-Merton sensitivity of the option price to changes in the implied volatility IV_{tk}. It is calculated at the given maturity τ_t and strike K_k as

$$\text{BSVega}_{tk} = S e^{-q\tau_t} n(d_{tk}) \sqrt{\tau_t}, \tag{3.6}$$

with

$$d_{tk} = \frac{\log(S/K_k) + (r - q + IV^2_{tk}/2)\tau_t}{IV_{tk}\sqrt{\tau_t}}, \tag{3.7}$$

where $n(x) = \exp(-x^2/2)/\sqrt{2\pi}$ represents the standard normal density function. In this thesis, we only used the MSE, RMSE and IVRMSE loss functions. In equations (3.2), (3.3), (3.4) and (3.5), $N = N_T N_K$ and $\sum_{t,k} = \sum_{t=1}^{N_T} \sum_{k=1}^{N_K}$.

3.3. Bias detection using a one-sample t-test

In this thesis, a one-sample Student's t-test is applied to evaluate whether the model's mean calibration error significantly differs from zero, which would indicate potential bias in its calibrated values. We explain in the next section what is this error approach. The t-test compares the sample mean of the error values to a hypothesized population mean of zero, under the assumption that the errors are normally distributed and the population variance is unknown.

The null hypothesis (H_0) assumes that the mean error is zero, suggesting that the model is unbiased:

$$H_0 : \mu = 0.$$

The alternative hypothesis (H_1) posits that the mean error is not equal to zero, indicating bias in the model's calibration:

$$H_1 : \mu \neq 0.$$

The MATLAB function `[h, p, ci] = ttest(errorData, 0)` is used to perform the test, where `errorData` represents the error values and 0 is the hypothesized mean. The function returns `h`, which indicates whether the null hypothesis can be rejected. If `h = 1`, the null hypothesis is rejected, implying that the mean error significantly differs from zero and that bias is detected in the model's calibrated values. If `h = 0`, the null hypothesis is not rejected, indicating that the mean error does not significantly differ from zero, suggesting that the model is unbiased.

The p-value returned by the function represents the probability of observing the data under the null hypothesis. If the p-value is below the chosen significance level of 0.05, the null hypothesis is rejected, indicating that the mean error is significantly different from zero and that bias is present in the model's calibration. Conversely, if the p-value exceeds 0.05, the null hypothesis is not rejected, implying that the model's calibrated values are unbiased. Additionally, the confidence interval (`ci`) provides a range within which the true population mean of the errors is likely to lie with 95% confidence. The t-statistic for the test is calculated using the formula

$$t = \frac{\bar{x} - \mu}{\frac{s}{\sqrt{n}}},$$

where $\bar{x}$ is the sample mean of the errors, $\mu = 0$ is the hypothesized population mean under the null hypothesis, s is the sample standard deviation, and n is the sample size.

Under the null hypothesis, the t-statistic follows a Student's t-distribution with $n - 1$ degrees of freedom.

3.4. Matlab program

The goal is to optimize the Heston model parameters to align model-generated prices with observed market prices, minimizing discrepancies in implied volatilities. The process starts by reading market data from CSV files, which include details such as option type, time to maturity, strike prices, implied volatilities, underlying mid price, continuous compounding interest rate (r), implied dividend yield (q), and other key metrics. For each option contract, the correct values of r and q are extracted from the data and considered constant until the end of the contract's life, though these values may vary between contracts. After loading the data, the script filters it to focus on options with specific maturities and strike prices within a defined range around the current underlying mid price.

Once the data is filtered, the script constructs a matrix of market implied volatilities. These values are then substituted into the Black-Scholes-Merton formula to compute the matrix of market prices. The core of the calibration process involves minimizing the error between these market prices and the theoretical prices derived from various Heston model formulations. This is achieved by using different loss functions. The script employs three main loss functions: the mean error sum of squares (MSE), the relative mean error sum of squares (RMSE), and the implied volatility relative mean squared error RMSE (IVRMSE). These loss functions are applied across five different Heston model formulations: Heston original, Heston single integrand, Attari, FFT, and FRFT. To speed up the computation for the first three formulations, the script uses a technique called Strike Vector Computation, which calculates each characteristic function once per maturity and reuses it for different strike prices. Since we have three loss functions and

5 model formulations, the script runs a total of 15 distinct calibration processes for each option type, aiming to find the optimal Heston parameters for each combination of loss function and model formulation.

The optimization for each combination of loss function and model formulation is performed using MATLAB's fmincon function, which is ideal for constrained optimization problems and it uses an interior point algorithm. fmincon adjusts the Heston parameters within predefined bounds to minimize the selected loss function. After determining the optimal parameters for each of the 15 distinct calibration processes for a given option type, these parameters are saved and used as starting points for the next day's calibration, thereby speeding up future optimizations.

Once the optimal parameters are determined, the script sums the difference errors between the implied market volatilities and the theoretical volatilities generated by each of the 15 distinct calibration processes for a given option type. By using the one-sample Student's t-test, we verify if our models are on average, overestimating or underestimating the implied volatilities for a given sample period. However, it is important to note that this error approach does not provide a holistic view of the model's performance for a given day, as large positive and negative errors can cancel each other out.

For the FFT and FRFT methods, this concept of difference errors is applied to determine the optimal parameters. For each day and for each combination of loss functions with the FFT and the FRFT, the script evaluates 98 different values of the α parameter, ranging from 0.75 to 25 in increments of 0.25. The α value that minimizes the sum of the difference errors in absolute value for that specific day is selected. It is important to note that each α value produces different Heston parameters, reflecting the sensitivity of Fourier methods to the choice of α.

Finally, each CSV file corresponds to a day in the sample period, with the script processing data for a total of 1,102 days. For each day, the program determines the optimal Heston parameters for the 15 distinct calibration processes for both call and put options. Once the calculations for a given day are complete, the results are written to CSV files, where the file name reflects the combination of the loss function, Heston model formulation, and option type. These CSV files contain eight key values: the date, the Heston model parameters, the time taken to perform the calibration, and the difference errors for that day. This results in 30 different CSV files for each day, 15 for calls and 15 for puts. Each new day appends its results to the existing CSV files, adding new lines for each day's results.

CHAPTER 4

Results

This chapter presents the in-sample results of the S&P 500 index options under alternative Heston (1993) model formulations using three different loss functions. Each loss function has its own section.

The Heston original formulation, Heston single integrand formulation, and Attari (2004) formulation produced the best results overall. Since the difference between the original formulation and the single integrand formulation lies in the number of numerical integrations, the results generated by these two methods were nearly identical across all loss functions. Due to their similarity, we chose to present the original formulation here in this chapter, as it forms the core of this thesis. The results for the single integrand formulation are presented in the Appendix. The Attari (2004) formulation is also included due to its strong performance. Overall, the FFT and FRFT produced worse results, which can be attributed to their high sensitivity to the values of parameters such as α, N, $\phi_{\max}$, η, and λ, as discussed earlier. Therefore, the results for the FFT and FRFT are also presented in the Appendix A.

Each subsection contains two tables, one for each chosen formulation, following the same structure as Table 3.1.2. presented in the previous chapter. Each table entry represents the percentage error between the averaged market-implied volatilities and the averaged implied volatilities generated by the respective model formulation for each moneyness and time-to-maturity category. These values can be either positive or negative, indicating whether the model overestimated or underestimated the implied volatilities.

Additionally, each section contains another two tables, one for each chosen formulation, containing the statistical analysis for both option types, covering the mean, standard deviation, minimum value, maximum value, and median for each Heston model parameter. This analysis also extends to the calibration time and the error employed, represented by the sum of the difference errors, as explained in the Matlab program section. We also present the results of the Student's t-test. In the Appendix B, we provide evolution plots for each Heston model parameter, across different combinations of loss function, model formulation, and option type. Although in the tables we have results for 6 different sample periods, the statistical analysis, the results of the Student's t-test and the evolution plots only covers the entire sample period, which extends from January 2$^{\text{nd}}$, 2018 through May 31$^{\text{st}}$, 2022.

Finally, the computations were executed over a span of 18 days, reflecting the complexity of the algorithms and the volume of data processed. The code was executed on a laptop with the following specifications: an AMD Ryzen 5 5600H processor, 8GB of

DDR4 RAM clocked at 3200 MHz, an NVIDIA GeForce GTX 1650 GPU, and a 512GB SSD. The system ran on Windows 11 (64-bit).

4.1. MSE loss function

The following tables present the percentage errors between the averaged market-implied volatilities and the averaged implied volatilities generated by the Heston original formulation and by the Attari formulation, broken down by moneyness and time-to-maturity categories. Positive values indicate overestimating, while negative values indicate underestimating.

Sample period	S/K	Call (Put) options				
		Time-to-maturity				
		21–70	**71–120**	**121–170**	**171–220**	**221–270**
Jan 2018 – May 2022	[0.88,0.94)	3.23 (3.26)	-2.01 (-1.70)	-1.66 (-1.50)	0.07 (0.18)	1.52 (1.63)
	[0.94,0.97)	4.37 (4.35)	-1.20 (-1.29)	-1.40 (-1.46)	-0.04 (-0.04)	1.15 (1.23)
	[0.97,1.00)	3.45 (3.39)	-0.48 (-0.50)	-1.13 (-1.14)	-0.23 (-0.20)	0.67 (0.73)
	[1.00,1.03)	4.03 (4.09)	-0.04 (8.00e-04)	-1.00 (-0.98)	-0.40 (-0.37)	0.33 (0.37)
	[1.03,1.06)	2.41 (2.47)	0.01 (0.06)	-0.92 (-0.90)	-0.42 (-0.40)	0.19 (0.21)
	[1.06,1.12)	-0.19 (-0.25)	-0.17 (-0.20)	-0.59 (-0.63)	-0.16 (-0.20)	0.30 (0.26)
Jan 2018 – Dec 2018	[0.88,0.94)	-0.84 (-0.32)	-3.26 (-1.84)	-0.93 (0.32)	1.00 (1.51)	1.71 (1.88)
	[0.94,0.97)	-0.13 (0.37)	-1.67 (-1.68)	-0.82 (-0.83)	0.28 (0.33)	0.59 (0.68)
	[0.97,1.00)	-0.52 (-0.67)	-0.78 (-0.88)	-0.66 (-0.73)	-0.11 (-0.08)	0.10 (0.16)
	[1.00,1.03)	3.53 (3.62)	0.27 (0.29)	-0.39 (-0.37)	-0.28 (-0.23)	-0.13 (-0.08)
	[1.03,1.06)	1.40 (1.51)	0.53 (0.57)	-0.34 (-0.31)	-0.35 (-0.31)	-0.21 (-0.17)
	[1.06,1.12)	-2.82 (-2.91)	-0.34 (-0.38)	-0.39 (-0.45)	-0.11 (-0.18)	-2.20e-03 (-0.06)
Jan 2019 – Dec 2019	[0.88,0.94)	-2.04 (-1.80)	-4.41 (-3.44)	-2.28 (-1.72)	0.23 (0.58)	1.79 (1.97)
	[0.94,0.97)	3.58 (3.41)	-1.64 (-1.90)	-1.03 (-1.09)	0.67 (0.72)	1.44 (1.57)
	[0.97,1.00)	3.33 (3.07)	-0.66 (-0.69)	-0.96 (-0.91)	0.05 (0.14)	0.60 (0.70)
	[1.00,1.03)	3.86 (3.86)	-0.18 (-0.12)	-0.98 (-0.91)	-0.40 (-0.33)	0.02 (0.08)
	[1.03,1.06)	2.12 (2.19)	0.08 (0.13)	-0.86 (-0.81)	-0.50 (-0.46)	-0.14 (-0.11)
	[1.06,1.12)	-1.55 (-1.65)	0.18 (0.11)	-0.14 (-0.20)	0.12 (0.04)	0.30 (0.22)
Jan 2020 – Dec 2020	[0.88,0.94)	3.01 (2.32)	-1.70 (-1.71)	-1.65 (-1.63)	0.23 (0.21)	1.39 (1.46)
	[0.94,0.97)	6.49 (6.33)	-0.26 (-0.29)	-1.47 (-1.49)	-0.14 (-0.14)	0.94 (0.99)
	[0.97,1.00)	6.03 (6.04)	0.03 (0.05)	-1.32 (-1.31)	-0.29 (-0.29)	0.69 (0.71)
	[1.00,1.03)	4.57 (4.60)	-0.07 (-0.04)	-1.30 (-1.27)	-0.38 (-0.37)	0.68 (0.70)
	[1.03,1.06)	2.52 (2.54)	-0.39 (-0.35)	-1.31 (-1.29)	-0.28 (-0.28)	0.80 (0.79)
	[1.06,1.12)	-0.20 (-0.25)	-0.82 (-0.82)	-1.11 (-1.12)	0.02 (-0.01)	1.08 (1.03)
Jan 2021 – Dec 2021	[0.88,0.94)	3.54 (4.24)	-0.70 (-0.84)	-1.65 (-1.69)	-0.32 (-0.15)	1.65 (1.92)
	[0.94,0.97)	5.08 (5.06)	-2.30 (-2.46)	-1.98 (-2.08)	-0.12 (-0.14)	1.68 (1.77)
	[0.97,1.00)	3.15 (3.12)	-1.19 (-1.24)	-1.34 (-1.38)	-0.08 (-0.07)	1.16 (1.24)
	[1.00,1.03)	5.14 (5.29)	-0.25 (-0.20)	-0.97 (-0.96)	-0.28 (-0.25)	0.54 (0.59)
	[1.03,1.06)	4.05 (4.16)	0.07 (0.12)	-0.83 (-0.81)	-0.47 (-0.45)	0.07 (0.10)
	[1.06,1.12)	1.95 (1.92)	0.18 (0.14)	-0.55 (-0.60)	-0.47 (-0.52)	-0.18 (-0.22)
Jan 2022 – Dec 2022	[0.88,0.94)	-3.31 (-2.17)	-1.97 (-1.87)	-1.30 (-1.27)	-0.03 (-0.05)	1.23 (1.27)
	[0.94,0.97)	1.99 (1.92)	-0.12 (-0.16)	-0.66 (-0.69)	-0.28 (-0.30)	0.47 (0.53)
	[0.97,1.00)	2.39 (2.40)	0.38 (0.41)	-0.69 (-0.67)	-0.66 (-0.64)	-0.03 (0.02)
	[1.00,1.03)	1.30 (1.33)	0.34 (0.38)	-0.71 (-0.69)	-0.75 (-0.72)	-0.16 (-0.15)
	[1.03,1.06)	0.17 (0.19)	0.26 (0.30)	-0.50 (-0.51)	-0.54 (-0.52)	-0.04 (-0.03)
	[1.06,1.12)	-1.36 (-1.40)	0.43 (0.41)	0.02 (-8.50e-03)	0.03 (-5.70e-03)	0.40 (0.37)

TABLE 4.1.1. MSE Heston original - implied volatility percentage errors

Sample period	S/K	Call (Put) options				
		Time-to-maturity				
		21–70	**71–120**	**121–170**	**171–220**	**221–270**
Jan 2018 – May 2022	[0.88,0.94)	3.22 (3.33)	-1.92 (-1.58)	-1.57 (-1.40)	0.13 (0.23)	1.55 (1.66)
	[0.94,0.97)	4.58 (4.58)	-1.04 (-1.12)	-1.32 (-1.38)	-4.70e-03 (-6.80e-03)	1.16 (1.24)
	[0.97,1.00)	3.67 (3.65)	-0.36 (-0.37)	-1.09 (-1.09)	-0.22 (-0.19)	0.67 (0.73)
	[1.00,1.03)	4.05 (4.13)	-1.90e-03 (0.04)	-1.00 (-0.97)	-0.41 (-0.38)	0.33 (0.36)
	[1.03,1.06)	2.30 (2.36)	-0.02 (0.02)	-0.95 (-0.93)	-0.44 (-0.43)	0.18 (0.20)
	[1.06,1.12)	-0.42 (-0.52)	-0.29 (-0.32)	-0.66 (-0.70)	-0.20 (-0.24)	0.28 (0.24)
Jan 2018 – Dec 2018	[0.88,0.94)	-0.77 (-0.40)	-3.20 (-1.75)	-0.89 (0.42)	1.05 (1.58)	1.76 (1.93)
	[0.94,0.97)	0.03 (0.63)	-1.47 (-1.46)	-0.63 (-0.64)	0.40 (0.45)	0.66 (0.74)
	[0.97,1.00)	-0.54 (-0.59)	-0.63 (-0.71)	-0.52 (-0.59)	-0.05 (-0.02)	0.13 (0.19)
	[1.00,1.03)	3.41 (3.53)	0.32 (0.34)	-0.34 (-0.32)	-0.28 (-0.23)	-0.14 (-0.09)
	[1.03,1.06)	1.22 (1.33)	0.49 (0.53)	-0.35 (-0.33)	-0.39 (-0.35)	-0.26 (-0.22)
	[1.06,1.12)	-2.99 (-3.21)	-0.45 (-0.51)	-0.47 (-0.54)	-0.20 (-0.27)	-0.09 (-0.14)
Jan 2019 – Dec 2019	[0.88,0.94)	-2.44 (-1.97)	-4.35 (-3.32)	-2.17 (-1.57)	0.31 (0.68)	1.83 (2.01)
	[0.94,0.97)	3.90 (3.77)	-1.33 (-1.58)	-0.85 (-0.92)	0.76 (0.80)	1.47 (1.59)
	[0.97,1.00)	3.77 (3.56)	-0.41 (-0.43)	-0.85 (-0.80)	0.10 (0.19)	0.61 (0.71)
	[1.00,1.03)	3.89 (3.91)	-0.10 (-0.04)	-0.94 (-0.88)	-0.40 (-0.33)	0.01 (0.08)
	[1.03,1.06)	1.91 (1.98)	4.80e-03 (0.05)	-0.91 (-0.86)	-0.54 (-0.50)	-0.17 (-0.14)
	[1.06,1.12)	-1.96 (-2.10)	-0.04 (-0.12)	-0.27 (-0.34)	0.02 (-0.05)	0.24 (0.16)
Jan 2020 – Dec 2020	[0.88,0.94)	3.08 (2.49)	-1.61 (-1.61)	-1.58 (-1.56)	0.26 (0.24)	1.42 (1.48)
	[0.94,0.97)	6.61 (6.45)	-0.20 (-0.23)	-1.44 (-1.46)	-0.15 (-0.15)	0.94 (0.98)
	[0.97,1.00)	6.14 (6.15)	0.07 (0.09)	-1.31 (-1.30)	-0.31 (-0.30)	0.68 (0.71)
	[1.00,1.03)	4.57 (4.60)	-0.07 (-0.03)	-1.30 (-1.28)	-0.39 (-0.38)	0.68 (0.69)
	[1.03,1.06)	2.46 (2.48)	-0.41 (-0.36)	-1.33 (-1.31)	-0.29 (-0.29)	0.79 (0.78)
	[1.06,1.12)	-0.33 (-0.37)	-0.87 (-0.87)	-1.14 (-1.15)	0.02 (-0.02)	1.07 (1.02)
Jan 2021 – Dec 2021	[0.88,0.94)	3.41 (4.20)	-0.62 (-0.70)	-1.55 (-1.57)	-0.24 (-0.07)	1.71 (1.98)
	[0.94,0.97)	5.34 (5.35)	-2.10 (-2.24)	-1.90 (-1.99)	-0.09 (-0.10)	1.70 (1.79)
	[0.97,1.00)	3.60 (3.62)	-1.04 (-1.09)	-1.29 (-1.34)	-0.07 (-0.06)	1.17 (1.25)
	[1.00,1.03)	5.28 (5.43)	-0.20 (-0.15)	-0.97 (-0.96)	-0.29 (-0.26)	0.54 (0.59)
	[1.03,1.06)	3.97 (4.08)	0.03 (0.08)	-0.87 (-0.85)	-0.50 (-0.48)	0.06 (0.09)
	[1.06,1.12)	1.64 (1.60)	0.05 (2.20e-03)	-0.64 (-0.69)	-0.53 (-0.57)	-0.21 (-0.24)
Jan 2022 – Dec 2022	[0.88,0.94)	-3.12 (-1.94)	-1.80 (-1.68)	-1.19 (-1.15)	0.02 (-8.50e-03)	1.24 (1.28)
	[0.94,0.97)	2.21 (2.14)	-4.00e-04 (-0.03)	-0.62 (-0.65)	-0.28 (-0.30)	0.46 (0.51)
	[0.97,1.00)	2.52 (2.53)	0.45 (0.47)	-0.67 (-0.66)	-0.66 (-0.64)	-0.04 (9.90e-03)
	[1.00,1.03)	1.29 (1.32)	0.36 (0.39)	-0.71 (-0.69)	-0.76 (-0.72)	-0.17 (-0.15)
	[1.03,1.06)	0.07 (0.09)	0.24 (0.28)	-0.52 (-0.53)	-0.55 (-0.53)	-0.04 (-0.03)
	[1.06,1.12)	-1.53 (-1.58)	0.35 (0.33)	-0.03 (-0.05)	0.01 (-0.02)	0.40 (0.38)

TABLE 4.1.2. MSE Attari - implied volatility percentage errors

By inspecting both tables, both formulations produced good results for any given sample period across the moneyness and time-to-maturity categories. For both formulations, we can also see that both calls and puts produced similar levels of mispricing for these same categories for all sample periods.

The results of the Student's t-test for the Heston original formulation were the following. For calls, `h = 0` indicating that the calibration of the Heston original formulation is not biased, a p-value `p = 0.24063` and a confidence interval `ci = [-0.00008, 0.00002]` with 95% confidence. For puts, `h = 1` indicating that the calibration of the Heston original formulation is biased, a p-value `p = 0.00297` and a confidence interval `ci = [0.00003, 0.00013]` with 95% confidence, overestimating on average.

The results of the Student's t-test for the Attari formulation were the following. For calls, `h = 0` indicating that the calibration of the Attari formulation is not biased, a p-value `p = 0.17776` and a confidence interval `ci = [-0.00009, 0.00002]` with 95% confidence. For puts, `h = 1` indicating that the calibration of the Attari formulation is biased, a p-value `p = 0.00550` and a confidence interval `ci = [0.00002, 0.00013]` with 95% confidence, overestimating on average.

We now present two tables, one for each formulation, with the statistical analysis for both option types.

Parameters	**Mean**	**Standard deviation**	**Minimum**	**Maximum**	**Median**
κ	2.45829 (2.39279)	1.30100 (1.26997)	0.03096 (0.03184)	10.12063 (9.71708)	2.33007 (2.25976)
θ	0.16320 (0.16744)	0.38317 (0.38772)	0.03310 (0.03400)	1.99910 (1.99899)	0.06596 (0.06717)
σ	1.10841 (1.10855)	0.37106 (0.36375)	0.53844 (0.56751)	2.00000 (2.00000)	1.00182 (1.00865)
v_0	0.04367 (0.04361)	0.05938 (0.05896)	0.00446 (0.00454)	0.68689 (0.68076)	0.02857 (0.02853)
ρ	-0.78994 (-0.79602)	0.04911 (0.04968)	-0.99900 (-0.99900)	-0.62707 (-0.64965)	-0.78342 (-0.78972)
Time	2.09387 (1.90994)	1.17363 (1.31304)	0.54046 (0.44715)	13.48915 (20.42345)	1.85651 (1.60835)
Error	-0.00003 (0.00008)	0.00090 (0.00088)	-0.00290 (-0.00344)	0.00452 (0.00478)	-0.00002 (0.00012)

TABLE 4.1.3. MSE Heston original - calls (puts) statistical analysis

Parameters	**Mean**	**Standard deviation**	**Minimum**	**Maximum**	**Median**
κ	2.38997 (2.30863)	1.31962 (1.27959)	0.03097 (0.03026)	10.12307 (9.71641)	2.23923 (2.14493)
θ	0.16795 (0.17348)	0.39238 (0.39882)	0.03087 (0.03220)	1.99969 (1.99975)	0.06698 (0.06850)
σ	1.08762 (1.08570)	0.36215 (0.35537)	0.54638 (0.55304)	2.00000 (2.00000)	0.99227 (0.99503)
v_0	0.04360 (0.04356)	0.05939 (0.05897)	0.00422 (0.00430)	0.68696 (0.68188)	0.02848 (0.02849)
ρ	-0.78947 (-0.79546)	0.04880 (0.04945)	-0.99900 (-0.99900)	-0.62518 (-0.64806)	-0.78304 (-0.78896)
Time	1.71564 (1.56805)	0.98400 (1.14292)	0.38836 (0.39163)	12.58123 (15.93984)	1.51921 (1.34847)
Error	-0.00004 (0.00007)	0.00091 (0.00089)	-0.00312 (-0.00343)	0.00455 (0.00481)	-0.00002 (0.00011)

TABLE 4.1.4. MSE Attari - calls (puts) statistical analysis

The tables above summarize the statistical analysis for both formulations covering both option types. We can see that, on average, the calibration time for puts was faster than the calibration time for calls for both formulations. The Attari formulation, on average, was faster than the Heston original formulation for both option types, which was expected.

4.2. RMSE loss function

The following tables present the percentage errors between the averaged market-implied volatilities and the averaged implied volatilities generated by the Heston original formulation and by the Attari formulation, broken down by moneyness and time-to-maturity categories. Positive values indicate overestimating, while negative values indicate underestimating.

Sample period	**S/K**	**Call (Put) options**				
		Time-to-maturity				
		21–70	**71–120**	**121–170**	**171–220**	**221–270**
Jan 2018 – May 2022	[0.88,0.94)	1.36 (1.59)	-2.13 (-2.83)	-1.32 (-1.64)	0.38 (0.87)	1.86 (2.77)
	[0.94,0.97)	3.65 (2.00)	-0.94 (-2.00)	-1.39 (-1.18)	-0.12 (0.71)	1.18 (2.21)
	[0.97,1.00)	5.27 (1.03)	-0.24 (-1.21)	-1.33 (-1.00)	-0.45 (0.30)	0.63 (1.43)
	[1.00,1.03)	3.54 (2.59)	-0.47 (-0.64)	-1.49 (-0.97)	-0.78 (-0.06)	0.24 (0.86)
	[1.03,1.06)	0.97 (1.69)	-1.01 (-0.44)	-1.68 (-0.96)	-0.95 (-0.25)	0.02 (0.51)
	[1.06,1.12)	-2.82 (-0.26)	-1.70 (-0.44)	-1.63 (-0.75)	-0.90 (-0.22)	1.40e-03 (0.30)
Jan 2018 – Dec 2018	[0.88,0.94)	-4.83 (0.09)	-3.73 (0.16)	-1.12 (2.92)	0.70 (4.16)	1.09 (4.06)
	[0.94,0.97)	0.89 (1.30)	0.37 (-0.75)	-0.11 (0.60)	-0.40 (1.65)	-0.28 (1.76)
	[0.97,1.00)	6.36 (-1.75)	1.46 (-1.36)	-0.34 (-0.54)	-0.95 (0.36)	-0.70 (0.57)
	[1.00,1.03)	4.49 (2.96)	0.64 (-0.28)	-1.16 (-0.54)	-1.43 (-0.17)	-1.00 (-0.02)
	[1.03,1.06)	-0.21 (1.74)	-0.78 (0.28)	-2.26 (-0.45)	-1.93 (-0.37)	-1.26 (-0.25)
	[1.06,1.12)	-7.61 (-1.62)	-3.23 (-0.15)	-3.63 (-0.42)	-2.33 (-0.28)	-1.36 (-0.22)
Jan 2019 – Dec 2019	[0.88,0.94)	-5.94 (-1.17)	-3.39 (-4.22)	-1.23 (-1.62)	0.76 (1.44)	2.01 (3.47)
	[0.94,0.97)	5.24 (1.76)	-0.35 (-2.37)	-0.99 (-0.51)	0.17 (1.74)	0.76 (2.93)
	[0.97,1.00)	7.20 (0.68)	0.12 (-1.30)	-1.23 (-0.64)	-0.48 (0.73)	0.04 (1.58)
	[1.00,1.03)	3.67 (2.66)	-0.34 (-0.66)	-1.50 (-0.89)	-0.94 (-0.08)	-0.38 (0.57)
	[1.03,1.06)	0.05 (1.78)	-0.99 (-0.25)	-1.72 (-0.91)	-1.15 (-0.42)	-0.40 (0.09)
	[1.06,1.12)	-5.79 (-1.16)	-1.82 (0.03)	-1.47 (-0.34)	-0.79 (-0.09)	0.09 (0.14)
Jan 2020 – Dec 2020	[0.88,0.94)	2.43 (0.22)	-1.88 (-3.60)	-1.28 (-1.93)	0.82 (0.85)	2.27 (2.64)
	[0.94,0.97)	3.88 (2.61)	-1.52 (-1.47)	-1.86 (-1.34)	-0.18 (0.55)	1.32 (1.99)
	[0.97,1.00)	3.85 (3.36)	-1.24 (-0.85)	-1.86 (-1.23)	-0.47 (0.22)	1.00 (1.47)
	[1.00,1.03)	2.77 (2.82)	-1.31 (-0.80)	-1.91 (-1.25)	-0.59 (0.01)	1.00 (1.35)
	[1.03,1.06)	1.60 (1.64)	-1.40 (-0.93)	-1.89 (-1.27)	-0.46 (-0.02)	1.07 (1.28)
	[1.06,1.12)	-0.15 (-0.17)	-1.31 (-1.01)	-1.51 (-1.16)	-0.07 (0.08)	1.33 (1.15)
Jan 2021 – Dec 2021	[0.88,0.94)	-0.27 (1.82)	-1.79 (-2.52)	-1.80 (-2.13)	-0.17 (0.26)	2.07 (2.86)
	[0.94,0.97)	4.94 (1.74)	-1.45 (-3.45)	-1.53 (-1.87)	0.14 (0.65)	2.03 (2.83)
	[0.97,1.00)	7.09 (-0.31)	-0.28 (-1.93)	-1.16 (-1.14)	-0.07 (0.61)	1.34 (2.11)
	[1.00,1.03)	5.00 (2.78)	-0.45 (-0.88)	-1.35 (-0.88)	-0.64 (0.20)	0.47 (1.22)
	[1.03,1.06)	1.62 (2.15)	-1.23 (-0.58)	-1.76 (-0.88)	-1.22 (-0.20)	-0.25 (0.52)
	[1.06,1.12)	-3.13 (0.37)	-2.29 (-0.56)	-2.17 (-0.81)	-1.77 (-0.50)	-0.88 (-0.06)
Jan 2022 – Dec 2022	[0.88,0.94)	-1.53 (-2.83)	-0.76 (-2.88)	-0.68 (-1.52)	0.20 (0.41)	1.24 (2.12)
	[0.94,0.97)	1.84 (0.06)	-0.47 (-1.07)	-1.02 (-0.80)	-0.64 (0.02)	0.18 (1.11)
	[0.97,1.00)	2.04 (1.40)	-0.05 (-0.27)	-1.06 (-0.80)	-0.97 (-0.49)	-0.26 (0.39)
	[1.00,1.03)	1.27 (1.17)	0.10 (-0.07)	-0.95 (-0.85)	-0.92 (-0.70)	-0.27 (0.04)
	[1.03,1.06)	0.48 (0.64)	0.25 (0.05)	-0.57 (-0.68)	-0.55 (-0.60)	-9.00e-03 (6.30e-03)
	[1.06,1.12)	-0.77 (-0.42)	0.69 (0.42)	0.18 (-0.16)	0.25 (-0.17)	0.64 (0.25)

Table 4.2.1. RMSE Heston original - implied volatility percentage errors

Sample period	S/K	Call (Put) options				
		Time-to-maturity				
		21–70	**71–120**	**121–170**	**171–220**	**221–270**
Jan 2018 – May 2022	[0.88,0.94)	3.26 (1.81)	-1.31 (-2.93)	-1.03 (-1.71)	0.56 (0.80)	1.96 (2.70)
	[0.94,0.97)	3.78 (1.99)	-1.33 (-2.10)	-1.37 (-1.22)	0.03 (0.69)	1.25 (2.20)
	[0.97,1.00)	2.72 (0.83)	-0.83 (-1.18)	-1.33 (-0.98)	-0.37 (0.32)	0.58 (1.45)
	[1.00,1.03)	3.58 (2.41)	-0.43 (-0.63)	-1.31 (-0.96)	-0.67 (-0.05)	0.14 (0.87)
	[1.03,1.06)	2.45 (1.41)	-0.28 (-0.49)	-1.25 (-0.98)	-0.76 (-0.25)	-0.08 (0.51)
	[1.06,1.12)	0.29 (-0.53)	-0.20 (-0.56)	-0.85 (-0.81)	-0.53 (-0.24)	-0.05 (0.29)
Jan 2018 – Dec 2018	[0.88,0.94)	-0.17 (0.82)	-1.13 (-0.25)	0.40 (2.17)	1.21 (3.60)	1.45 (3.81)
	[0.94,0.97)	2.19 (1.02)	-0.37 (-1.20)	-0.43 (0.28)	-0.29 (1.55)	-0.25 (1.76)
	[0.97,1.00)	1.11 (-2.97)	-0.15 (-1.51)	-0.73 (-0.49)	-0.93 (0.43)	-0.87 (0.65)
	[1.00,1.03)	5.15 (2.21)	0.82 (-0.36)	-0.57 (-0.47)	-1.17 (-0.11)	-1.13 (0.02)
	[1.03,1.06)	3.50 (1.05)	1.22 (0.19)	-0.46 (-0.43)	-1.21 (-0.35)	-1.18 (-0.27)
	[1.06,1.12)	-0.44 (-1.70)	0.64 (-0.27)	-0.34 (-0.46)	-0.87 (-0.32)	-0.90 (-0.30)
Jan 2019 – Dec 2019	[0.88,0.94)	-0.25 (-1.31)	-1.96 (-4.84)	-0.67 (-2.05)	1.17 (1.14)	2.34 (3.30)
	[0.94,0.97)	4.60 (1.42)	-1.30 (-2.62)	-1.08 (-0.57)	0.41 (1.73)	1.11 (2.96)
	[0.97,1.00)	2.93 (0.15)	-1.05 (-1.21)	-1.37 (-0.54)	-0.45 (0.83)	0.11 (1.64)
	[1.00,1.03)	4.12 (2.28)	-0.37 (-0.62)	-1.29 (-0.81)	-0.86 (-0.01)	-0.48 (0.60)
	[1.03,1.06)	3.04 (1.30)	0.28 (-0.33)	-0.96 (-0.92)	-0.83 (-0.40)	-0.55 (0.08)
	[1.06,1.12)	0.12 (-1.61)	0.85 (-0.18)	0.09 (-0.44)	0.01 (-0.16)	0.02 (0.06)
Jan 2020 – Dec 2020	[0.88,0.94)	2.52 (0.42)	-1.74 (-3.55)	-1.21 (-1.88)	0.84 (0.87)	2.29 (2.62)
	[0.94,0.97)	3.90 (2.68)	-1.55 (-1.45)	-1.83 (-1.35)	-0.14 (0.53)	1.38 (1.97)
	[0.97,1.00)	3.56 (3.43)	-1.31 (-0.82)	-1.85 (-1.23)	-0.45 (0.21)	1.02 (1.46)
	[1.00,1.03)	2.86 (2.81)	-1.28 (-0.79)	-1.87 (-1.25)	-0.59 (1.90e-03)	0.98 (1.35)
	[1.03,1.06)	1.87 (1.54)	-1.26 (-0.94)	-1.81 (-1.29)	-0.46 (-0.03)	1.04 (1.28)
	[1.06,1.12)	0.31 (-0.37)	-1.06 (-1.08)	-1.37 (-1.19)	-0.06 (0.08)	1.31 (1.15)
Jan 2021 – Dec 2021	[0.88,0.94)	2.70 (1.61)	-1.09 (-2.68)	-1.54 (-2.18)	0.07 (0.18)	2.15 (2.81)
	[0.94,0.97)	4.18 (1.57)	-2.02 (-3.54)	-1.43 (-1.89)	0.41 (0.63)	2.08 (2.83)
	[0.97,1.00)	2.88 (-0.27)	-0.93 (-1.87)	-1.04 (-1.12)	0.12 (0.63)	1.23 (2.14)
	[1.00,1.03)	4.49 (2.75)	-0.42 (-0.85)	-1.08 (-0.87)	-0.46 (0.22)	0.27 (1.25)
	[1.03,1.06)	3.25 (1.93)	-0.44 (-0.63)	-1.26 (-0.91)	-0.96 (-0.20)	-0.48 (0.54)
	[1.06,1.12)	0.90 (-0.07)	-0.61 (-0.72)	-1.31 (-0.90)	-1.32 (-0.53)	-1.08 (-0.07)
Jan 2022 – Dec 2022	[0.88,0.94)	-1.47 (-2.75)	-0.68 (-2.71)	-0.62 (-1.44)	0.24 (0.41)	1.25 (2.09)
	[0.94,0.97)	1.99 (0.33)	-0.34 (-0.94)	-0.93 (-0.77)	-0.58 (-3.60e-03)	0.20 (1.08)
	[0.97,1.00)	2.01 (1.58)	0.03 (-0.19)	-1.00 (-0.79)	-0.93 (-0.50)	-0.25 (0.37)
	[1.00,1.03)	1.16 (1.17)	0.13 (-0.05)	-0.91 (-0.86)	-0.90 (-0.71)	-0.28 (0.04)
	[1.03,1.06)	0.32 (0.51)	0.23 (0.02)	-0.55 (-0.70)	-0.56 (-0.61)	-0.03 (0.01)
	[1.06,1.12)	-0.95 (-0.67)	0.62 (0.34)	0.17 (-0.20)	0.22 (-0.17)	0.60 (0.27)

TABLE 4.2.2. RMSE Attari - implied volatility percentage errors

By inspecting both tables, both formulations produced good results for any given sample period across the moneyness and time-to-maturity categories. For both formulations, we can also see that both calls and puts produced similar levels of mispricing for these same categories for all sample periods.

The results of the Student's t-test for the Heston original formulation were the following. For calls, `h = 1` indicating that the calibration of the Heston original formulation is biased, a p-value `p = 0.00000` and a confidence interval `ci = [-0.00117, -0.00101]` with 95% confidence, underestimating on average. For puts, `h = 1` indicating that the calibration of the Heston original formulation is biased, a p-value `p = 0.00000` and a confidence interval `ci = [-0.00029, -0.00019]` with 95% confidence, underestimating on average.

The results of the Student's t-test for the Attari formulation were the following. For calls, `h = 1` indicating that the calibration of the Attari formulation is biased, a p-value `p = 0.00012` and a confidence interval `ci = [0.00004, 0.00014]` with 95% confidence, overestimating on average. For puts, `h = 1` indicating that the calibration of the Attari formulation is biased, a p-value `p = 0.00000` and a confidence interval `ci = [-0.00047, -0.00037]` with 95% confidence, underestimating on average.

We now present two tables, one for each formulation, with the statistical analysis for both option types.

Parameters	**Mean**	**Standard deviation**	**Minimum**	**Maximum**	**Median**
κ	1.57749 (3.21187)	1.42149 (1.62776)	0.01164 (0.02937)	9.29185 (12.01620)	1.48371 (3.03987)
θ	0.50732 (0.12076)	0.74238 (0.27629)	0.03042 (0.03228)	1.99730 (1.99904)	0.10946 (0.06533)
σ	0.95630 (1.23015)	0.42595 (0.36417)	0.23837 (0.54566)	2.00000 (2.00000)	0.90183 (1.15124)
v_0	0.04324 (0.04285)	0.05667 (0.06094)	0.00615 (0.00383)	0.65455 (0.68535)	0.02753 (0.02696)
ρ	-0.78374 (-0.79038)	0.04542 (0.06033)	-0.99271 (-0.99900)	-0.60237 (-0.58335)	-0.78279 (-0.78528)
Time	5.51197 (2.49458)	3.75331 (1.63449)	0.84195 (0.44569)	25.64791 (15.07684)	4.47463 (2.06734)
Error	-0.00109 (-0.00024)	0.00137 (0.00089)	-0.00818 (-0.00401)	0.00163 (0.00280)	-0.00060 (-0.00017)

TABLE 4.2.3. RMSE Heston original - calls (puts) statistical analysis

Parameters	**Mean**	**Standard deviation**	**Minimum**	**Maximum**	**Median**
κ	3.00516 (3.21560)	1.70335 (1.66154)	0.03283 (0.03247)	11.37919 (11.94851)	2.68553 (2.98542)
θ	0.13160 (0.12223)	0.30926 (0.28322)	0.02356 (0.03099)	1.99945 (1.99929)	0.06157 (0.06321)
σ	1.20313 (1.21135)	0.36049 (0.35354)	0.59174 (0.57236)	2.00000 (2.00000)	1.17175 (1.14436)
v_0	0.04323 (0.04253)	0.05663 (0.06106)	0.00528 (0.00269)	0.65479 (0.68615)	0.02817 (0.02684)
ρ	-0.77388 (-0.79444)	0.04702 (0.05893)	-0.99434 (-0.99900)	-0.60155 (-0.60041)	-0.76873 (-0.79000)
Time	2.46497 (1.58608)	1.46599 (1.20143)	0.60629 (0.37690)	16.34896 (15.84824)	2.08486 (1.30159)
Error	0.00009 (-0.00042)	0.00077 (0.00082)	-0.00253 (-0.00389)	0.00286 (0.00224)	-0.00002 (-0.00035)

TABLE 4.2.4. RMSE Attari - calls (puts) statistical analysis

The tables above summarize the statistical analysis for both formulations covering both option types. We can see that, on average, the calibration time for puts was faster than the calibration time for calls for both formulations. The Attari formulation, on average, was faster than the Heston original formulation for both option types, which was expected.

4.3. IVRMSE loss function

The following tables present the percentage errors between the averaged market-implied volatilities and the averaged implied volatilities generated by the Heston original formulation and by the Attari formulation, broken down by moneyness and time-to-maturity categories. Positive values indicate overestimating, while negative values indicate underestimating.

Sample period	S/K	Call (Put) options				
		Time-to-maturity				
		21–70	71–120	121–170	171–220	221–270
Jan 2018 – May 2022	[0.88,0.94)	1.15 (1.17)	-2.01 (-1.47)	-1.19 (-0.52)	0.61 (1.58)	2.24 (3.29)
	[0.94,0.97)	4.48 (3.47)	0.03 (-0.71)	-0.52 (-0.63)	0.61 (0.96)	1.81 (2.46)
	[0.97,1.00)	7.68 (4.60)	1.06 (-0.05)	-0.35 (-0.73)	0.31 (0.37)	1.23 (1.58)
	[1.00,1.03)	5.62 (4.03)	0.74 (-0.09)	-0.59 (-0.95)	-0.05 (-0.11)	0.79 (0.96)
	[1.03,1.06)	2.78 (2.08)	0.05 (-0.43)	-0.85 (-1.13)	-0.28 (-0.38)	0.52 (0.57)
	[1.06,1.12)	-1.46 (-1.22)	-0.73 (-0.93)	-0.91 (-1.13)	-0.30 (-0.47)	0.38 (0.29)
Jan 2018 – Dec 2018	[0.88,0.94)	-3.92 (-2.46)	-2.80 (0.21)	-1.36 (2.89)	0.10 (3.43)	0.54 (2.68)
	[0.94,0.97)	3.51 (3.34)	2.78 (1.81)	2.21 (2.19)	0.69 (1.76)	0.23 (1.32)
	[0.97,1.00)	12.09 (6.05)	4.47 (1.89)	2.41 (0.91)	0.28 (0.35)	-0.36 (0.16)
	[1.00,1.03)	10.00 (6.44)	3.56 (1.52)	1.63 (0.22)	-0.18 (-0.46)	-0.84 (-0.52)
	[1.03,1.06)	5.15 (3.24)	1.98 (0.81)	0.49 (-0.42)	-0.69 (-0.90)	-1.28 (-0.80)
	[1.06,1.12)	-3.21 (-3.17)	-0.52 (-1.00)	-0.86 (-1.36)	-1.10 (-1.33)	-1.48 (-1.03)
Jan 2019 – Dec 2019	[0.88,0.94)	-4.93 (-2.31)	-3.49 (-0.27)	-1.48 (1.05)	0.10 (3.10)	1.91 (4.81)
	[0.94,0.97)	8.26 (5.60)	2.45 (0.53)	1.27 (0.49)	1.86 (2.00)	1.66 (3.02)
	[0.97,1.00)	12.49 (5.89)	3.13 (0.52)	1.02 (-0.32)	1.11 (0.56)	0.74 (1.39)
	[1.00,1.03)	8.17 (4.63)	2.32 (0.21)	0.36 (-0.87)	0.34 (-0.30)	-0.03 (0.46)
	[1.03,1.06)	3.97 (2.28)	1.29 (-0.13)	-0.11 (-1.12)	-0.11 (-0.68)	-0.25 (-0.10)
	[1.06,1.12)	-2.09 (-2.14)	0.29 (-0.54)	-0.10 (-0.86)	9.00e-04 (-0.45)	-0.13 (-0.08)
Jan 2020 – Dec 2020	[0.88,0.94)	1.37 (0.53)	-2.07 (-2.12)	-0.82 (-0.72)	1.82 (1.87)	3.45 (3.83)
	[0.94,0.97)	3.24 (2.79)	-1.63 (-1.80)	-1.39 (-1.41)	0.52 (0.60)	2.28 (2.62)
	[0.97,1.00)	3.83 (3.45)	-1.26 (-1.34)	-1.46 (-1.48)	0.06 (0.13)	1.77 (2.03)
	[1.00,1.03)	2.79 (2.73)	-1.28 (-1.28)	-1.55 (-1.55)	-0.14 (-0.09)	1.66 (1.80)
	[1.03,1.06)	1.52 (1.62)	-1.38 (-1.28)	-1.56 (-1.54)	-0.07 (-0.05)	1.65 (1.76)
	[1.06,1.12)	-0.27 (-0.11)	-1.27 (-1.14)	-1.27 (-1.24)	0.27 (0.24)	1.69 (1.74)
Jan 2021 – Dec 2021	[0.88,0.94)	-1.02 (-0.40)	-2.37 (-2.29)	-2.05 (-1.65)	-0.48 (0.74)	1.86 (3.16)
	[0.94,0.97)	6.15 (4.24)	-0.30 (-1.32)	-0.83 (-0.87)	0.75 (1.28)	2.46 (3.23)
	[0.97,1.00)	10.46 (5.95)	1.46 (0.19)	-0.12 (-0.40)	0.86 (1.04)	2.04 (2.42)
	[1.00,1.03)	7.31 (5.24)	1.12 (0.27)	-0.29 (-0.56)	0.38 (0.40)	1.32 (1.43)
	[1.03,1.06)	3.22 (2.48)	0.08 (-0.41)	-0.74 (-0.98)	-0.17 (-0.26)	0.68 (0.58)
	[1.06,1.12)	-2.22 (-1.73)	-1.29 (-1.44)	-1.25 (-1.47)	-0.75 (-0.95)	0.08 (-0.24)
Jan 2022 – Dec 2022	[0.88,0.94)	-1.15 (-0.77)	-0.83 (-1.17)	-0.39 (-0.48)	0.89 (0.94)	2.21 (2.35)
	[0.94,0.97)	1.18 (1.24)	-0.89 (-0.77)	-1.01 (-0.76)	-0.36 (-0.15)	0.71 (0.96)
	[0.97,1.00)	1.74 (1.91)	-0.51 (-0.34)	-1.21 (-0.97)	-0.92 (-0.74)	0.01 (0.20)
	[1.00,1.03)	1.35 (1.43)	-0.33 (-0.20)	-1.20 (-1.04)	-1.05 (-0.92)	-0.20 (-0.11)
	[1.03,1.06)	0.87 (0.82)	-0.10 (-0.06)	-0.88 (-0.84)	-0.79 (-0.74)	-0.09 (-0.07)
	[1.06,1.12)	-0.07 (-0.25)	0.48 (0.38)	-0.16 (-0.24)	-0.09 (-0.17)	0.40 (0.29)

TABLE 4.3.1. IVRMSE Heston original - implied volatility percentage errors

Sample period	S/K	Call (Put) options				
		Time-to-maturity				
		21–70	**71–120**	**121–170**	**171–220**	**221–270**
Jan 2018 – May 2022	[0.88,0.94)	2.50 (2.07)	-1.49 (-2.41)	-0.60 (-1.12)	1.50 (1.31)	3.18 (3.23)
	[0.94,0.97)	2.60 (1.78)	-1.62 (-1.82)	-1.14 (-0.91)	0.62 (0.96)	2.11 (2.57)
	[0.97,1.00)	2.21 (1.96)	-1.20 (-0.80)	-1.23 (-0.78)	0.08 (0.49)	1.30 (1.70)
	[1.00,1.03)	2.86 (2.92)	-0.86 (-0.47)	-1.29 (-0.91)	-0.30 (-6.90e-03)	0.78 (1.03)
	[1.03,1.06)	1.63 (1.60)	-0.76 (-0.58)	-1.28 (-1.08)	-0.45 (-0.32)	0.49 (0.57)
	[1.06,1.12)	-0.74 (-0.84)	-0.76 (-0.84)	-0.97 (-1.01)	-0.30 (-0.42)	0.43 (0.24)
Jan 2018 – Dec 2018	[0.88,0.94)	0.19 (-0.09)	0.06 (-0.74)	2.19 (0.94)	3.54 (2.60)	3.50 (2.81)
	[0.94,0.97)	1.42 (1.04)	-0.22 (-0.70)	0.17 (0.26)	0.68 (1.15)	0.55 (1.10)
	[0.97,1.00)	0.26 (-0.19)	-0.80 (-0.33)	-0.79 (-0.18)	-0.50 (0.13)	-0.46 (0.13)
	[1.00,1.03)	4.04 (3.92)	-0.02 (0.38)	-0.87 (-0.29)	-0.93 (-0.52)	-0.90 (-0.45)
	[1.03,1.06)	2.40 (2.17)	0.36 (0.42)	-0.85 (-0.49)	-1.07 (-0.88)	-1.05 (-0.80)
	[1.06,1.12)	-1.53 (-1.79)	-0.17 (-0.56)	-0.81 (-0.86)	-0.85 (-1.08)	-0.84 (-0.94)
Jan 2019 – Dec 2019	[0.88,0.94)	-1.33 (-1.80)	-2.10 (-3.20)	-0.03 (-0.68)	2.24 (2.13)	3.86 (3.87)
	[0.94,0.97)	4.06 (2.18)	-1.03 (-1.79)	-0.53 (-0.24)	1.18 (1.86)	2.13 (2.92)
	[0.97,1.00)	3.33 (1.64)	-1.05 (-0.78)	-1.17 (-0.52)	0.04 (0.74)	0.87 (1.49)
	[1.00,1.03)	3.35 (2.95)	-0.76 (-0.46)	-1.39 (-0.91)	-0.61 (-0.16)	0.09 (0.41)
	[1.03,1.06)	1.71 (1.66)	-0.48 (-0.33)	-1.31 (-1.05)	-0.78 (-0.56)	-0.13 (-0.11)
	[1.06,1.12)	-2.00 (-1.66)	-0.26 (-0.34)	-0.57 (-0.65)	-0.20 (-0.35)	0.29 (-0.16)
Jan 2020 – Dec 2020	[0.88,0.94)	1.75 (0.86)	-2.13 (-2.30)	-0.74 (-0.82)	1.96 (1.88)	3.64 (3.77)
	[0.94,0.97)	2.61 (2.27)	-1.98 (-2.07)	-1.50 (-1.50)	0.62 (0.66)	2.43 (2.56)
	[0.97,1.00)	2.70 (2.63)	-1.67 (-1.59)	-1.63 (-1.56)	0.12 (0.17)	1.84 (1.93)
	[1.00,1.03)	2.19 (2.28)	-1.57 (-1.45)	-1.67 (-1.59)	-0.11 (-0.07)	1.71 (1.74)
	[1.03,1.06)	1.28 (1.32)	-1.54 (-1.45)	-1.64 (-1.59)	-0.05 (-0.04)	1.67 (1.65)
	[1.06,1.12)	-0.17 (-0.24)	-1.31 (-1.29)	-1.28 (-1.29)	0.28 (0.22)	1.71 (1.60)
Jan 2021 – Dec 2021	[0.88,0.94)	1.07 (-0.02)	-1.78 (-4.05)	-1.51 (-2.41)	0.55 (0.33)	3.05 (3.29)
	[0.94,0.97)	2.72 (1.05)	-2.51 (-2.56)	-1.42 (-0.94)	0.87 (1.38)	2.92 (3.60)
	[0.97,1.00)	2.49 (2.70)	-1.25 (-0.41)	-0.95 (-0.18)	0.65 (1.28)	2.14 (2.74)
	[1.00,1.03)	3.65 (3.99)	-0.75 (0.02)	-0.94 (-0.30)	0.12 (0.60)	1.23 (1.65)
	[1.03,1.06)	2.05 (2.06)	-0.86 (-0.46)	-1.13 (-0.76)	-0.37 (-0.14)	0.51 (0.66)
	[1.06,1.12)	-0.90 (-1.28)	-1.20 (-1.22)	-1.21 (-1.22)	-0.74 (-0.87)	-0.06 (-0.25)
Jan 2022 – Dec 2022	[0.88,0.94)	-1.39 (-1.22)	-0.85 (-1.65)	-0.35 (-0.83)	0.97 (0.81)	2.29 (2.32)
	[0.94,0.97)	1.04 (0.68)	-0.90 (-0.82)	-0.97 (-0.74)	-0.28 (-0.05)	0.77 (1.04)
	[0.97,1.00)	1.41 (1.63)	-0.58 (-0.28)	-1.21 (-0.89)	-0.87 (-0.64)	0.05 (0.27)
	[1.00,1.03)	1.09 (1.23)	-0.40 (-0.16)	-1.22 (-0.98)	-1.02 (-0.86)	-0.18 (-0.07)
	[1.03,1.06)	0.66 (0.62)	-0.17 (-0.08)	-0.90 (-0.82)	-0.79 (-0.73)	-0.09 (-0.08)
	[1.06,1.12)	-0.22 (-0.49)	0.41 (0.29)	-0.19 (-0.29)	-0.12 (-0.24)	0.38 (0.22)

TABLE 4.3.2. IVRMSE Attari - implied volatility percentage errors

By inspecting both tables, both formulations produced good results for any given sample period across the moneyness and time-to-maturity categories. For both formulations, we can also see that both calls and puts produced similar levels of mispricing for these same categories for all sample periods.

The results of the Student's t-test for the Heston original formulation were the following. For calls, `h = 1` indicating that the calibration of the Heston original formulation is biased, a p-value `p = 0.00000` and a confidence interval `ci = [0.00040, 0.00088]` with 95% confidence, overestimating on average. For puts, `h = 1` indicating that the calibration of the Heston original formulation is biased, a p-value `p = 0.00222` and a confidence interval `ci = [0.00014, 0.00062]` with 95% confidence, overestimating on average.

The results of the Student's t-test for the Attari formulation were the following. For calls, `h = 1` indicating that the calibration of the Attari formulation is biased, a p-value `p = 0.03093` and a confidence interval `ci = [-0.00011, -0.00001]` with 95% confidence, underestimating on average. For puts, `h = 1` indicating that the calibration of the Attari formulation is biased, a p-value `p = 0.00029` and a confidence interval `ci = [-0.00032, -0.00010]` with 95% confidence, underestimating on average.

We now present two tables, one for each formulation, with the statistical analysis for both option types.

Parameters	**Mean**	**Standard deviation**	**Minimum**	**Maximum**	**Median**
κ	2.00106 (2.49319)	1.73706 (2.06152)	0.02973 (0.02206)	12.19936 (19.93529)	1.79206 (2.13108)
θ	0.19490 (0.15681)	0.24532 (0.20770)	0.01216 (0.01159)	1.60093 (1.37623)	0.10173 (0.08721)
σ	0.98791 (1.09160)	0.42219 (0.40530)	0.24616 (0.27357)	1.99907 (1.99909)	0.93994 (1.03919)
v_0	0.04528 (0.04413)	0.05901 (0.05919)	0.00666 (0.00125)	0.66134 (0.65771)	0.02887 (0.02795)
ρ	-0.80033 (-0.78405)	0.06903 (0.07045)	-0.99872 (-0.99865)	-0.55512 (-0.18213)	-0.79766 (-0.78664)
Time	3.26435 (3.02271)	4.23749 (3.39718)	0.41126 (0.40933)	32.07864 (32.37330)	1.80740 (1.84586)
Error	0.00064 (0.00038)	0.00411 (0.00410)	-0.00169 (-0.00801)	0.06959 (0.06859)	-0.00005 (-0.00007)

Table 4.3.3. IVRMSE Heston original - calls (puts) statistical analysis

Parameters	**Mean**	**Standard deviation**	**Minimum**	**Maximum**	**Median**
κ	2.74267 (3.11920)	1.57015 (1.89934)	0.04470 (0.03360)	12.10968 (14.59549)	2.51828 (2.80533)
θ	0.10424 (0.10590)	0.11879 (0.14068)	0.02705 (0.02560)	1.03693 (1.33942)	0.07462 (0.06847)
σ	1.16579 (1.16557)	0.34822 (0.35658)	0.46782 (0.30772)	1.99995 (1.99994)	1.13682 (1.12110)
v_0	0.04337 (0.04294)	0.05975 (0.05964)	0.00463 (0.00338)	0.66200 (0.65835)	0.02723 (0.02733)
ρ	-0.76960 (-0.79501)	0.05127 (0.06256)	-0.99898 (-0.99897)	-0.57820 (-0.60215)	-0.76697 (-0.79041)
Time	1.63267 (1.88322)	1.71057 (2.13418)	0.31370 (0.32361)	18.19945 (21.56241)	1.26871 (1.38016)
Error	-0.00006 (-0.00021)	0.00091 (0.00192)	-0.00156 (-0.00752)	0.01453 (0.05970)	-0.00013 (-0.00021)

Table 4.3.4. IVRMSE Attari - calls (puts) statistical analysis

The tables above summarize the statistical analysis for both formulations covering both option types. We can see that, on average, the calibration time for puts was faster than the calibration time for calls for the Heston original formulation and the other way around for the Attari formulation. The Attari formulation, on average, was faster than the Heston original formulation for both option types, which was expected.

CHAPTER 5

Conclusions

The objective of this thesis was to calibrate the S&P 500 index options under alternative formulations of the Heston (1993) model. The five formulations used were: Heston original, Heston single integrand, Attari, FFT, and FRFT. To conduct this study, we estimated five parameters for each Heston model formulation using three different loss functions: the MSE, RMSE, and IVRMSE. For each combination of Heston model formulation and loss function, we performed two calibrations, one for calls and one for puts, resulting in a total of 30 calibrations: 15 for calls and 15 for puts.

We found that, in terms of accuracy, Heston original, Heston single integrand, and Attari were the formulations that generally produced the best results across the three loss functions. However, we did not conduct any formal statistical tests to definitively conclude which formulation had the best performance. Future work could incorporate statistical comparisons to draw more definitive conclusions regarding the relative performance of the models. The only thing we can actually conclude is what formulation provided the best balance between computational speed and accuracy for the loss functions. The results between these three formulations were comparable for every loss function, with the Attari formulation being the fastest. Consequently, the Attari formulation prevails when using this criterion.

On average, when considering the call options, out of the 15 different calibrations, 9 underestimated (60%), 3 overestimated (20%) and 3 were non biased (20%). On average, when considering the put options, out of the 15 different calibrations, 10 underestimated (66.67%), 5 overestimated (33.33%) and 0 were non biased. The 3 non biased are all under the MSE loss function for the formulations, Heston original, Heston single integrand and Attari. Therefore, we can conclude that, in general, our calibrations underestimated on average.

The other two model formulations, FFT and FRFT, overall presented worse results. As explained earlier, this can be attributed to their sensitivity to the choice of parameters such as α, N, $\phi_{\max}$, η, and λ. Exploring more effective strategies for parameter optimization could significantly improve the performance of the FFT and FRFT formulations, as better-tuned parameters would likely result in more accurate and reliable outcomes. Nevertheless, in terms of computational speed, from fastest to slowest, we have: FRFT, FFT, Attari, Heston single integrand, and Heston original, with the last two being practically tied. This verifies what was theoretically presented earlier, except for the tied formulations, where in practice, the Heston single integrand was expected to be faster.

Appendix A. Additional results

Here is presented the results for the remaining formulations: the Heston single integrand, FFT and FRFT. We present the tables containing the percentage errors between the averaged market implied volatilities and the averaged implied volatilities generated by each model formulation. Just like before, we have a section for each loss function. We also present the tables with the statistical analysis and the results of the Student's t-test.

A.1. MSE loss function

The following tables present the percentage errors between the averaged market-implied volatilities and the averaged implied volatilities generated by the Heston single integrand formulation, the FFT formulation and the FRFT formulation, broken down by moneyness and time-to-maturity categories. Positive values indicate overestimating, while negative values indicate underestimating.

Sample period	S/K	Call (Put) options				
		Time-to-maturity				
		21–70	71–120	121–170	171–220	221–270
Jan 2018 – May 2022	[0.88,0.94)	3.23 (3.26)	-2.01 (-1.70)	-1.66 (-1.50)	0.07 (0.18)	1.52 (1.63)
	[0.94,0.97)	4.37 (4.35)	-1.20 (-1.29)	-1.40 (-1.46)	-0.04 (-0.04)	1.15 (1.23)
	[0.97,1.00)	3.45 (3.39)	-0.48 (-0.50)	-1.13 (-1.14)	-0.23 (-0.20)	0.67 (0.73)
	[1.00,1.03)	4.03 (4.09)	-0.04 (8.00e-04)	-1.00 (-0.98)	-0.40 (-0.37)	0.33 (0.37)
	[1.03,1.06)	2.41 (2.47)	0.01 (0.06)	-0.92 (-0.90)	-0.42 (-0.40)	0.19 (0.21)
	[1.06,1.12)	-0.19 (-0.25)	-0.17 (-0.20)	-0.59 (-0.63)	-0.16 (-0.20)	0.30 (0.26)
Jan 2018 – Dec 2018	[0.88,0.94)	-0.84 (-0.32)	-3.26 (-1.84)	-0.93 (0.32)	1.00 (1.51)	1.71 (1.88)
	[0.94,0.97)	-0.13 (0.37)	-1.67 (-1.68)	-0.82 (-0.83)	0.28 (0.33)	0.59 (0.68)
	[0.97,1.00)	-0.52 (-0.67)	-0.78 (-0.88)	-0.66 (-0.73)	-0.11 (-0.08)	0.10 (0.16)
	[1.00,1.03)	3.53 (3.62)	0.27 (0.29)	-0.39 (-0.37)	-0.28 (-0.23)	-0.13 (-0.08)
	[1.03,1.06)	1.40 (1.51)	0.53 (0.57)	-0.34 (-0.31)	-0.35 (-0.31)	-0.21 (-0.17)
	[1.06,1.12)	-2.82 (-2.91)	-0.34 (-0.38)	-0.39 (-0.45)	-0.11 (-0.18)	-2.20e-03 (-0.06)
Jan 2019 – Dec 2019	[0.88,0.94)	-2.04 (-1.80)	-4.41 (-3.44)	-2.28 (-1.72)	0.23 (0.58)	1.79 (1.97)
	[0.94,0.97)	3.58 (3.41)	-1.64 (-1.90)	-1.03 (-1.09)	0.67 (0.72)	1.44 (1.57)
	[0.97,1.00)	3.33 (3.07)	-0.66 (-0.69)	-0.96 (-0.91)	0.05 (0.14)	0.60 (0.70)
	[1.00,1.03)	3.86 (3.86)	-0.18 (-0.12)	-0.98 (-0.91)	-0.40 (-0.33)	0.02 (0.08)
	[1.03,1.06)	2.12 (2.19)	0.08 (0.13)	-0.86 (-0.81)	-0.50 (-0.46)	-0.14 (-0.11)
	[1.06,1.12)	-1.55 (-1.65)	0.18 (0.11)	-0.14 (-0.20)	0.12 (0.04)	0.30 (0.22)
Jan 2020 – Dec 2020	[0.88,0.94)	3.01 (2.32)	-1.70 (-1.71)	-1.65 (-1.63)	0.23 (0.21)	1.39 (1.46)
	[0.94,0.97)	6.49 (6.33)	-0.26 (-0.29)	-1.47 (-1.49)	-0.14 (-0.14)	0.94 (0.99)
	[0.97,1.00)	6.03 (6.04)	0.03 (0.05)	-1.32 (-1.31)	-0.29 (-0.29)	0.69 (0.71)
	[1.00,1.03)	4.57 (4.60)	-0.07 (-0.04)	-1.30 (-1.27)	-0.38 (-0.37)	0.68 (0.70)
	[1.03,1.06)	2.52 (2.54)	-0.39 (-0.35)	-1.31 (-1.29)	-0.28 (-0.28)	0.80 (0.79)
	[1.06,1.12)	-0.20 (-0.25)	-0.82 (-0.82)	-1.11 (-1.12)	0.02 (-0.01)	1.08 (1.03)
Jan 2021 – Dec 2021	[0.88,0.94)	3.54 (4.24)	-0.70 (-0.84)	-1.65 (-1.69)	-0.32 (-0.15)	1.65 (1.92)
	[0.94,0.97)	5.08 (5.06)	-2.30 (-2.46)	-1.98 (-2.08)	-0.12 (-0.14)	1.68 (1.77)
	[0.97,1.00)	3.15 (3.13)	-1.19 (-1.24)	-1.34 (-1.38)	-0.08 (-0.07)	1.16 (1.24)
	[1.00,1.03)	5.14 (5.29)	-0.25 (-0.20)	-0.97 (-0.96)	-0.28 (-0.25)	0.54 (0.59)
	[1.03,1.06)	4.05 (4.16)	0.07 (0.12)	-0.83 (-0.81)	-0.47 (-0.45)	0.07 (0.10)
	[1.06,1.12)	1.95 (1.92)	0.18 (0.14)	-0.55 (-0.60)	-0.47 (-0.52)	-0.18 (-0.22)
Jan 2022 – Dec 2022	[0.88,0.94)	-3.31 (-2.17)	-1.97 (-1.87)	-1.30 (-1.27)	-0.03 (-0.05)	1.23 (1.27)
	[0.94,0.97)	1.99 (1.92)	-0.12 (-0.16)	-0.66 (-0.69)	-0.28 (-0.30)	0.47 (0.53)
	[0.97,1.00)	2.39 (2.40)	0.38 (0.41)	-0.69 (-0.67)	-0.66 (-0.64)	-0.03 (0.02)
	[1.00,1.03)	1.30 (1.33)	0.34 (0.38)	-0.71 (-0.69)	-0.75 (-0.72)	-0.16 (-0.15)
	[1.03,1.06)	0.17 (0.19)	0.26 (0.30)	-0.50 (-0.51)	-0.54 (-0.52)	-0.04 (-0.03)
	[1.06,1.12)	-1.36 (-1.40)	0.43 (0.41)	0.02 (-8.50e-03)	0.03 (-5.70e-03)	0.40 (0.37)

Table A.1.1. MSE Heston single integrand - implied volatility percentage errors

Sample period	S/K	Call (Put) options				
		Time-to-maturity				
		21–70	**71–120**	**121–170**	**171–220**	**221–270**
Jan 2018 – May 2022	[0.88,0.94)	6.14 (4.39)	-5.77 (-6.24)	-6.03 (-6.04)	-4.29 (-4.53)	-3.64 (-4.43)
	[0.94,0.97)	4.67 (3.15)	-3.08 (-4.72)	-4.71 (-5.77)	-4.09 (-5.11)	-3.98 (-5.49)
	[0.97,1.00)	-0.29 (-1.82)	-5.80 (-7.07)	-8.12 (-8.99)	-8.38 (-8.60)	-8.84 (-10.06)
	[1.00,1.03)	-0.79 (-1.18)	-5.75 (-6.22)	-7.66 (-7.79)	-7.32 (-7.24)	-7.38 (-7.99)
	[1.03,1.06)	-1.98 (-2.47)	-5.88 (-6.12)	-8.19 (-8.24)	-8.69 (-8.54)	-9.25 (-9.58)
	[1.06,1.12)	-3.41 (-3.73)	-5.99 (-5.76)	-7.66 (-7.35)	-8.00 (-7.71)	-8.55 (-8.45)
Jan 2018 – Dec 2018	[0.88,0.94)	2.12 (0.48)	-9.07 (-8.87)	-8.50 (-7.42)	-4.10 (-3.52)	-4.72 (-5.90)
	[0.94,0.97)	-5.63 (-5.17)	-8.70 (-9.36)	-9.00 (-9.22)	-5.62 (-3.98)	-8.40 (-8.62)
	[0.97,1.00)	-12.29 (-11.06)	-10.07 (-10.79)	-11.46 (-10.90)	-7.86 (-4.85)	-9.48 (-10.31)
	[1.00,1.03)	-6.52 (-5.25)	-8.34 (-9.02)	-10.42 (-9.85)	-7.88 (-5.18)	-10.87 (-11.23)
	[1.03,1.06)	-6.03 (-4.78)	-6.50 (-6.50)	-8.04 (-7.58)	-6.82 (-4.38)	-9.00 (-8.65)
	[1.06,1.12)	-6.14 (-5.82)	-5.81 (-6.27)	-7.21 (-6.97)	-5.75 (-4.30)	-8.36 (-8.52)
Jan 2019 – Dec 2019	[0.88,0.94)	7.20e-03 (-0.99)	-9.68 (-8.81)	-6.84 (-6.19)	-3.72 (-1.90)	-2.42 (-2.71)
	[0.94,0.97)	0.43 (-0.23)	-5.07 (-5.40)	-4.46 (-4.30)	-3.09 (-0.59)	-3.95 (-3.51)
	[0.97,1.00)	-1.85 (-1.83)	-5.76 (-4.50)	-5.87 (-4.58)	-5.03 (-1.48)	-4.98 (-4.71)
	[1.00,1.03)	-0.60 (0.62)	-4.72 (-2.91)	-5.81 (-4.01)	-6.00 (-1.74)	-6.57 (-4.67)
	[1.03,1.06)	-0.38 (0.17)	-3.26 (-2.06)	-4.61 (-3.48)	-4.82 (-2.07)	-4.50 (-4.17)
	[1.06,1.12)	-2.11 (-1.99)	-2.35 (-1.33)	-3.28 (-2.20)	-4.15 (-1.59)	-4.58 (-3.35)
Jan 2020 – Dec 2020	[0.88,0.94)	2.53 (2.76)	-3.60 (-3.01)	-3.25 (-2.39)	-0.76 (-0.50)	0.70 (0.90)
	[0.94,0.97)	8.73 (9.79)	0.49 (1.12)	-1.39 (-1.10)	-0.87 (-0.97)	0.53 (0.73)
	[0.97,1.00)	6.21 (6.00)	-0.86 (-1.32)	-3.39 (-3.55)	-2.10 (-2.84)	-1.63 (-1.57)
	[1.00,1.03)	3.59 (3.30)	-1.84 (-2.19)	-3.74 (-4.00)	-2.54 (-3.48)	-1.62 (-0.95)
	[1.03,1.06)	1.56 (0.64)	-2.78 (-3.36)	-4.49 (-4.80)	-2.97 (-4.11)	-2.31 (-1.64)
	[1.06,1.12)	-1.31 (-2.51)	-3.68 (-4.58)	-4.67 (-5.36)	-3.17 (-4.96)	-2.33 (-1.61)
Jan 2021 – Dec 2021	[0.88,0.94)	13.63 (5.59)	-6.42 (-12.14)	-10.60 (-14.50)	-11.16 (-15.51)	-10.70 (-15.08)
	[0.94,0.97)	4.31 (-3.40)	-7.39 (-13.16)	-10.75 (-14.70)	-10.74 (-14.92)	-10.21 (-14.19)
	[0.97,1.00)	-4.13 (-10.75)	-13.79 (-17.74)	-17.65 (-20.83)	-19.21 (-20.89)	-19.48 (-22.05)
	[1.00,1.03)	-5.43 (-7.85)	-13.46 (-14.88)	-15.94 (-17.09)	-16.07 (-16.81)	-15.16 (-17.28)
	[1.03,1.06)	-6.96 (-8.19)	-14.43 (-14.53)	-18.12 (-18.16)	-19.41 (-19.04)	-20.07 (-21.03)
	[1.06,1.12)	-7.28 (-6.69)	-13.90 (-11.79)	-16.84 (-15.13)	-17.73 (-16.18)	-18.05 (-18.00)
Jan 2022 – Dec 2022	[0.88,0.94)	-8.08 (-6.65)	-7.45 (-6.93)	-4.67 (-4.14)	-1.55 (-0.91)	0.13 (0.05)
	[0.94,0.97)	1.03 (1.51)	0.41 (0.20)	-0.70 (-0.46)	-0.22 (0.57)	1.01 (0.48)
	[0.97,1.00)	1.77 (2.18)	0.70 (0.43)	-1.51 (-1.59)	-1.28 (-1.01)	-1.31 (-1.90)
	[1.00,1.03)	0.58 (0.47)	0.15 (-0.19)	-1.61 (-1.89)	-1.39 (-1.28)	-1.12 (-1.66)
	[1.03,1.06)	-1.16 (-1.45)	-0.66 (-1.09)	-2.14 (-2.66)	-1.90 (-1.97)	-2.26 (-2.82)
	[1.06,1.12)	-2.92 (-3.37)	-1.01 (-1.39)	-1.96 (-2.65)	-1.82 (-1.99)	-2.15 (-2.86)

Table A.1.2. MSE FFT - implied volatility percentage errors

Sample period	S/K	Call (Put) options				
		Time-to-maturity				
		21–70	**71–120**	**121–170**	**171–220**	**221–270**
Jan 2018 – May 2022	[0.88,0.94)	9.29 (1.81)	-3.50 (-7.42)	-4.82 (-7.29)	-4.89 (-5.16)	-4.07 (-3.71)
	[0.94,0.97)	7.71 (1.31)	-2.46 (-5.70)	-4.92 (-6.60)	-5.10 (-4.94)	-5.59 (-4.72)
	[0.97,1.00)	1.34 (-3.02)	-5.71 (-8.05)	-8.05 (-9.54)	-8.83 (-8.67)	-9.76 (-9.14)
	[1.00,1.03)	0.23 (-1.84)	-5.82 (-6.64)	-7.72 (-7.69)	-7.90 (-6.73)	-8.36 (-7.01)
	[1.03,1.06)	-1.98 (-2.59)	-6.19 (-6.46)	-8.37 (-8.21)	-9.15 (-8.47)	-9.97 (-8.55)
	[1.06,1.12)	-3.86 (-3.43)	-6.52 (-5.55)	-8.10 (-6.75)	-8.52 (-7.11)	-9.36 (-7.27)
Jan 2018 – Dec 2018	[0.88,0.94)	4.91 (1.90)	-2.47 (-7.81)	1.15 (-6.96)	-3.05 (-3.29)	3.69 (-5.70)
	[0.94,0.97)	-1.88 (-5.72)	-5.73 (-9.55)	-3.31 (-10.13)	-4.63 (-5.11)	-4.64 (-8.72)
	[0.97,1.00)	-9.38 (-11.81)	-9.09 (-10.20)	-7.60 (-11.23)	-6.23 (-5.69)	-8.56 (-9.25)
	[1.00,1.03)	-6.29 (-6.28)	-9.04 (-8.70)	-8.93 (-10.52)	-6.41 (-6.20)	-11.06 (-10.16)
	[1.03,1.06)	-7.81 (-5.32)	-8.46 (-6.21)	-8.92 (-8.12)	-5.54 (-4.86)	-11.09 (-7.83)
	[1.06,1.12)	-9.38 (-6.31)	-9.02 (-5.74)	-10.08 (-7.07)	-5.32 (-4.97)	-12.73 (-7.41)
Jan 2019 – Dec 2019	[0.88,0.94)	1.49 (0.84)	-7.50 (-6.73)	-6.14 (-5.73)	-3.87 (-2.38)	-4.55 (-5.24)
	[0.94,0.97)	1.39 (1.17)	-5.82 (-6.23)	-6.07 (-5.68)	-4.86 (-2.23)	-7.59 (-7.96)
	[0.97,1.00)	-2.67 (-1.71)	-7.29 (-7.04)	-7.86 (-6.05)	-6.66 (-3.37)	-7.83 (-8.62)
	[1.00,1.03)	-1.07 (0.43)	-6.12 (-5.00)	-7.45 (-5.03)	-7.30 (-3.48)	-8.77 (-8.47)
	[1.03,1.06)	-0.71 (-0.12)	-3.99 (-3.80)	-5.62 (-4.05)	-6.18 (-3.13)	-6.73 (-6.43)
	[1.06,1.12)	-1.77 (-2.16)	-2.34 (-2.32)	-3.65 (-2.55)	-4.45 (-2.30)	-5.06 (-5.30)
Jan 2020 – Dec 2020	[0.88,0.94)	0.45 (-1.23)	-5.00 (-5.81)	-3.95 (-5.31)	-1.79 (-2.65)	0.66 (-3.10e-03)
	[0.94,0.97)	5.89 (5.71)	-0.80 (-2.22)	-2.36 (-4.31)	-0.50 (-1.70)	-5.50e-03 (-1.50)
	[0.97,1.00)	3.56 (1.69)	-2.03 (-4.96)	-3.38 (-6.67)	-2.99 (-4.95)	-1.34 (-3.81)
	[1.00,1.03)	2.10 (1.03)	-2.33 (-4.08)	-3.22 (-5.21)	-2.09 (-3.33)	-1.21 (-2.15)
	[1.03,1.06)	0.36 (-0.38)	-2.70 (-4.62)	-3.68 (-5.85)	-3.18 (-4.88)	-1.12 (-3.24)
	[1.06,1.12)	-1.73 (-2.03)	-3.42 (-4.42)	-3.79 (-5.21)	-3.00 (-4.23)	-1.25 (-2.32)
Jan 2021 – Dec 2021	[0.88,0.94)	29.83 (2.24)	0.26 (-12.78)	-7.68 (-14.51)	-11.64 (-14.13)	-12.86 (-11.37)
	[0.94,0.97)	19.06 (-5.43)	-3.76 (-12.31)	-10.47 (-13.15)	-12.70 (-12.31)	-13.28 (-9.24)
	[0.97,1.00)	4.99 (-10.39)	-11.15 (-16.33)	-17.10 (-19.07)	-19.52 (-18.80)	-21.28 (-17.88)
	[1.00,1.03)	1.04 (-7.62)	-11.34 (-13.63)	-16.02 (-15.20)	-17.26 (-14.48)	-17.16 (-13.22)
	[1.03,1.06)	-4.17 (-7.98)	-13.78 (-13.97)	-18.97 (-17.14)	-20.16 (-18.05)	-21.69 (-17.48)
	[1.06,1.12)	-6.95 (-6.31)	-14.13 (-11.29)	-18.47 (-13.77)	-18.90 (-14.82)	-19.70 (-14.76)
Jan 2022 – Dec 2022	[0.88,0.94)	-6.82 (-7.19)	-7.13 (-7.73)	-5.04 (-4.41)	-1.57 (-1.19)	-0.80 (0.50)
	[0.94,0.97)	1.39 (1.29)	-0.02 (0.72)	-1.24 (-0.05)	-0.18 (0.32)	-0.91 (0.60)
	[0.97,1.00)	2.19 (2.88)	-0.06 (0.74)	-1.63 (-0.75)	-0.87 (-0.55)	-1.81 (-0.84)
	[1.00,1.03)	0.66 (1.54)	-0.59 (0.62)	-2.01 (-0.74)	-1.41 (-0.80)	-2.24 (-0.93)
	[1.03,1.06)	-1.23 (-0.35)	-1.20 (-0.28)	-2.18 (-1.32)	-1.59 (-1.20)	-2.41 (-1.50)
	[1.06,1.12)	-3.23 (-2.33)	-1.81 (-0.76)	-2.45 (-1.31)	-1.84 (-1.29)	-2.65 (-1.51)

TABLE A.1.3. MSE FRFT - implied volatility percentage errors

By inspecting the tables above, the Heston single integrand produced good results for any given sample period across the moneyness and time-to-maturity categories, the FFT and the FRFT produced worst results but comparable between each other. For each model formulation, we can also see that both calls and puts produced similar levels of mispricing for these same categories for all sample periods.

The results of the Student's t-test for the Heston single integrand formulation were the following. For calls, `h = 0` indicating that the calibration of the Heston single integrand formulation is not biased, a p-value `p = 0.24041` and a confidence interval `ci =`

`[-0.00008, 0.00002]` with 95% confidence. For puts, `h = 1` indicating that the calibration of the Heston single integrand formulation is biased, a p-value `p = 0.00297` and a confidence interval `ci = [0.00003, 0.00013]` with 95% confidence, overestimating on average.

The results of the Student's t-test for the FFT formulation were the following. For calls, `h = 1` indicating that the calibration of the FFT formulation is biased, a p-value `p = 0.00000` and a confidence interval `ci = [-0.00059, -0.00052]` with 95% confidence, underestimating on average. For puts, `h = 1` indicating that the calibration of the FFT formulation is biased, a p-value `p = 0.00000` and a confidence interval `ci = [-0.00050, -0.00043]` with 95% confidence, underestimating on average.

The results of the Student's t-test for the FRFT formulation were the following. For calls, `h = 1` indicating that the calibration of the FRFT formulation is biased, a p-value `p = 0.00000` and a confidence interval `ci = [-0.00048, -0.00041]` with 95% confidence, underestimating on average. For puts, `h = 1` indicating that the calibration of the FRFT formulation is biased, a p-value `p = 0.00000` and a confidence interval `ci = [-0.00044, -0.00038]` with 95% confidence, underestimating on average.

We now present three tables, one for each formulation, with the statistical analysis for both option types.

Parameters	**Mean**	**Standard deviation**	**Minimum**	**Maximum**	**Median**
κ	2.45826 (2.39274)	1.30101 (1.26987)	0.03106 (0.03161)	10.12063 (9.71708)	2.33011 (2.25972)
θ	0.16328 (0.16722)	0.38352 (0.38671)	0.03310 (0.03400)	1.99889 (1.99917)	0.06594 (0.06718)
σ	1.10840 (1.10854)	0.37104 (0.36371)	0.53844 (0.56752)	2.00000 (2.00000)	1.00184 (1.00864)
v_0	0.04367 (0.04361)	0.05938 (0.05896)	0.00446 (0.00454)	0.68689 (0.68076)	0.02857 (0.02853)
ρ	-0.78994 (-0.79602)	0.04911 (0.04968)	-0.99900 (-0.99900)	-0.62707 (-0.64965)	-0.78342 (-0.78972)
Time	2.46352 (2.20492)	1.35965 (1.46534)	0.57407 (0.49430)	14.18748 (19.73512)	2.19143 (1.87640)
Error	-0.00003 (0.00008)	0.00090 (0.00088)	-0.00290 (-0.00344)	0.00452 (0.00478)	-0.00002 (0.00012)

Table A.1.4. MSE Heston single integrand - calls (puts) statistical analysis

Parameters	**Mean**	**Standard deviation**	**Minimum**	**Maximum**	**Median**
κ	4.03894 (3.11105)	4.06383 (1.92079)	0.00459 (0.00468)	20.00000 (19.91529)	2.77239 (2.64978)
θ	0.08920 (0.10108)	0.17299 (0.19479)	0.00001 (0.00049)	2.00000 (2.00000)	0.05569 (0.05832)
σ	1.08141 (1.11478)	0.52413 (0.47830)	0.00001 (0.00001)	2.00000 (2.00000)	0.97671 (1.00922)
v_0	0.04243 (0.04292)	0.06009 (0.05923)	0.00001 (0.00001)	0.68272 (0.67846)	0.02647 (0.02825)
ρ	-0.75848 (-0.76931)	0.28726 (0.27402)	-0.99900 (-0.99900)	0.99900 (0.99900)	-0.79558 (-0.80426)
α	14.31171 (14.29673)	3.11921 (3.25353)	8.25000 (8.25000)	25.00000 (25.00000)	13.75000 (13.50000)
Time	0.67593 (0.76498)	0.61831 (0.58711)	0.05984 (0.10257)	8.19054 (7.68872)	0.57931 (0.66276)
Error	-0.00056 (-0.00046)	0.00066 (0.00062)	-0.00505 (-0.00468)	0.00211 (0.00193)	-0.00038 (-0.00025)

Table A.1.5. MSE FFT - calls (puts) statistical analysis

Parameters	**Mean**	**Standard deviation**	**Minimum**	**Maximum**	**Median**
κ	4.73338 (3.00947)	5.18192 (1.80947)	0.03253 (0.00001)	20.00000 (11.78514)	2.79818 (2.54828)
θ	0.10785 (0.11979)	0.26332 (0.27658)	0.00652 (0.01870)	2.00000 (2.00000)	0.05554 (0.05995)
σ	1.03053 (1.14631)	0.54825 (0.42917)	0.00001 (0.00005)	2.00000 (2.00000)	0.95710 (1.02733)
v_0	0.04214 (0.04305)	0.06024 (0.05913)	0.00001 (0.00001)	0.68344 (0.67843)	0.02548 (0.02810)
ρ	-0.71420 (-0.81047)	0.39886 (0.06294)	-0.99900 (-0.99900)	0.99900 (0.04976)	-0.79272 (-0.80250)
α	14.44306 (14.03675)	4.08586 (4.19084)	5.75000 (5.50000)	25.00000 (25.00000)	13.75000 (13.50000)
Time	0.40103 (0.44803)	0.39009 (0.47142)	0.02280 (0.02115)	5.71388 (5.30612)	0.33215 (0.36033)
Error	-0.00045 (-0.00041)	0.00056 (0.00056)	-0.00305 (-0.00291)	0.00159 (0.00165)	-0.00025 (-0.00019)

Table A.1.6. MSE FRFT - calls (puts) statistical analysis

The tables above summarize the statistical analysis for the three formulations covering both option types. On average, the damping factor α was similar between the FFT and FRFT formulations. We explained earlier that we used the equation (2.81) to price OTM, ATM and ITM options for a wide range of maturities, by using this formulae for OTM options and for very short maturities, the integrand of the equation (2.81) can be high oscillatory, these high oscilations explains the high values of α. We can see that on average, the calibration time for puts was faster than the calibration time for calls for the Heston single integrand formulation and the other way around for the FFT and FRFT formulations. The FRFT formulation, was, on average, the fastest followed by the FFT and Heston single integrand for both option types, which was expected.

A.2. RMSE loss function

The following tables present the percentage errors between the averaged market-implied volatilities and the averaged implied volatilities generated by the Heston single integrand formulation, the FFT formulation and the FRFT formulation, broken down by moneyness and time-to-maturity categories. Positive values indicate overestimating, while negative values indicate underestimating.

Sample period	S/K	Call (Put) options				
		Time-to-maturity				
		21–70	71–120	121–170	171–220	221–270
Jan 2018 – May 2022	[0.88,0.94)	1.36 (1.59)	-2.13 (-2.83)	-1.32 (-1.64)	0.38 (0.87)	1.86 (2.77)
	[0.94,0.97)	3.65 (2.00)	-0.94 (-2.00)	-1.39 (-1.18)	-0.12 (0.71)	1.18 (2.21)
	[0.97,1.00)	5.27 (1.03)	-0.24 (-1.21)	-1.33 (-1.00)	-0.45 (0.30)	0.63 (1.43)
	[1.00,1.03)	3.54 (2.59)	-0.47 (-0.64)	-1.49 (-0.97)	-0.78 (-0.06)	0.24 (0.86)
	[1.03,1.06)	0.97 (1.69)	-1.01 (-0.44)	-1.68 (-0.96)	-0.95 (-0.25)	0.02 (0.51)
	[1.06,1.12)	-2.83 (-0.26)	-1.70 (-0.44)	-1.63 (-0.75)	-0.90 (-0.22)	1.70e-03 (0.30)
Jan 2018 – Dec 2018	[0.88,0.94)	-4.83 (0.09)	-3.73 (0.16)	-1.12 (2.92)	0.70 (4.16)	1.09 (4.06)
	[0.94,0.97)	0.89 (1.30)	0.37 (-0.75)	-0.11 (0.60)	-0.40 (1.65)	-0.28 (1.76)
	[0.97,1.00)	6.36 (-1.75)	1.46 (-1.36)	-0.34 (-0.54)	-0.95 (0.36)	-0.70 (0.57)
	[1.00,1.03)	4.49 (2.96)	0.64 (-0.28)	-1.16 (-0.54)	-1.43 (-0.17)	-1.00 (-0.02)
	[1.03,1.06)	-0.21 (1.74)	-0.78 (0.28)	-2.26 (-0.45)	-1.93 (-0.37)	-1.26 (-0.25)
	[1.06,1.12)	-7.61 (-1.62)	-3.23 (-0.15)	-3.63 (-0.42)	-2.33 (-0.28)	-1.36 (-0.22)
Jan 2019 – Dec 2019	[0.88,0.94)	-5.95 (-1.17)	-3.39 (-4.22)	-1.23 (-1.62)	0.76 (1.44)	2.01 (3.47)
	[0.94,0.97)	5.24 (1.76)	-0.35 (-2.37)	-0.99 (-0.51)	0.17 (1.74)	0.76 (2.93)
	[0.97,1.00)	7.20 (0.68)	0.12 (-1.30)	-1.23 (-0.64)	-0.48 (0.73)	0.04 (1.58)
	[1.00,1.03)	3.67 (2.66)	-0.34 (-0.66)	-1.50 (-0.89)	-0.94 (-0.08)	-0.38 (0.57)
	[1.03,1.06)	0.05 (1.78)	-0.99 (-0.25)	-1.72 (-0.91)	-1.15 (-0.42)	-0.40 (0.09)
	[1.06,1.12)	-5.79 (-1.16)	-1.82 (0.03)	-1.47 (-0.34)	-0.79 (-0.09)	0.09 (0.14)
Jan 2020 – Dec 2020	[0.88,0.94)	2.43 (0.22)	-1.88 (-3.60)	-1.28 (-1.93)	0.82 (0.85)	2.27 (2.64)
	[0.94,0.97)	3.88 (2.61)	-1.52 (-1.47)	-1.86 (-1.34)	-0.18 (0.55)	1.32 (1.99)
	[0.97,1.00)	3.85 (3.36)	-1.24 (-0.85)	-1.86 (-1.23)	-0.47 (0.22)	1.00 (1.47)
	[1.00,1.03)	2.77 (2.82)	-1.31 (-0.80)	-1.91 (-1.25)	-0.59 (0.01)	1.00 (1.35)
	[1.03,1.06)	1.60 (1.64)	-1.40 (-0.93)	-1.89 (-1.27)	-0.46 (-0.02)	1.07 (1.28)
	[1.06,1.12)	-0.16 (-0.17)	-1.31 (-1.01)	-1.51 (-1.16)	-0.07 (0.08)	1.33 (1.15)
Jan 2021 – Dec 2021	[0.88,0.94)	-0.26 (1.82)	-1.79 (-2.52)	-1.80 (-2.13)	-0.17 (0.26)	2.07 (2.86)
	[0.94,0.97)	4.94 (1.74)	-1.45 (-3.45)	-1.53 (-1.87)	0.14 (0.65)	2.03 (2.83)
	[0.97,1.00)	7.09 (-0.31)	-0.28 (-1.93)	-1.16 (-1.14)	-0.07 (0.61)	1.34 (2.11)
	[1.00,1.03)	5.00 (2.78)	-0.45 (-0.88)	-1.35 (-0.88)	-0.64 (0.20)	0.47 (1.22)
	[1.03,1.06)	1.62 (2.15)	-1.23 (-0.58)	-1.76 (-0.88)	-1.22 (-0.20)	-0.25 (0.52)
	[1.06,1.12)	-3.13 (0.37)	-2.29 (-0.56)	-2.17 (-0.81)	-1.77 (-0.50)	-0.88 (-0.06)
Jan 2022 – Dec 2022	[0.88,0.94)	-1.53 (-2.83)	-0.76 (-2.88)	-0.68 (-1.52)	0.20 (0.41)	1.24 (2.12)
	[0.94,0.97)	1.84 (0.06)	-0.47 (-1.07)	-1.02 (-0.80)	-0.64 (0.02)	0.18 (1.11)
	[0.97,1.00)	2.04 (1.40)	-0.05 (-0.27)	-1.06 (-0.80)	-0.97 (-0.49)	-0.26 (0.39)
	[1.00,1.03)	1.27 (1.17)	0.10 (-0.07)	-0.95 (-0.85)	-0.92 (-0.70)	-0.27 (0.04)
	[1.03,1.06)	0.48 (0.64)	0.25 (0.05)	-0.57 (-0.68)	-0.55 (-0.60)	-9.00e-03 (6.30e-03)
	[1.06,1.12)	-0.77 (-0.42)	0.69 (0.42)	0.18 (-0.16)	0.25 (-0.17)	0.64 (0.25)

TABLE A.2.1. RMSE Heston single integrand - implied volatility percentage errors

Sample period	S/K	Call (Put) options				
		Time-to-maturity				
		21–70	71–120	121–170	171–220	221–270
Jan 2018 – May 2022	[0.88,0.94)	3.46 (0.16)	-5.96 (-9.35)	-6.98 (-7.48)	-6.31 (-4.41)	-4.96 (-3.11)
	[0.94,0.97)	0.96 (-1.86)	-6.40 (-6.50)	-7.59 (-5.81)	-7.36 (-4.79)	-6.75 (-4.54)
	[0.97,1.00)	-5.00 (-5.14)	-9.77 (-8.03)	-11.68 (-8.28)	-12.21 (-8.41)	-11.76 (-9.13)
	[1.00,1.03)	-3.84 (-3.15)	-9.18 (-6.60)	-10.67 (-6.92)	-10.58 (-7.12)	-9.88 (-7.05)
	[1.03,1.06)	-4.15 (-2.81)	-9.15 (-5.70)	-11.73 (-6.64)	-12.63 (-7.82)	-12.12 (-8.50)
	[1.06,1.12)	-4.01 (-2.77)	-7.95 (-4.80)	-10.56 (-5.62)	-11.02 (-6.45)	-10.80 (-7.16)
Jan 2018 – Dec 2018	[0.88,0.94)	1.82 (3.91)	-3.34 (-9.08)	-2.74 (-8.40)	-0.33 (-6.25)	-1.93 (-7.59)
	[0.94,0.97)	-1.23 (-8.10)	-5.45 (-12.80)	-5.02 (-10.54)	-3.96 (-9.69)	-6.84 (-12.30)
	[0.97,1.00)	-7.55 (-16.08)	-7.63 (-15.00)	-6.98 (-12.34)	-5.86 (-10.87)	-7.94 (-13.63)
	[1.00,1.03)	-1.85 (-8.99)	-6.74 (-12.06)	-7.50 (-10.49)	-7.25 (-10.94)	-9.27 (-14.24)
	[1.03,1.06)	-0.96 (-7.16)	-5.06 (-8.99)	-6.69 (-8.33)	-7.30 (-8.47)	-8.26 (-11.14)
	[1.06,1.12)	-1.81 (-5.41)	-4.49 (-7.24)	-6.15 (-7.39)	-7.51 (-7.11)	-8.16 (-10.98)
Jan 2019 – Dec 2019	[0.88,0.94)	2.06 (-0.53)	-4.47 (-10.25)	-2.81 (-6.60)	-0.13 (-1.19)	-1.26 (-1.74)
	[0.94,0.97)	2.40 (-2.21)	-4.43 (-6.08)	-3.69 (-3.40)	-1.41 (1.28)	-5.24 (-1.33)
	[0.97,1.00)	-3.91 (-3.82)	-6.59 (-4.28)	-6.32 (-3.35)	-4.20 (0.55)	-8.09 (-2.81)
	[1.00,1.03)	-0.65 (-0.25)	-6.24 (-3.03)	-7.02 (-3.20)	-5.63 (-0.44)	-9.55 (-3.42)
	[1.03,1.06)	1.20 (-0.10)	-4.46 (-2.08)	-6.22 (-2.82)	-6.02 (-0.98)	-8.93 (-3.22)
	[1.06,1.12)	2.12 (-1.96)	-2.61 (-1.30)	-5.11 (-1.98)	-5.65 (-0.91)	-8.53 (-2.72)
Jan 2020 – Dec 2020	[0.88,0.94)	1.52 (-4.09)	-4.97 (-8.25)	-4.55 (-4.94)	-3.55 (-0.53)	1.02 (2.04)
	[0.94,0.97)	4.29 (1.47)	-3.42 (-2.02)	-4.10 (-1.83)	-3.60 (0.20)	-0.11 (1.82)
	[0.97,1.00)	-0.42 (1.58)	-6.49 (-2.32)	-8.09 (-2.74)	-7.21 (-0.73)	-2.16 (-0.10)
	[1.00,1.03)	-2.25 (1.17)	-7.35 (-2.10)	-7.49 (-2.54)	-5.96 (-0.93)	-2.75 (0.27)
	[1.03,1.06)	-4.13 (0.53)	-8.59 (-2.14)	-10.25 (-2.60)	-8.44 (-1.16)	-4.79 (-0.11)
	[1.06,1.12)	-5.83 (-1.06)	-8.64 (-2.26)	-10.51 (-2.60)	-8.16 (-1.44)	-4.56 (-0.30)
Jan 2021 – Dec 2021	[0.88,0.94)	4.39 (0.96)	-11.56 (-15.27)	-15.32 (-15.87)	-15.51 (-15.10)	-13.80 (-13.18)
	[0.94,0.97)	-6.55 (-9.34)	-14.75 (-14.99)	-15.97 (-14.78)	-16.10 (-14.98)	-14.20 (-12.98)
	[0.97,1.00)	-13.04 (-15.21)	-20.19 (-19.03)	-22.49 (-20.56)	-24.30 (-22.09)	-23.49 (-21.68)
	[1.00,1.03)	-10.05 (-11.46)	-17.21 (-15.76)	-19.06 (-16.82)	-19.68 (-18.33)	-17.67 (-16.21)
	[1.03,1.06)	-9.24 (-10.04)	-17.24 (-14.65)	-20.07 (-16.78)	-22.87 (-19.76)	-22.48 (-20.28)
	[1.06,1.12)	-6.27 (-7.05)	-13.65 (-11.79)	-16.30 (-13.66)	-18.56 (-15.95)	-18.97 (-16.31)
Jan 2022 – Dec 2022	[0.88,0.94)	-4.56 (-9.11)	-4.52 (-9.24)	-4.24 (-4.85)	-2.77 (-1.18)	-3.28 (1.04)
	[0.94,0.97)	0.84 (-2.51)	-1.37 (-1.38)	-4.01 (-1.20)	-3.93 (-0.13)	-5.21 (0.59)
	[0.97,1.00)	-1.79 (1.10)	-3.39 (-0.40)	-5.84 (-1.25)	-5.43 (-0.66)	-6.74 (-0.33)
	[1.00,1.03)	-3.42 (0.82)	-4.33 (-0.39)	-6.53 (-1.45)	-6.72 (-1.06)	-7.73 (-0.94)
	[1.03,1.06)	-4.00 (0.12)	-4.00 (-0.51)	-6.19 (-1.40)	-6.37 (-1.17)	-7.27 (-1.08)
	[1.06,1.12)	-4.54 (-1.20)	-4.03 (-0.44)	-5.97 (-1.26)	-6.26 (-1.18)	-7.26 (-1.26)

Table A.2.2. RMSE FFT - implied volatility percentage errors

Sample period	S/K	Call (Put) options				
		Time-to-maturity				
		21–70	71–120	121–170	171–220	221–270
Jan 2018 – May 2022	[0.88,0.94)	4.04 (-0.18)	-6.07 (-9.19)	-7.00 (-7.25)	-5.88 (-4.30)	-4.61 (-2.49)
	[0.94,0.97)	0.67 (-1.75)	-6.84 (-6.31)	-7.84 (-5.67)	-6.65 (-4.15)	-6.78 (-4.41)
	[0.97,1.00)	-5.78 (-4.98)	-10.23 (-7.74)	-12.15 (-8.09)	-11.34 (-7.05)	-10.75 (-7.75)
	[1.00,1.03)	-4.38 (-2.40)	-9.45 (-6.10)	-10.95 (-6.69)	-9.52 (-5.64)	-9.90 (-6.35)
	[1.03,1.06)	-4.30 (-2.25)	-9.14 (-5.50)	-11.97 (-6.59)	-11.63 (-6.59)	-11.41 (-7.18)
	[1.06,1.12)	-4.15 (-2.47)	-7.89 (-4.42)	-10.86 (-5.47)	-10.56 (-5.58)	-10.43 (-6.38)
Jan 2018 – Dec 2018	[0.88,0.94)	0.70 (2.94)	-4.50 (-8.60)	-4.02 (-8.42)	-0.87 (-6.03)	-5.11 (-8.79)
	[0.94,0.97)	-2.19 (-8.35)	-6.83 (-12.32)	-7.44 (-11.48)	-3.82 (-8.13)	-10.51 (-13.83)
	[0.97,1.00)	-8.30 (-17.40)	-9.67 (-14.91)	-10.06 (-14.13)	-5.67 (-8.56)	-12.00 (-15.17)
	[1.00,1.03)	-2.12 (-9.13)	-8.44 (-12.06)	-9.89 (-12.27)	-6.96 (-9.05)	-12.98 (-15.54)
	[1.03,1.06)	-0.53 (-7.24)	-5.98 (-9.13)	-8.40 (-9.55)	-6.44 (-7.06)	-10.90 (-11.76)
	[1.06,1.12)	-1.07 (-5.18)	-4.72 (-7.02)	-6.92 (-7.98)	-6.70 (-6.77)	-10.35 (-11.06)
Jan 2019 – Dec 2019	[0.88,0.94)	4.41 (1.14)	-4.54 (-7.60)	-4.11 (-5.62)	-1.90 (-0.78)	-4.20 (-1.76)
	[0.94,0.97)	1.25 (-0.47)	-6.84 (-5.96)	-6.82 (-4.17)	-4.39 (0.60)	-9.66 (-3.27)
	[0.97,1.00)	-6.73 (-3.78)	-9.45 (-5.70)	-9.04 (-5.21)	-6.57 (-1.11)	-11.44 (-4.76)
	[1.00,1.03)	-2.11 (-0.66)	-7.81 (-4.31)	-8.71 (-4.77)	-7.16 (-1.79)	-12.19 (-5.89)
	[1.03,1.06)	0.10 (-0.59)	-5.25 (-3.31)	-7.17 (-4.10)	-6.68 (-2.06)	-10.70 (-4.33)
	[1.06,1.12)	1.80 (-2.13)	-2.75 (-2.14)	-5.29 (-2.83)	-5.64 (-1.52)	-9.71 (-4.13)
Jan 2020 – Dec 2020	[0.88,0.94)	2.96 (-3.48)	-4.91 (-7.82)	-5.05 (-4.59)	-3.91 (-1.07)	0.27 (2.53)
	[0.94,0.97)	4.36 (1.38)	-3.37 (-2.72)	-4.13 (-2.27)	-2.59 (-0.07)	-0.86 (1.71)
	[0.97,1.00)	-1.09 (1.20)	-7.94 (-3.23)	-9.24 (-3.27)	-9.34 (-2.48)	-2.83 (0.49)
	[1.00,1.03)	-2.50 (1.32)	-7.78 (-2.34)	-7.70 (-2.64)	-5.37 (-1.34)	-3.03 (0.57)
	[1.03,1.06)	-4.44 (0.23)	-9.35 (-2.86)	-10.76 (-3.09)	-9.97 (-2.44)	-5.18 (0.11)
	[1.06,1.12)	-6.25 (-1.02)	-9.40 (-2.64)	-11.34 (-2.86)	-9.18 (-1.96)	-4.60 (-0.11)
Jan 2021 – Dec 2021	[0.88,0.94)	3.24 (-2.09)	-11.70 (-15.95)	-14.64 (-14.72)	-13.42 (-12.28)	-12.24 (-9.91)
	[0.94,0.97)	-7.35 (-9.12)	-13.73 (-12.82)	-15.37 (-12.34)	-13.38 (-10.84)	-13.14 (-10.28)
	[0.97,1.00)	-14.64 (-12.21)	-18.19 (-15.07)	-22.18 (-17.09)	-20.16 (-15.53)	-20.20 (-16.42)
	[1.00,1.03)	-11.69 (-7.71)	-15.78 (-11.95)	-19.09 (-13.78)	-16.71 (-12.17)	-17.03 (-12.35)
	[1.03,1.06)	-9.79 (-6.63)	-15.48 (-11.56)	-20.20 (-14.39)	-19.29 (-14.19)	-20.32 (-15.75)
	[1.06,1.12)	-6.90 (-5.51)	-12.44 (-9.10)	-16.80 (-11.73)	-16.70 (-11.86)	-17.95 (-13.26)
Jan 2022 – Dec 2022	[0.88,0.94)	-4.54 (-8.86)	-3.18 (-9.05)	-2.27 (-5.94)	-0.47 (-1.95)	0.24 (-0.23)
	[0.94,0.97)	3.17 (-1.63)	1.25 (-2.13)	-0.76 (-2.59)	-0.87 (-1.07)	-0.86 (-0.95)
	[0.97,1.00)	2.37 (0.66)	0.40 (-1.65)	-2.02 (-2.74)	-2.37 (-1.55)	-2.76 (-1.78)
	[1.00,1.03)	0.21 (0.74)	-1.14 (-1.23)	-3.28 (-2.51)	-3.26 (-1.73)	-3.63 (-2.05)
	[1.03,1.06)	-1.31 (-0.33)	-1.68 (-1.25)	-3.45 (-2.33)	-3.59 (-1.74)	-3.91 (-2.06)
	[1.06,1.12)	-3.27 (-1.51)	-2.40 (-1.10)	-3.84 (-2.08)	-3.97 (-1.70)	-4.55 (-2.11)

Table A.2.3. RMSE FRFT - implied volatility percentage errors

By inspecting the tables above, the Heston single integrand produced good results for any given sample period across the moneyness and time-to-maturity categories, the FFT and the FRFT produced worst results but comparable between each other. For each model formulation, we can also see that both calls and puts produced similar levels of mispricing for these same categories for all sample periods.

The results of the Student's t-test for the Heston single integrand formulation were the following. For calls, `h = 1` indicating that the calibration of the Heston single integrand formulation is biased, a p-value `p = 0.00000` and a confidence interval `ci = [-0.00117,`

-0.00101] with 95% confidence, underestimating on average. For puts, `h = 1` indicating that the calibration of the Heston single integrand formulation is biased, a p-value `p = 0.00000` and a confidence interval `ci = [-0.00029, -0.00019]` with 95% confidence, underestimating on average.

The results of the Student's t-test for the FFT formulation were the following. For calls, `h = 1` indicating that the calibration of the FFT formulation is biased, a p-value `p = 0.00000` and a confidence interval `ci = [-0.00061, -0.00052]` with 95% confidence, underestimating on average. For puts, `h = 1` indicating that the calibration of the FFT formulation is biased, a p-value `p = 0.00000` and a confidence interval `ci = [-0.00101, -0.00090]` with 95% confidence, underestimating on average.

The results of the Student's t-test for the FRFT formulation were the following. For calls, `h = 1` indicating that the calibration of the FRFT formulation is biased, a p-value `p = 0.00000` and a confidence interval `ci = [-0.00048, -0.00041]` with 95% confidence, underestimating on average. For puts, `h = 1` indicating that the calibration of the FRFT formulation is biased, a p-value `p = 0.00000` and a confidence interval `ci = [-0.00084, -0.00074]` with 95% confidence, underestimating on average.

We now present three tables, one for each formulation, with the statistical analysis for both option types.

Parameters	**Mean**	**Standard deviation**	**Minimum**	**Maximum**	**Median**
κ	1.57734 (3.21192)	1.42162 (1.62784)	0.01162 (0.03025)	9.29185 (12.01448)	1.48376 (3.04001)
θ	0.50470 (0.12047)	0.73685 (0.27446)	0.03042 (0.03228)	1.99858 (1.99899)	0.10947 (0.06533)
σ	0.95627 (1.23016)	0.42595 (0.36418)	0.23837 (0.54573)	2.00000 (2.00000)	0.90184 (1.15123)
v_0	0.04324 (0.04285)	0.05667 (0.06094)	0.00616 (0.00383)	0.65455 (0.68535)	0.02753 (0.02696)
ρ	-0.78374 (-0.79038)	0.04542 (0.06032)	-0.99271 (-0.99900)	-0.60237 (-0.58335)	-0.78279 (-0.78531)
Time	6.15500 (2.80888)	4.23292 (1.68779)	0.83886 (0.54345)	31.94626 (15.42622)	4.92947 (2.42948)
Error	-0.00109 (-0.00024)	0.00137 (0.00089)	-0.00818 (-0.00401)	0.00163 (0.00280)	-0.00060 (-0.00017)

Table A.2.4. RMSE Heston single integrand - calls (puts) statistical analysis

Parameters	**Mean**	**Standard deviation**	**Minimum**	**Maximum**	**Median**
κ	4.86949 (3.85350)	3.45058 (1.87325)	0.03437 (0.03309)	19.52024 (15.96551)	3.86320 (3.54293)
θ	0.10045 (0.07710)	0.24337 (0.10827)	0.02082 (0.01929)	2.00000 (1.99225)	0.05517 (0.05856)
σ	1.38549 (1.24387)	0.46607 (0.38006)	0.27892 (0.38924)	2.00000 (2.00000)	1.30768 (1.16844)
v_0	0.04290 (0.04204)	0.05724 (0.06094)	0.00044 (0.00001)	0.65716 (0.68189)	0.02735 (0.02658)
ρ	-0.78510 (-0.81157)	0.06585 (0.06538)	-0.99853 (-0.99900)	-0.56131 (-0.56609)	-0.77333 (-0.80461)
α	14.77246 (14.17446)	4.14660 (3.11610)	9.00000 (9.25000)	25.00000 (25.00000)	13.00000 (13.25000)
Time	0.91833 (0.80694)	1.01412 (0.59582)	0.02993 (0.02774)	8.70647 (8.61818)	0.72527 (0.72052)
Error	-0.00056 (-0.00096)	0.00078 (0.00091)	-0.00604 (-0.00523)	0.00202 (0.00251)	-0.00027 (-0.00071)

Table A.2.5. RMSE FFT - calls (puts) statistical analysis

Parameters	**Mean**	**Standard deviation**	**Minimum**	**Maximum**	**Median**
κ	4.48775 (3.76743)	3.09259 (1.88286)	0.03579 (0.03167)	19.17004 (11.95100)	3.67024 (3.43872)
θ	0.09660 (0.09258)	0.22202 (0.19452)	0.02063 (0.02361)	1.99998 (1.99972)	0.05519 (0.05959)
σ	1.34698 (1.24505)	0.46599 (0.38229)	0.52709 (0.46854)	2.00000 (2.00000)	1.27159 (1.16627)
v_0	0.04315 (0.04209)	0.05693 (0.06089)	0.00036 (0.00001)	0.65521 (0.68192)	0.02820 (0.02660)
ρ	-0.78339 (-0.80882)	0.06333 (0.06516)	-0.99835 (-0.99900)	-0.60027 (-0.47199)	-0.77346 (-0.80306)
α	13.75204 (14.08575)	4.95664 (4.01325)	7.00000 (5.50000)	25.00000 (25.00000)	13.00000 (13.25000)
Time	0.58379 (0.44896)	0.66846 (0.37508)	0.01968 (0.01794)	5.69296 (6.20455)	0.44202 (0.38578)
Error	-0.00045 (-0.00079)	0.00061 (0.00081)	-0.00363 (-0.00388)	0.00156 (0.00257)	-0.00027 (-0.00061)

Table A.2.6. RMSE FRFT - calls (puts) statistical analysis

The tables above summarize the statistical analysis for the three formulations covering both option types. On average, the damping factor α was similar between the FFT and FRFT formulations. Here, the value of the damping factor α is again high for the same reasons discussed before in the MSE section. We can see that on average, the calibration time for puts was faster than the calibration time for calls across every formulation. The FRFT formulation, was, on average, the fastest followed by the FFT and Heston single integrand for both option types, which was expected.

A.3. IVRMSE loss function

The following tables present the percentage errors between the averaged market-implied volatilities and the averaged implied volatilities generated by the Heston single integrand formulation, the FFT formulation and the FRFT formulation, broken down by moneyness and time-to-maturity categories. Positive values indicate overestimating, while negative values indicate underestimating.

Sample period	**S/K**	**Call (Put) options**				
		Time-to-maturity				
		21–70	**71–120**	**121–170**	**171–220**	**221–270**
Jan 2018 – May 2022	[0.88,0.94)	1.10 (1.10)	-2.20 (-1.51)	-1.24 (-0.54)	0.50 (1.50)	2.18 (3.18)
	[0.94,0.97)	4.38 (3.47)	-0.05 (-0.71)	-0.57 (-0.65)	0.56 (0.91)	1.76 (2.38)
	[0.97,1.00)	7.60 (4.61)	1.00 (-0.05)	-0.40 (-0.73)	0.28 (0.33)	1.18 (1.54)
	[1.00,1.03)	5.53 (4.05)	0.67 (-0.09)	-0.63 (-0.96)	-0.08 (-0.15)	0.74 (0.92)
	[1.03,1.06)	2.67 (2.12)	-0.04 (-0.41)	-0.90 (-1.13)	-0.32 (-0.41)	0.45 (0.54)
	[1.06,1.12)	-1.56 (-1.17)	-0.82 (-0.88)	-0.96 (-1.11)	-0.35 (-0.47)	0.31 (0.28)
Jan 2018 – Dec 2018	[0.88,0.94)	-3.85 (-2.26)	-2.52 (0.66)	-0.26 (3.26)	0.42 (3.55)	0.82 (3.20)
	[0.94,0.97)	3.49 (3.90)	2.83 (2.38)	2.30 (2.47)	0.74 (2.11)	0.06 (1.92)
	[0.97,1.00)	11.85 (6.62)	4.33 (2.38)	2.21 (1.29)	0.31 (0.58)	-0.52 (0.78)
	[1.00,1.03)	9.69 (6.96)	3.38 (1.97)	1.41 (0.46)	-0.15 (-0.17)	-1.09 (0.08)
	[1.03,1.06)	4.91 (3.75)	1.85 (1.23)	0.32 (-0.19)	-0.65 (-0.69)	-1.51 (-0.29)
	[1.06,1.12)	-3.35 (-2.62)	-0.57 (-0.49)	-0.95 (-1.07)	-1.01 (-1.11)	-1.72 (-0.50)
Jan 2019 – Dec 2019	[0.88,0.94)	-5.15 (-2.72)	-4.23 (-0.62)	-1.86 (0.98)	-0.58 (2.81)	1.56 (3.96)
	[0.94,0.97)	8.01 (5.46)	2.20 (0.33)	1.07 (0.46)	1.50 (1.87)	1.43 (2.52)
	[0.97,1.00)	12.39 (5.69)	3.03 (0.34)	0.88 (-0.37)	0.88 (0.47)	0.53 (1.08)
	[1.00,1.03)	8.07 (4.43)	2.20 (0.04)	0.27 (-0.92)	0.11 (-0.40)	-0.16 (0.12)
	[1.03,1.06)	3.81 (2.18)	1.07 (-0.21)	-0.25 (-1.12)	-0.40 (-0.70)	-0.44 (-0.30)
	[1.06,1.12)	-2.28 (-2.19)	7.80e-03 (-0.55)	-0.24 (-0.82)	-0.36 (-0.41)	-0.27 (-0.19)
Jan 2020 – Dec 2020	[0.88,0.94)	1.42 (0.46)	-2.11 (-2.18)	-0.86 (-0.75)	1.84 (1.86)	3.44 (3.81)
	[0.94,0.97)	3.19 (2.76)	-1.67 (-1.78)	-1.42 (-1.41)	0.53 (0.62)	2.29 (2.60)
	[0.97,1.00)	3.78 (3.46)	-1.30 (-1.31)	-1.49 (-1.48)	0.06 (0.15)	1.73 (2.01)
	[1.00,1.03)	2.75 (2.74)	-1.32 (-1.27)	-1.57 (-1.55)	-0.14 (-0.09)	1.63 (1.79)
	[1.03,1.06)	1.47 (1.62)	-1.44 (-1.27)	-1.59 (-1.53)	-0.07 (-0.05)	1.59 (1.74)
	[1.06,1.12)	-0.32 (-0.10)	-1.34 (-1.14)	-1.31 (-1.25)	0.27 (0.22)	1.61 (1.71)
Jan 2021 – Dec 2021	[0.88,0.94)	-1.31 (-0.56)	-2.65 (-2.47)	-2.16 (-1.72)	-0.69 (0.52)	1.72 (2.92)
	[0.94,0.97)	5.98 (4.04)	-0.42 (-1.50)	-0.87 (-0.98)	0.70 (1.09)	2.43 (3.03)
	[0.97,1.00)	10.40 (5.78)	1.44 (0.03)	-0.13 (-0.48)	0.85 (0.88)	2.04 (2.24)
	[1.00,1.03)	7.23 (5.14)	1.10 (0.14)	-0.29 (-0.62)	0.37 (0.25)	1.31 (1.27)
	[1.03,1.06)	3.09 (2.40)	9.30e-03 (-0.51)	-0.76 (-1.03)	-0.21 (-0.39)	0.65 (0.43)
	[1.06,1.12)	-2.36 (-1.76)	-1.38 (-1.49)	-1.28 (-1.49)	-0.81 (-1.03)	0.05 (-0.35)
Jan 2022 – Dec 2022	[0.88,0.94)	-1.15 (-0.77)	-0.82 (-1.17)	-0.40 (-0.48)	0.89 (0.94)	2.21 (2.35)
	[0.94,0.97)	1.19 (1.24)	-0.89 (-0.78)	-1.02 (-0.76)	-0.37 (-0.14)	0.70 (0.96)
	[0.97,1.00)	1.75 (1.90)	-0.51 (-0.34)	-1.22 (-0.97)	-0.93 (-0.74)	0.01 (0.20)
	[1.00,1.03)	1.35 (1.43)	-0.33 (-0.20)	-1.21 (-1.04)	-1.05 (-0.91)	-0.19 (-0.10)
	[1.03,1.06)	0.87 (0.82)	-0.10 (-0.06)	-0.88 (-0.83)	-0.79 (-0.73)	-0.08 (-0.07)
	[1.06,1.12)	-0.08 (-0.25)	0.48 (0.39)	-0.16 (-0.24)	-0.09 (-0.16)	0.42 (0.29)

TABLE A.3.1. IVRMSE Heston single integrand - implied volatility percentage errors

Sample period	S/K	Call (Put) options				
		Time-to-maturity				
		21–70	71–120	121–170	171–220	221–270
Jan 2018 – May 2022	[0.88,0.94)	6.88 (4.61)	-0.69 (-2.61)	0.85 (-0.24)	0.98 (0.90)	1.30 (2.46)
	[0.94,0.97)	6.82 (4.87)	0.53 (-0.69)	-0.03 (-0.21)	-1.05 (-0.43)	-1.47 (-0.05)
	[0.97,1.00)	1.20 (1.32)	-3.22 (-2.53)	-3.83 (-2.58)	-5.29 (-3.40)	-6.28 (-3.05)
	[1.00,1.03)	1.25 (1.98)	-3.38 (-2.55)	-4.14 (-3.05)	-5.84 (-4.09)	-6.18 (-3.73)
	[1.03,1.06)	0.94 (1.31)	-3.46 (-2.63)	-4.77 (-3.56)	-6.72 (-4.93)	-7.67 (-4.55)
	[1.06,1.12)	0.35 (-0.08)	-3.05 (-2.82)	-4.40 (-3.74)	-6.57 (-5.19)	-7.16 (-5.05)
Jan 2018 – Dec 2018	[0.88,0.94)	1.13 (2.54)	-6.57 (-4.96)	-3.14 (-3.03)	-4.74 (-1.28)	-0.59 (-2.28)
	[0.94,0.97)	-4.05 (-2.45)	-7.94 (-6.57)	-5.92 (-4.97)	-8.39 (-4.06)	-5.66 (-5.85)
	[0.97,1.00)	-12.76 (-10.81)	-11.71 (-9.21)	-9.66 (-7.49)	-10.14 (-5.67)	-8.89 (-7.85)
	[1.00,1.03)	-6.95 (-3.43)	-9.63 (-6.86)	-9.10 (-6.64)	-11.41 (-6.64)	-9.02 (-7.89)
	[1.03,1.06)	-4.56 (-2.78)	-7.53 (-5.53)	-8.73 (-6.26)	-9.36 (-6.11)	-9.09 (-7.68)
	[1.06,1.12)	-4.28 (-2.99)	-6.35 (-4.85)	-7.53 (-5.66)	-9.88 (-6.52)	-8.75 (-7.58)
Jan 2019 – Dec 2019	[0.88,0.94)	3.11 (2.23)	-3.21 (-2.58)	-1.11 (0.56)	3.21 (1.79)	-1.27 (4.10)
	[0.94,0.97)	2.17 (2.95)	-2.25 (-1.69)	-1.86 (0.80)	2.42 (1.21)	-5.15 (1.01)
	[0.97,1.00)	-4.46 (0.32)	-5.33 (-2.21)	-5.05 (-0.60)	-0.74 (-1.31)	-7.98 (-1.08)
	[1.00,1.03)	-1.37 (1.99)	-4.55 (-2.16)	-5.16 (-1.88)	-2.22 (-2.58)	-8.67 (-2.87)
	[1.03,1.06)	-1.25 (1.53)	-4.41 (-1.85)	-5.77 (-2.35)	-3.45 (-3.19)	-8.79 (-3.51)
	[1.06,1.12)	-0.53 (-0.11)	-2.57 (-1.32)	-4.29 (-2.01)	-3.50 (-3.18)	-7.98 (-3.79)
Jan 2020 – Dec 2020	[0.88,0.94)	6.45 (2.28)	1.91 (-2.44)	3.89 (1.47)	3.83 (2.30)	4.85 (4.57)
	[0.94,0.97)	11.40 (8.00)	4.91 (1.08)	4.05 (1.84)	2.65 (1.36)	3.41 (2.69)
	[0.97,1.00)	8.99 (5.73)	3.08 (-0.29)	1.65 (-0.50)	0.02 (-0.50)	1.22 (1.21)
	[1.00,1.03)	7.17 (3.88)	2.42 (-0.97)	1.44 (-0.97)	-0.60 (-1.33)	2.21 (0.67)
	[1.03,1.06)	5.91 (3.23)	1.74 (-1.31)	0.48 (-1.21)	-1.58 (-2.06)	0.45 (0.32)
	[1.06,1.12)	4.16 (1.39)	1.16 (-1.78)	0.38 (-1.62)	-1.44 (-2.22)	0.22 (-0.23)
Jan 2021 – Dec 2021	[0.88,0.94)	6.15 (2.57)	-2.87 (-5.44)	-3.06 (-4.41)	-4.18 (-2.84)	-3.47 (-0.59)
	[0.94,0.97)	4.51 (2.00)	-2.10 (-2.79)	-4.31 (-3.72)	-6.49 (-3.37)	-6.03 (-2.33)
	[0.97,1.00)	-1.65 (-0.37)	-8.50 (-5.02)	-10.39 (-6.75)	-13.49 (-7.76)	-14.08 (-6.91)
	[1.00,1.03)	-2.36 (0.73)	-9.05 (-4.74)	-10.68 (-6.54)	-13.18 (-7.85)	-13.89 (-7.40)
	[1.03,1.06)	-2.72 (-0.25)	-9.48 (-5.19)	-11.23 (-7.61)	-14.50 (-9.23)	-16.21 (-8.98)
	[1.06,1.12)	-2.78 (-1.67)	-8.29 (-5.30)	-10.55 (-7.57)	-13.44 (-9.19)	-14.52 (-9.36)
Jan 2022 – Dec 2022	[0.88,0.94)	-0.04 (1.79)	0.35 (0.54)	2.14 (1.79)	4.51 (3.11)	5.44 (4.23)
	[0.94,0.97)	7.49 (7.51)	5.13 (5.10)	3.85 (3.40)	3.60 (2.53)	3.69 (2.39)
	[0.97,1.00)	7.49 (7.45)	4.16 (3.98)	1.94 (1.65)	1.57 (0.35)	1.14 (0.39)
	[1.00,1.03)	5.60 (5.61)	3.14 (2.65)	0.88 (0.38)	0.29 (-0.71)	0.15 (-0.91)
	[1.03,1.06)	3.55 (3.78)	2.03 (1.94)	-0.22 (-0.24)	-0.68 (-1.38)	-0.86 (-1.52)
	[1.06,1.12)	1.41 (1.42)	1.05 (0.74)	-0.81 (-1.10)	-1.37 (-2.23)	-1.56 (-2.48)

TABLE A.3.2. IVRMSE FFT - implied volatility percentage errors

Sample period	S/K	Call (Put) options				
		Time-to-maturity				
		21–70	**71–120**	**121–170**	**171–220**	**221–270**
Jan 2018 – May 2022	[0.88,0.94)	11.48 (8.82)	1.60 (0.57)	2.51 (0.61)	1.42 (1.25)	3.10 (4.78)
	[0.94,0.97)	10.07 (6.99)	2.33 (1.62)	1.87 (0.19)	0.07 (-0.68)	0.89 (1.66)
	[0.97,1.00)	1.77 (1.96)	-2.55 (-0.97)	-2.57 (-2.42)	-4.27 (-3.43)	-3.50 (-1.24)
	[1.00,1.03)	2.27 (2.03)	-2.17 (-1.46)	-2.55 (-3.25)	-4.57 (-4.25)	-3.56 (-2.38)
	[1.03,1.06)	1.75 (2.22)	-2.57 (-1.22)	-3.27 (-3.10)	-5.64 (-5.13)	-4.96 (-3.02)
	[1.06,1.12)	0.88 (0.69)	-2.45 (-1.72)	-3.44 (-3.46)	-5.56 (-5.46)	-5.23 (-3.71)
Jan 2018 – Dec 2018	[0.88,0.94)	9.08 (18.80)	-3.51 (17.80)	-0.40 (11.49)	-2.89 (5.93)	-4.13 (15.84)
	[0.94,0.97)	-0.76 (7.40)	-8.89 (7.98)	-6.71 (4.01)	-6.98 (-1.48)	-10.41 (6.75)
	[0.97,1.00)	-13.88 (-6.15)	-13.91 (-1.26)	-10.63 (-3.42)	-9.37 (-3.76)	-13.71 (0.86)
	[1.00,1.03)	-6.71 (-0.05)	-10.73 (0.74)	-9.43 (-1.97)	-9.76 (-4.28)	-13.01 (0.32)
	[1.03,1.06)	-4.46 (0.93)	-8.23 (1.50)	-8.34 (-1.62)	-8.39 (-3.21)	-11.77 (0.47)
	[1.06,1.12)	-3.21 (0.34)	-6.36 (0.92)	-6.59 (-1.70)	-8.00 (-4.23)	-10.57 (-0.51)
Jan 2019 – Dec 2019	[0.88,0.94)	3.63 (0.09)	-3.12 (-4.90)	-1.87 (-2.75)	1.99 (1.64)	-3.26 (-0.24)
	[0.94,0.97)	2.22 (0.59)	-3.91 (-4.08)	-3.69 (-2.25)	0.21 (0.73)	-7.63 (-2.79)
	[0.97,1.00)	-6.24 (-3.92)	-7.81 (-4.83)	-7.16 (-3.83)	-3.09 (-1.11)	-10.12 (-5.25)
	[1.00,1.03)	-3.10 (-1.35)	-6.34 (-4.44)	-6.89 (-4.27)	-3.99 (-2.83)	-10.06 (-6.27)
	[1.03,1.06)	-2.08 (-0.67)	-5.40 (-3.10)	-6.57 (-3.79)	-4.70 (-2.88)	-9.76 (-6.04)
	[1.06,1.12)	-1.36 (-1.80)	-3.39 (-2.37)	-4.93 (-3.21)	-4.18 (-2.81)	-8.31 (-5.80)
Jan 2020 – Dec 2020	[0.88,0.94)	10.01 (7.13)	0.43 (-0.25)	1.28 (2.13)	1.51 (1.41)	3.81 (7.31)
	[0.94,0.97)	12.26 (9.41)	1.13 (1.86)	0.47 (1.63)	-0.41 (-0.27)	2.46 (4.21)
	[0.97,1.00)	5.22 (5.44)	-3.49 (-0.60)	-4.14 (-1.60)	-6.14 (-4.19)	0.21 (1.87)
	[1.00,1.03)	4.44 (2.77)	-2.64 (-1.93)	-3.00 (-2.77)	-4.30 (-4.46)	0.30 (0.69)
	[1.03,1.06)	3.96 (4.35)	-2.98 (-1.24)	-3.03 (-1.64)	-5.75 (-5.94)	-0.53 (1.39)
	[1.06,1.12)	2.37 (2.48)	-2.88 (-1.82)	-3.22 (-2.14)	-4.71 (-5.56)	-1.23 (0.88)
Jan 2021 – Dec 2021	[0.88,0.94)	16.67 (2.07)	8.23 (-5.89)	7.14 (-4.49)	1.57 (-2.43)	4.87 (0.26)
	[0.94,0.97)	16.37 (3.13)	11.39 (-0.28)	7.36 (-2.20)	1.41 (-2.63)	3.40 (-0.55)
	[0.97,1.00)	7.47 (0.80)	4.02 (-1.66)	1.04 (-4.58)	-4.44 (-5.78)	-4.05 (-3.90)
	[1.00,1.03)	6.24 (1.91)	2.98 (-2.06)	0.55 (-5.00)	-5.18 (-6.15)	-3.76 (-4.86)
	[1.03,1.06)	3.72 (0.90)	0.55 (-2.86)	-1.84 (-5.89)	-7.01 (-7.41)	-7.01 (-6.87)
	[1.06,1.12)	1.58 (-0.96)	-0.77 (-3.55)	-2.99 (-6.16)	-7.36 (-7.84)	-7.45 (-7.61)
Jan 2022 – Dec 2022	[0.88,0.94)	0.34 (6.24)	-0.41 (1.44)	1.96 (4.13)	2.94 (4.52)	4.59 (5.13)
	[0.94,0.97)	7.99 (10.86)	5.47 (5.52)	3.82 (4.49)	2.46 (3.09)	2.70 (2.79)
	[0.97,1.00)	8.57 (10.62)	4.90 (5.00)	2.36 (2.84)	0.84 (1.29)	0.88 (0.90)
	[1.00,1.03)	6.61 (7.57)	3.69 (3.40)	1.00 (1.15)	-0.39 (-0.17)	-0.45 (-0.59)
	[1.03,1.06)	4.35 (5.33)	2.30 (2.29)	-0.06 (0.11)	-1.28 (-1.08)	-1.48 (-1.54)
	[1.06,1.12)	2.00 (2.52)	1.33 (1.15)	-0.88 (-0.91)	-1.96 (-1.95)	-2.33 (-2.50)

Table A.3.3. IVRMSE FRFT - implied volatility percentage errors

By inspecting the tables above, the Heston single integrand produced good results for any given sample period across the moneyness and time-to-maturity categories, the FFT and the FRFT produced worst results but comparable between each other. For each model formulation, we can also see that both calls and puts produced similar levels of mispricing for these same categories for all sample periods.

The results of the Student's t-test for the Heston single integrand formulation were the following. For calls, `h = 1` indicating that the calibration of the Heston single integrand formulation is biased, a p-value `p = 0.00000` and a confidence interval `ci = [0.00028,` `0.00067]` with 95% confidence, overestimating on average. For puts, `h = 1` indicating that the calibration of the Heston single integrand formulation is biased, a p-value `p = 0.00030` and a confidence interval `ci = [0.00021, 0.00069]` with 95% confidence, overestimating on average.

The results of the Student's t-test for the FFT formulation were the following. For calls, `h = 1` indicating that the calibration of the FFT formulation is biased, a p-value `p = 0.00000` and a confidence interval `ci = [-0.00056, -0.00050]` with 95% confidence, underestimating on average. For puts, `h = 1` indicating that the calibration of the FFT formulation is biased, a p-value `p = 0.00000` and a confidence interval `ci = [-0.00057, -0.00051]` with 95% confidence, underestimating on average.

The results of the Student's t-test for the FRFT formulation were the following. For calls, `h = 1` indicating that the calibration of the FRFT formulation is biased, a p-value `p = 0.00000` and a confidence interval `ci = [-0.00042, -0.00037]` with 95% confidence, underestimating on average. For puts, `h = 1` indicating that the calibration of the FRFT formulation is biased, a p-value `p = 0.00000` and a confidence interval `ci = [-0.00043, -0.00038]` with 95% confidence, underestimating on average.

We now present three tables, one for each formulation, with the statistical analysis for both option types.

Parameters	**Mean**	**Standard deviation**	**Minimum**	**Maximum**	**Median**
κ	2.01801 (2.50198)	1.80900 (2.05177)	0.02566 (0.02830)	19.94577 (19.93600)	1.76149 (2.14293)
θ	0.19310 (0.15910)	0.24412 (0.21038)	0.01123 (0.01146)	1.76311 (1.31547)	0.10098 (0.08720)
σ	0.98578 (1.09640)	0.42188 (0.40369)	0.25306 (0.27361)	1.99907 (1.99909)	0.94044 (1.04664)
v_0	0.04522 (0.04414)	0.05904 (0.05918)	0.00653 (0.00012)	0.66134 (0.65771)	0.02859 (0.02800)
ρ	-0.80014 (-0.78370)	0.07185 (0.07053)	-0.99863 (-0.99865)	-0.12721 (-0.18216)	-0.79781 (-0.78675)
Time	3.70263 (3.25651)	4.59755 (3.59450)	0.44364 (0.45605)	32.42315 (35.25967)	2.04291 (2.06357)
Error	0.00048 (0.00045)	0.00335 (0.00410)	-0.00721 (-0.00802)	0.06930 (0.06792)	-0.00005 (-0.00007)

Table A.3.4. IVRMSE Heston single integrand - calls (puts) statistical analysis

Parameters	**Mean**	**Standard deviation**	**Minimum**	**Maximum**	**Median**
κ	4.86286 (4.47421)	2.28139 (2.03638)	1.15707 (0.08298)	15.25511 (15.20703)	4.52960 (4.24268)
θ	0.06248 (0.06595)	0.03006 (0.05572)	0.01954 (0.02078)	0.18481 (1.59602)	0.05625 (0.05667)
σ	1.33321 (1.26153)	0.37502 (0.35684)	0.38029 (0.56758)	1.99995 (1.99994)	1.31145 (1.22894)
v_0	0.04308 (0.04289)	0.06046 (0.06014)	0.00216 (0.00007)	0.66190 (0.65826)	0.02704 (0.02707)
ρ	-0.78365 (-0.80720)	0.07081 (0.07167)	-0.99898 (-0.99897)	-0.49777 (-0.60260)	-0.77035 (-0.80084)
α	15.29446 (16.13022)	3.90768 (3.98635)	10.00000 (10.00000)	25.00000 (25.00000)	13.75000 (14.75000)
Time	0.82638 (0.96990)	1.28849 (1.45824)	0.02976 (0.04130)	9.41132 (9.18008)	0.55169 (0.61586)
Error	-0.00053 (-0.00054)	0.00053 (0.00052)	-0.00434 (-0.00403)	0.00115 (0.00188)	-0.00041 (-0.00043)

Table A.3.5. IVRMSE FFT - calls (puts) statistical analysis

Parameters	**Mean**	**Standard deviation**	**Minimum**	**Maximum**	**Median**
κ	4.52784 (4.20732)	2.14787 (2.00449)	0.11086 (0.03033)	15.09135 (14.13811)	4.38418 (4.00746)
θ	0.06767 (0.07528)	0.06246 (0.10489)	0.02139 (0.02275)	1.40343 (1.92801)	0.05743 (0.05891)
σ	1.30312 (1.26178)	0.38009 (0.36722)	0.23259 (0.50778)	1.99995 (1.99999)	1.25257 (1.22703)
v_0	0.04316 (0.04276)	0.06035 (0.06021)	0.00180 (0.00075)	0.66199 (0.65816)	0.02726 (0.02675)
ρ	-0.78241 (-0.80288)	0.06889 (0.06797)	-0.99898 (-0.99900)	-0.56715 (-0.57695)	-0.76951 (-0.79868)
α	14.69896 (15.19170)	4.52332 (4.44722)	6.75000 (6.00000)	25.00000 (25.00000)	13.25000 (14.00000)
Time	0.62093 (0.57533)	1.06207 (0.88410)	0.03130 (0.02189)	6.65846 (6.26406)	0.35901 (0.35849)
Error	-0.00040 (-0.00041)	0.00046 (0.00044)	-0.00280 (-0.00235)	0.00115 (0.00137)	-0.00022 (-0.00029)

Table A.3.6. IVRMSE FRFT - calls (puts) statistical analysis

The tables above summarize the statistical analysis for the three formulations covering both option types. On average, the damping factor α was similar between the FFT and FRFT formulations. Here, the value of the damping factor α is again high for the same reasons discussed before in the MSE section. We can see that on average, the calibration time for puts was faster than the calibration time for calls for the Heston single integrand formulation and for the FRFT formulation and the other way around for the FFT formulation. The FRFT formulation, was, on average, the fastest followed by the FFT and Heston single integrand for both option types, which was expected.

Appendix B. Evolution plots

Here, we present the evolution plots for each Heston model parameter. Each parameter has its own section, where we show its evolution across all combinations of model formulations and loss functions.

B.1. Evolution plots of κ

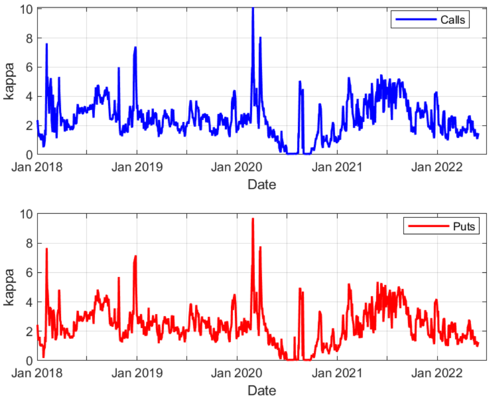

FIGURE B.1.1. MSE Heston original

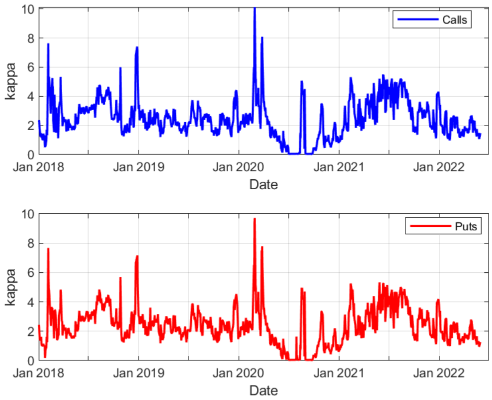

FIGURE B.1.2. MSE Heston single integrand

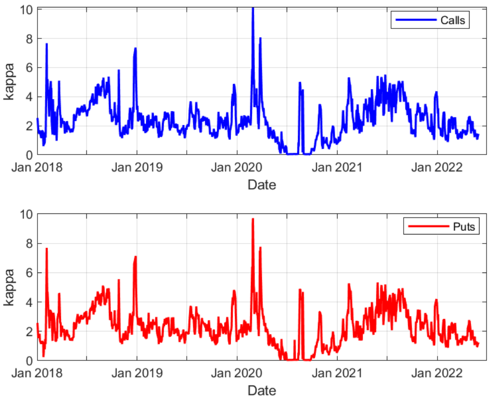

FIGURE B.1.3. MSE Attari

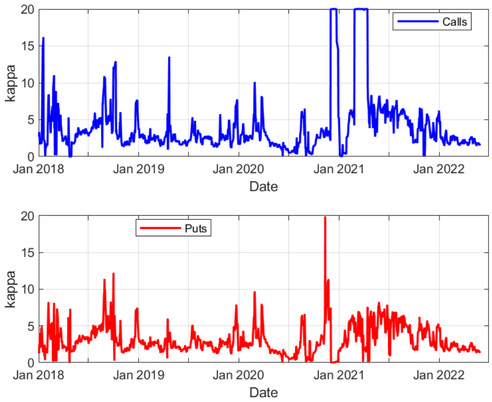

FIGURE B.1.4. MSE FFT

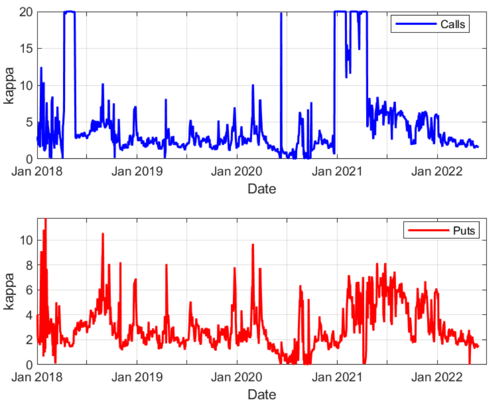

FIGURE B.1.5. MSE FRFT

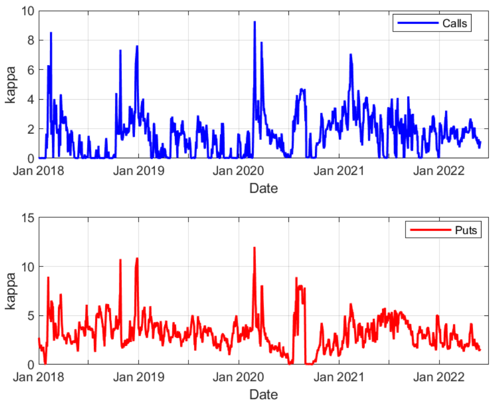

FIGURE B.1.6. RMSE Heston original

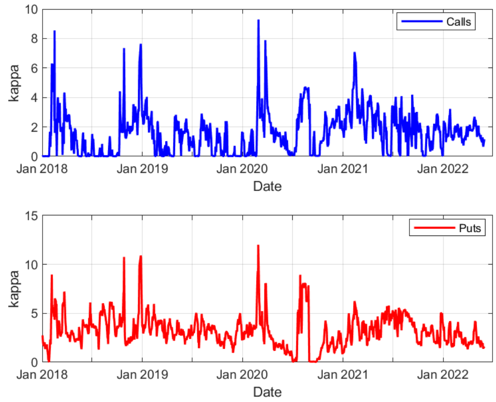

FIGURE B.1.7. RMSE Heston single integrand

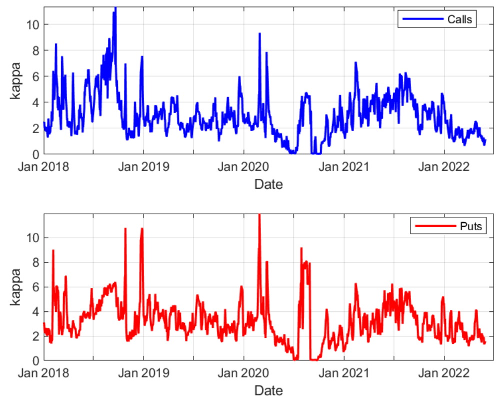

FIGURE B.1.8. RMSE Attari

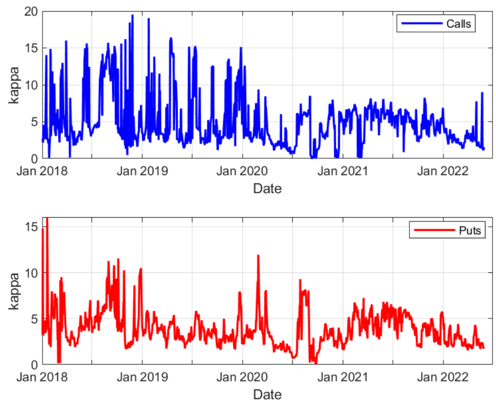

FIGURE B.1.9. RMSE FFT

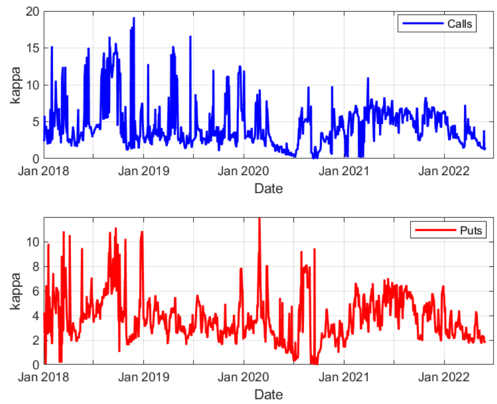

FIGURE B.1.10. RMSE FRFT

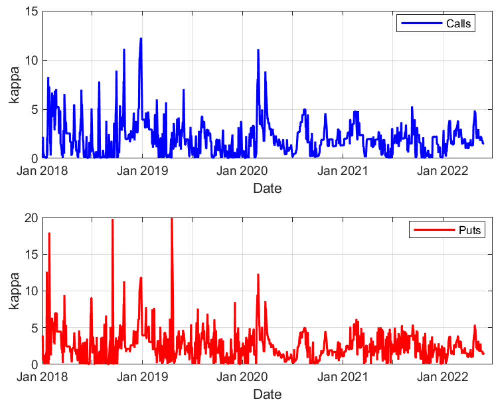

FIGURE B.1.11. IVRMSE Heston original

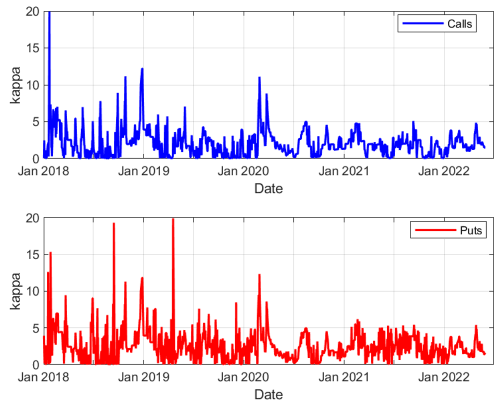

FIGURE B.1.12. IVRMSE Heston single integrand

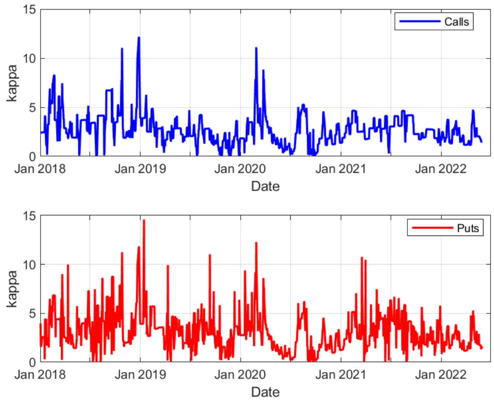

FIGURE B.1.13. IVRMSE Attari

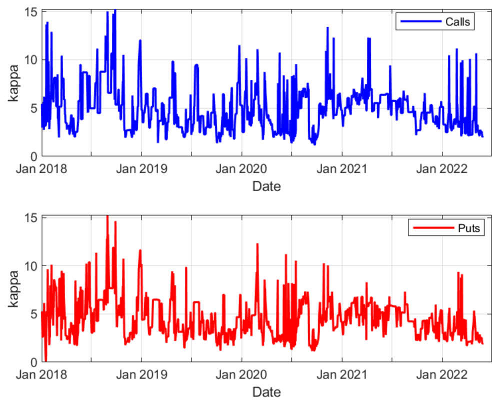

FIGURE B.1.14. IVRMSE FFT

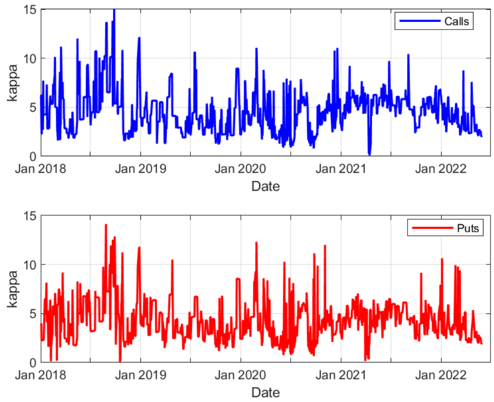

FIGURE B.1.15. IVRMSE FRFT

B.2. Evolution plots of θ

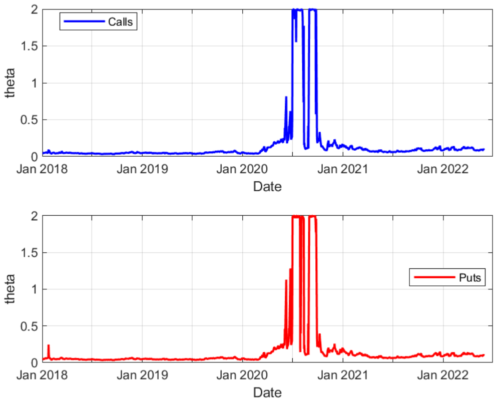

FIGURE B.2.1. MSE Heston original

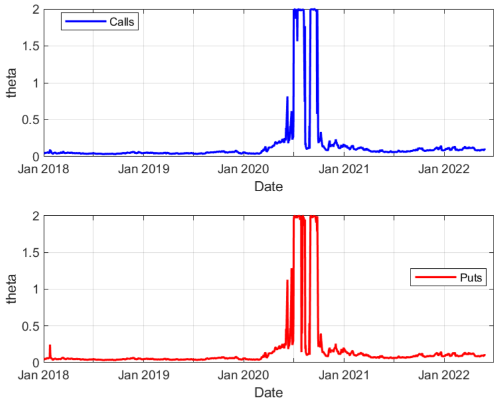

FIGURE B.2.2. MSE Heston single integrand

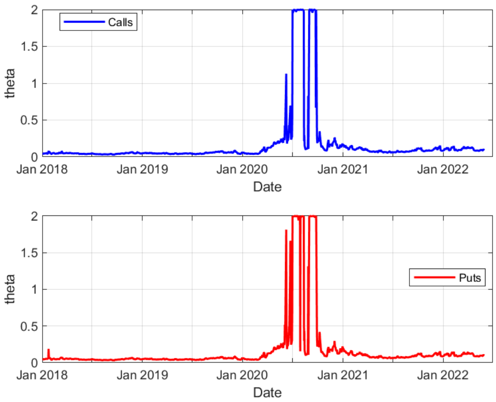

FIGURE B.2.3. MSE Attari

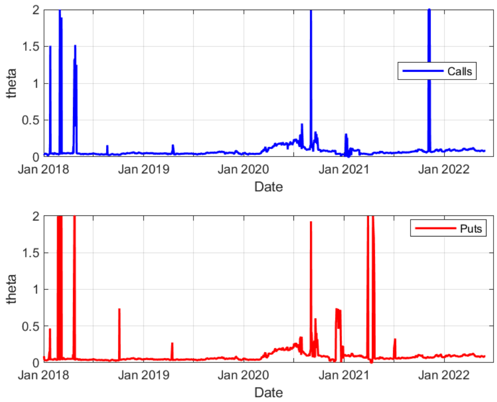

FIGURE B.2.4. MSE FFT

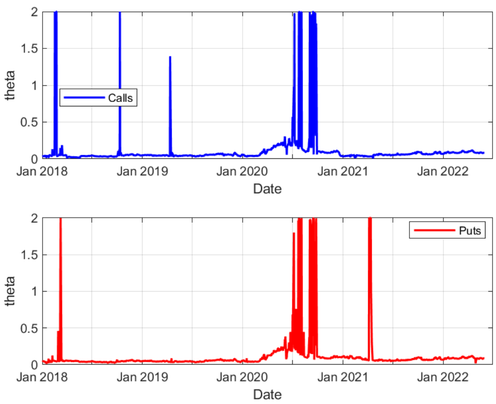

FIGURE B.2.5. MSE FRFT

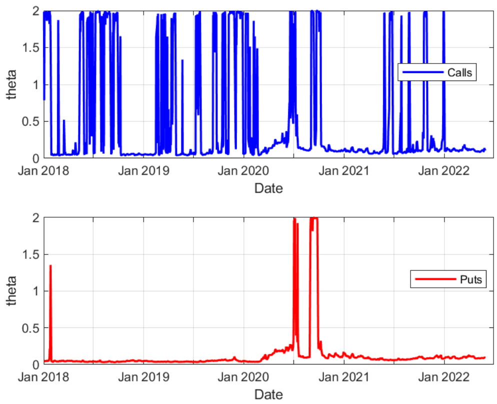

FIGURE B.2.6. RMSE Heston original

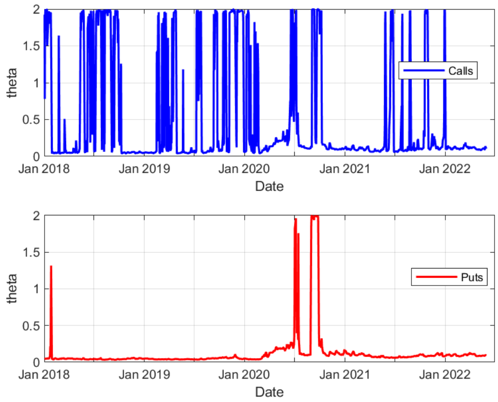

FIGURE B.2.7. RMSE Heston single integrand

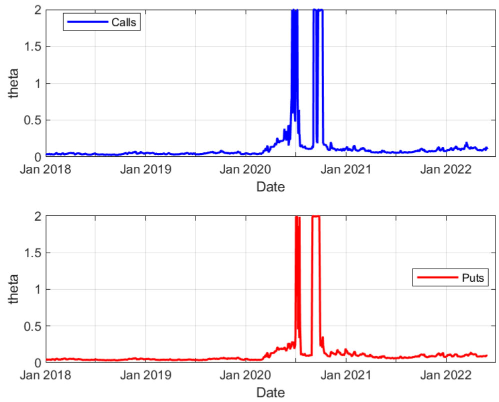

FIGURE B.2.8. RMSE Attari

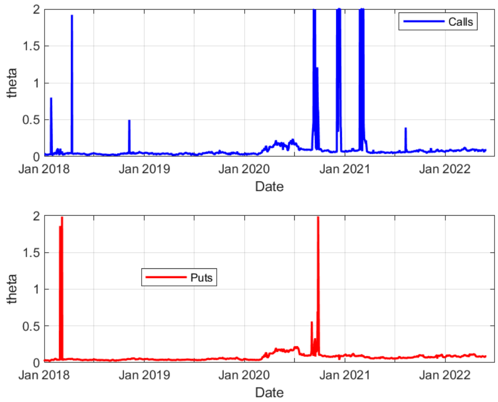

FIGURE B.2.9. RMSE FFT

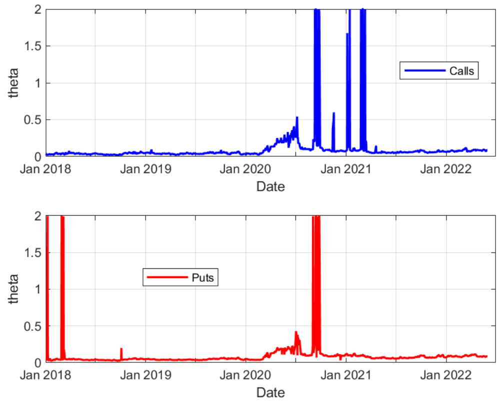

FIGURE B.2.10. RMSE FRFT

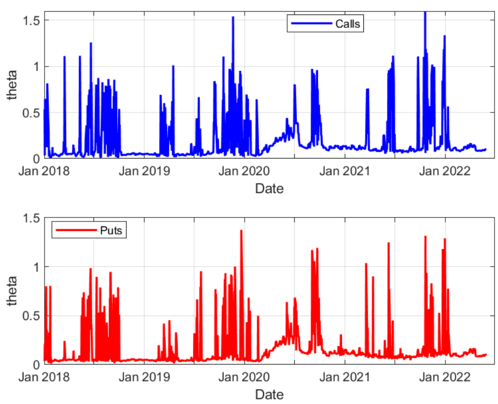

FIGURE B.2.11. IVRMSE Heston original

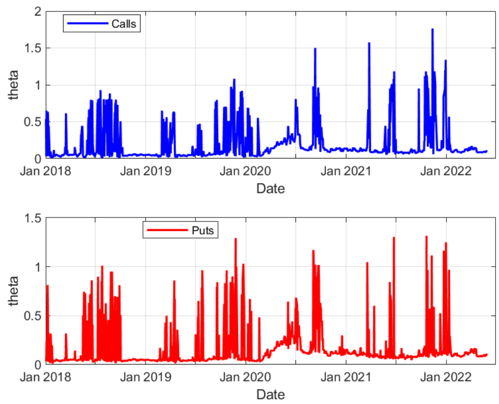

FIGURE B.2.12. IVRMSE Heston single integrand

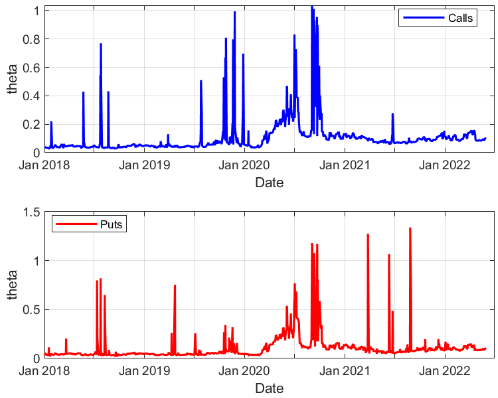

FIGURE B.2.13. IVRMSE Attari

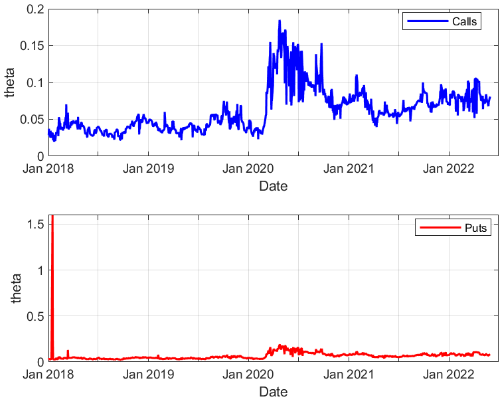

FIGURE B.2.14. IVRMSE FFT

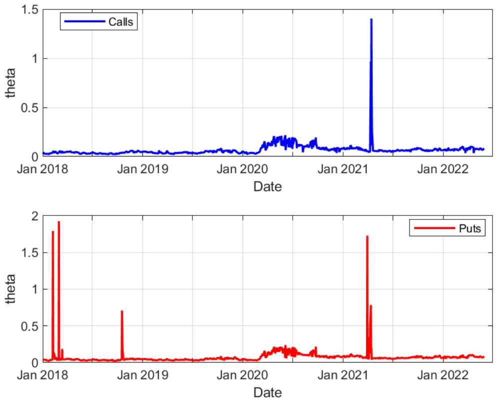

FIGURE B.2.15. IVRMSE FRFT

B.3. Evolution plots of σ

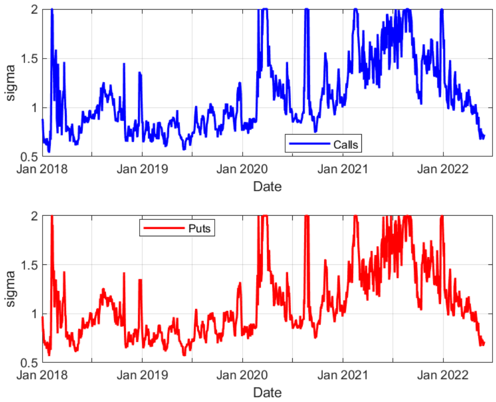

FIGURE B.3.1. MSE Heston original

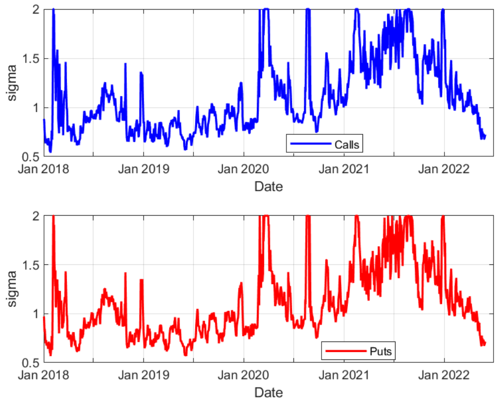

FIGURE B.3.2. MSE Heston single integrand

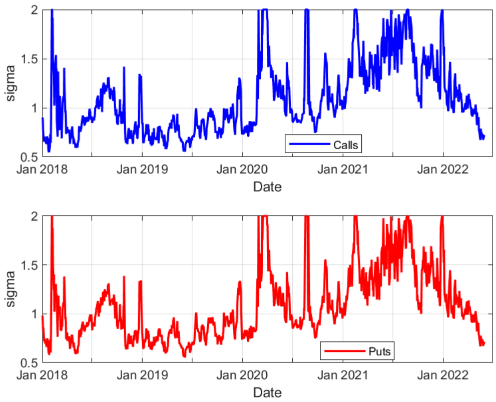

FIGURE B.3.3. MSE Attari

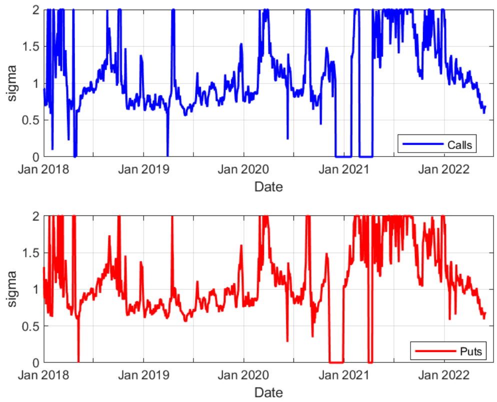

FIGURE B.3.4. MSE FFT

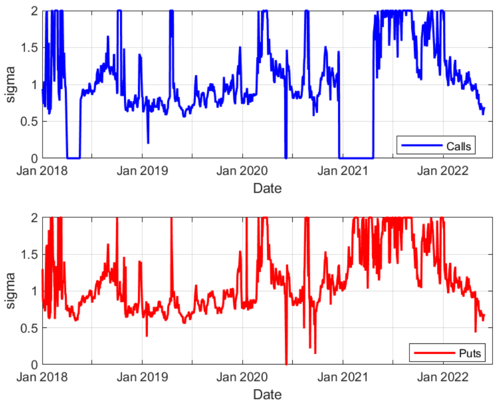

FIGURE B.3.5. MSE FRFT

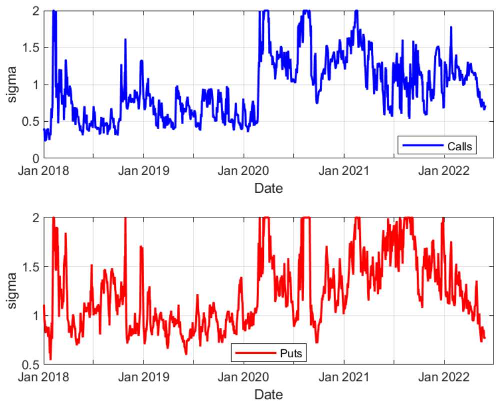

FIGURE B.3.6. RMSE Heston original

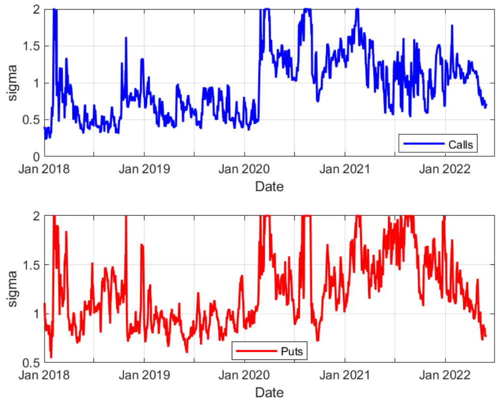

FIGURE B.3.7. RMSE Heston single integrand

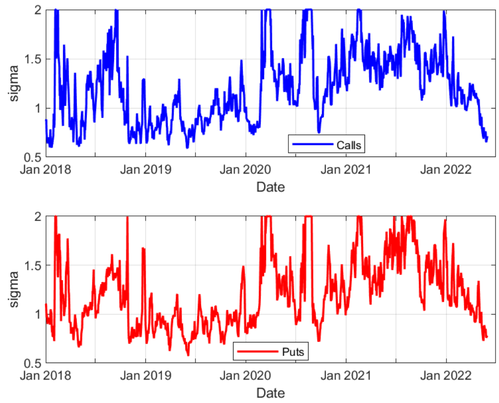

FIGURE B.3.8. RMSE Attari

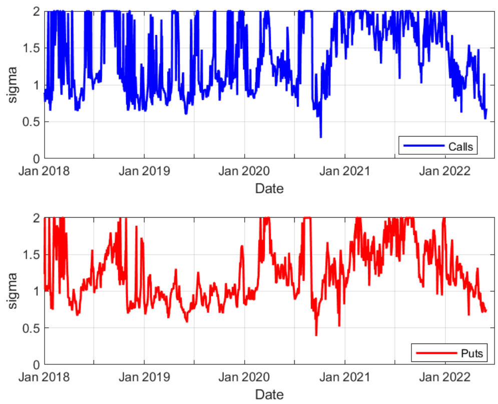

FIGURE B.3.9. RMSE FFT

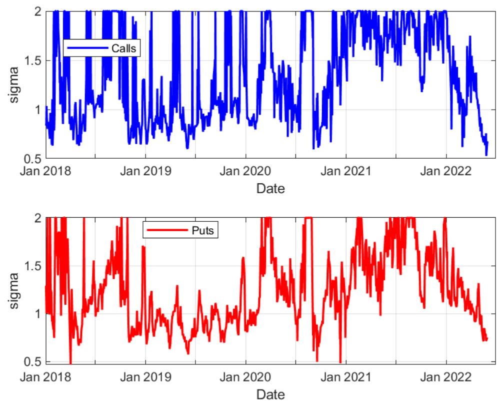

FIGURE B.3.10. RMSE FRFT

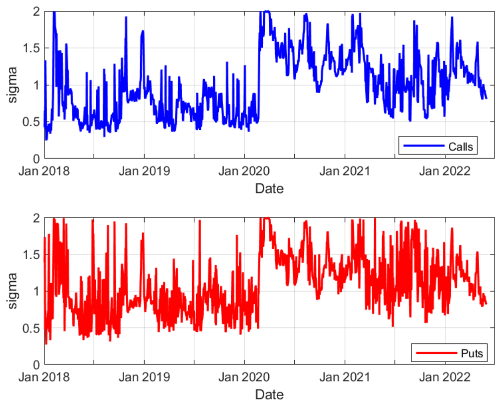

FIGURE B.3.11. IVRMSE Heston original

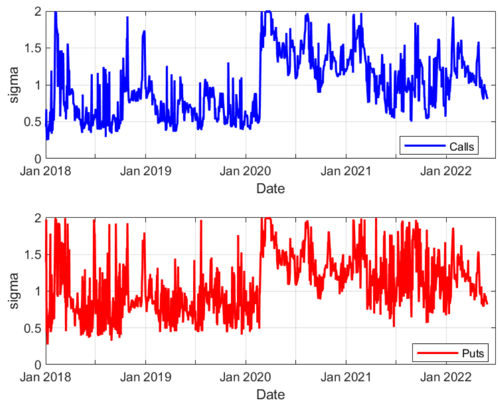

FIGURE B.3.12. IVRMSE Heston single integrand

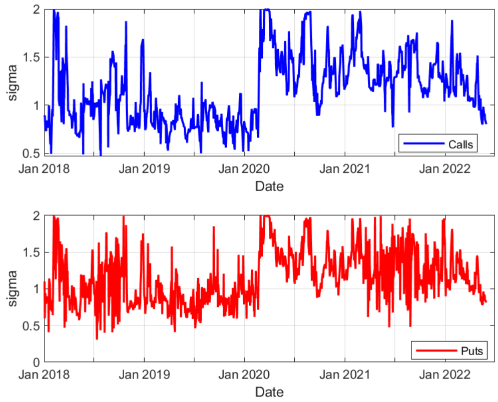

FIGURE B.3.13. IVRMSE Attari

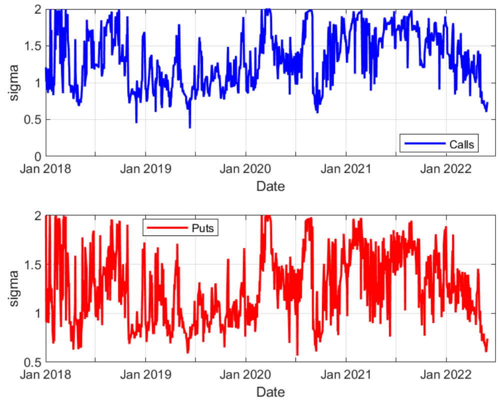

FIGURE B.3.14. IVRMSE FFT

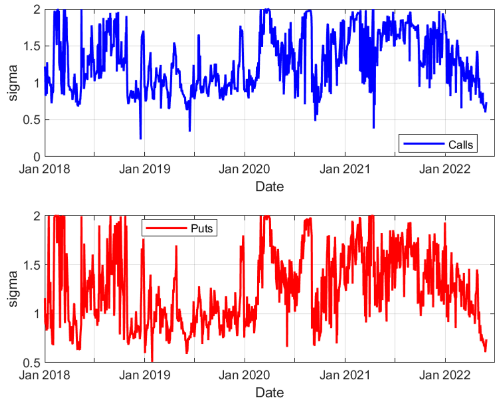

FIGURE B.3.15. IVRMSE FRFT

B.4. Evolution plots of v_0

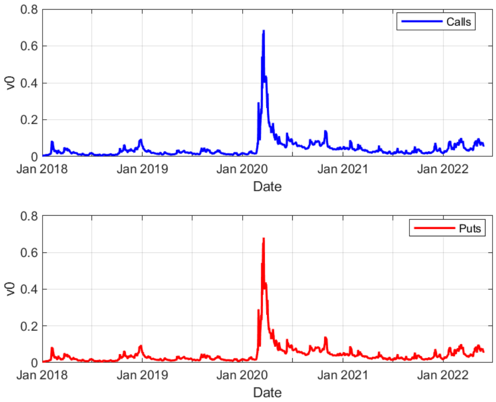

FIGURE B.4.1. MSE Heston original

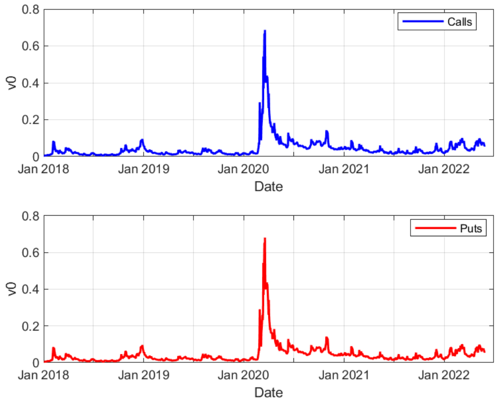

FIGURE B.4.2. MSE Heston single integrand

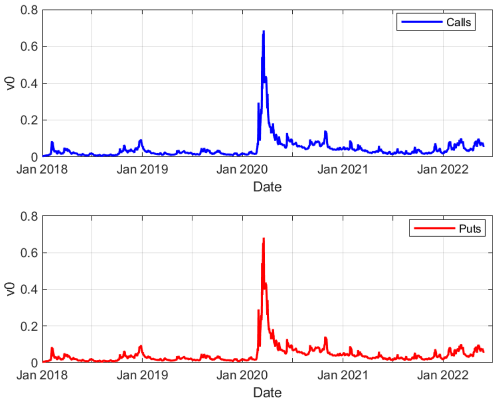

FIGURE B.4.3. MSE Attari

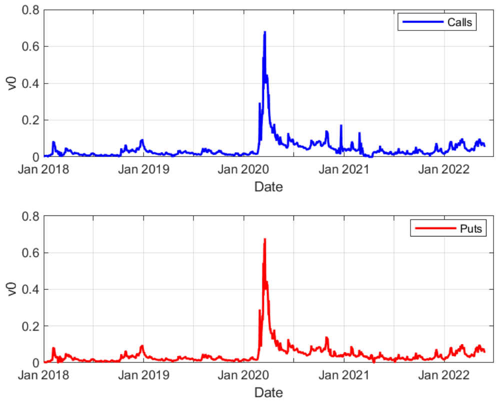

FIGURE B.4.4. MSE FFT

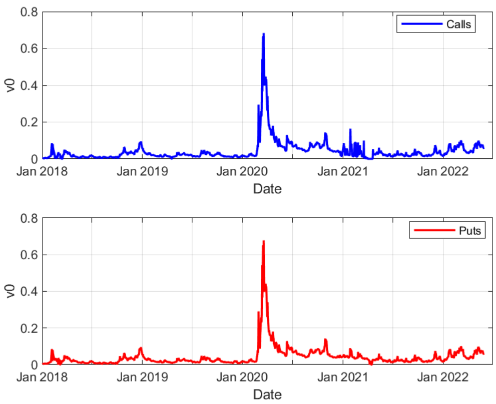

FIGURE B.4.5. MSE FRFT

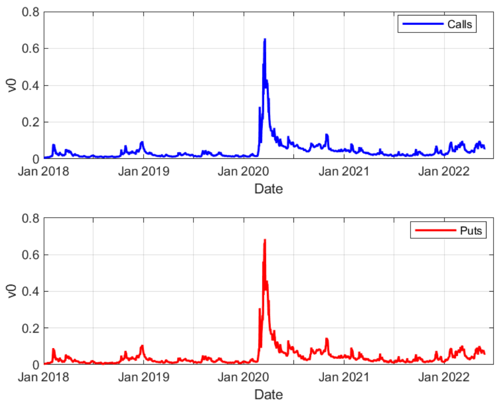

FIGURE B.4.6. RMSE Heston original

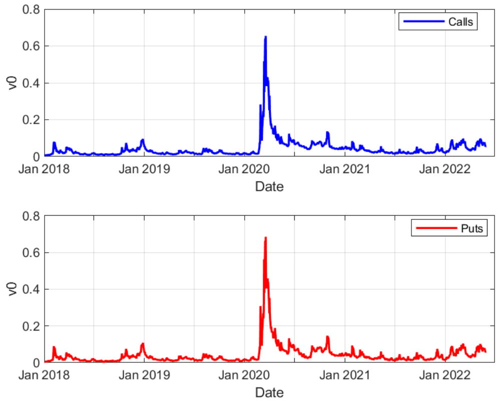

Figure B.4.7. RMSE Heston single integrand

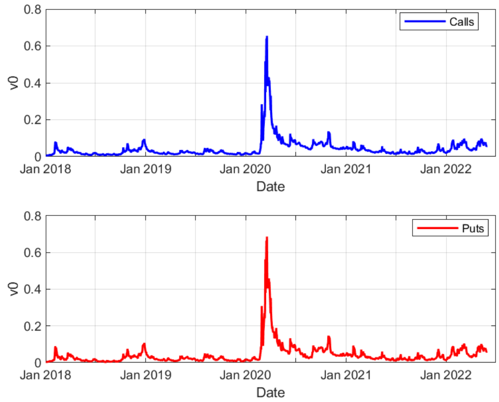

Figure B.4.8. RMSE Attari

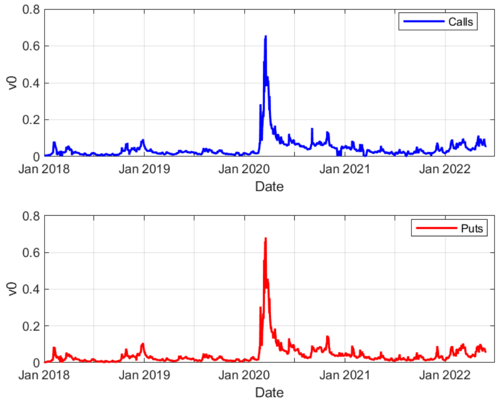

Figure B.4.9. RMSE FFT

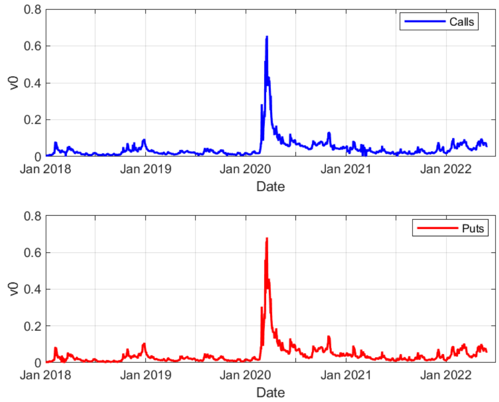

Figure B.4.10. RMSE FRFT

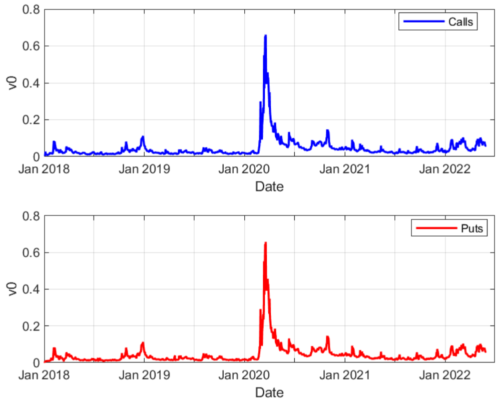

Figure B.4.11. IVRMSE Heston original

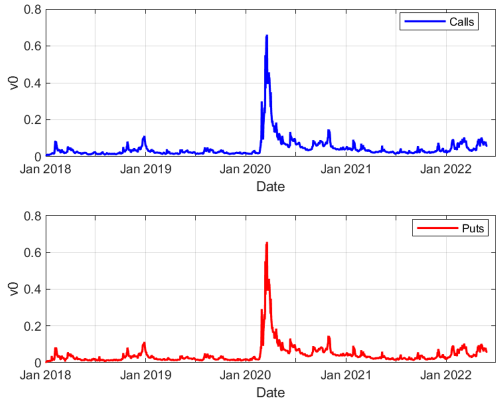

Figure B.4.12. IVRMSE Heston single integrand

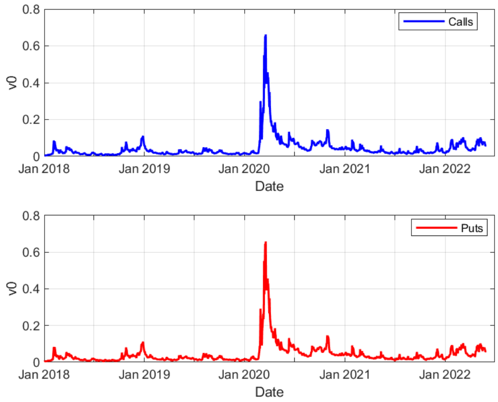

FIGURE B.4.13. IVRMSE Attari

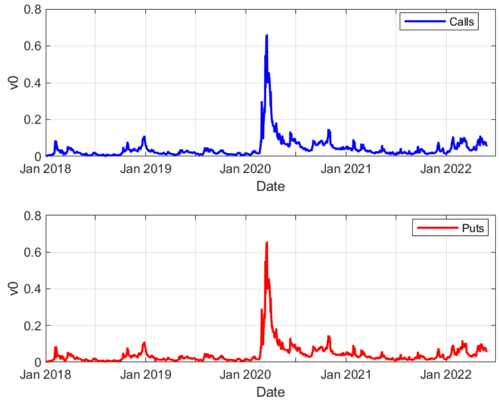

FIGURE B.4.14. IVRMSE FFT

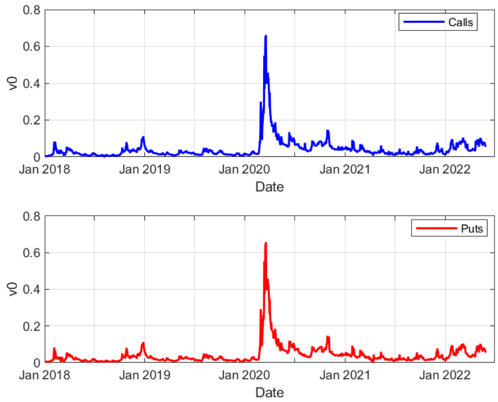

FIGURE B.4.15. IVRMSE FRFT

B.5. Evolution plots of ρ

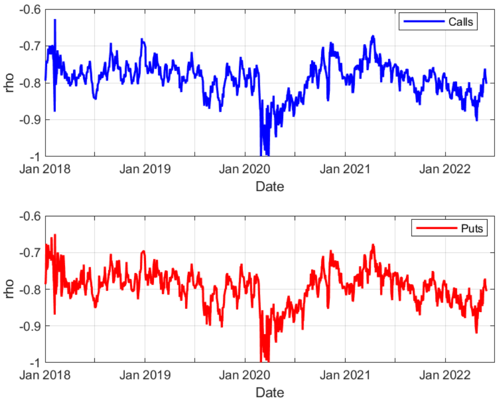

FIGURE B.5.1. MSE Heston original

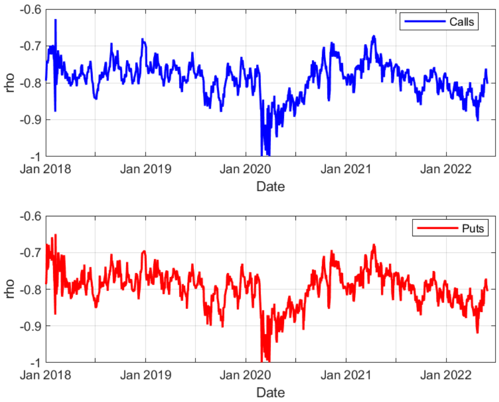

FIGURE B.5.2. MSE Heston single integrand

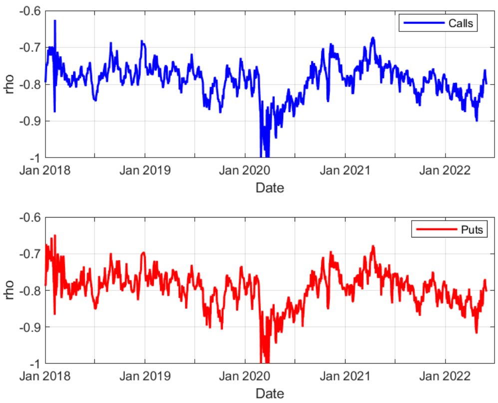

FIGURE B.5.3. MSE Attari

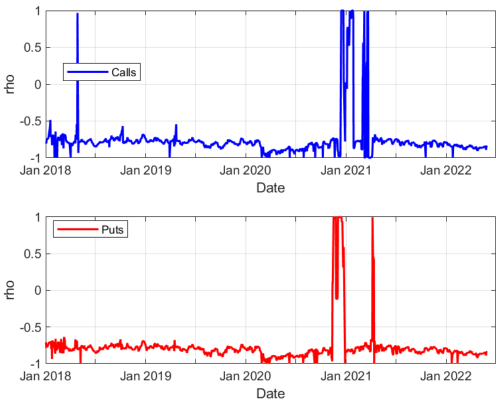

FIGURE B.5.4. MSE FFT

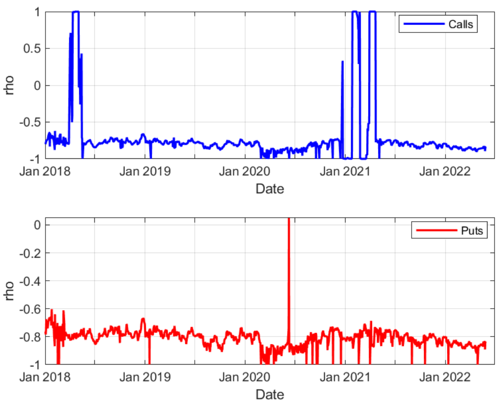

FIGURE B.5.5. MSE FRFT

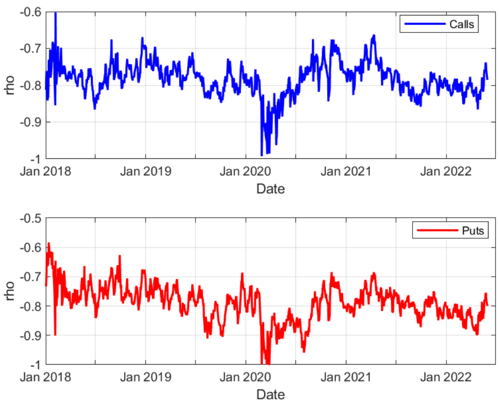

FIGURE B.5.6. RMSE Heston original

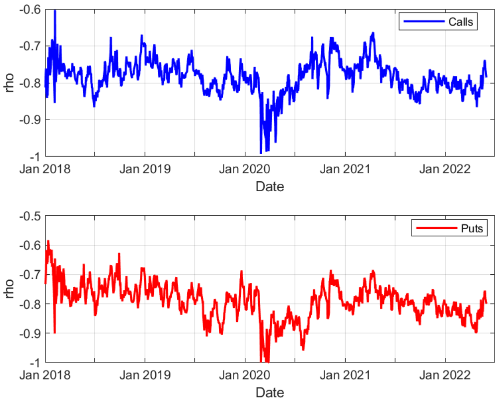

FIGURE B.5.7. RMSE Heston single integrand

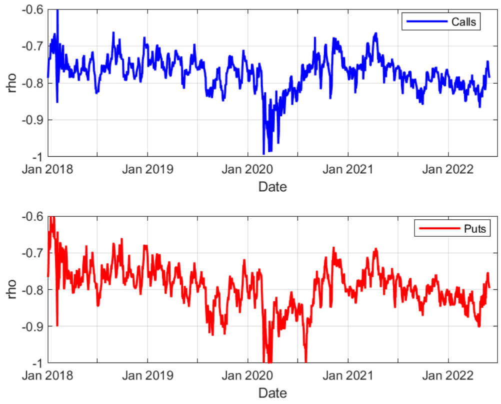

FIGURE B.5.8. RMSE Attari

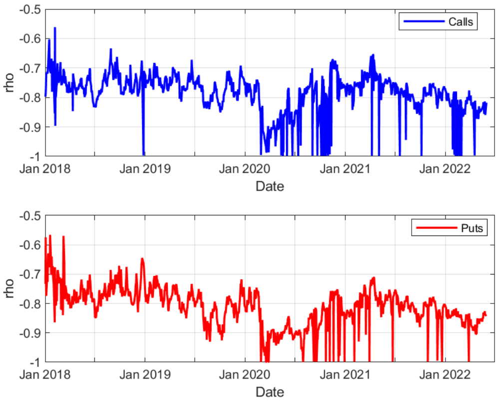

FIGURE B.5.9. RMSE FFT

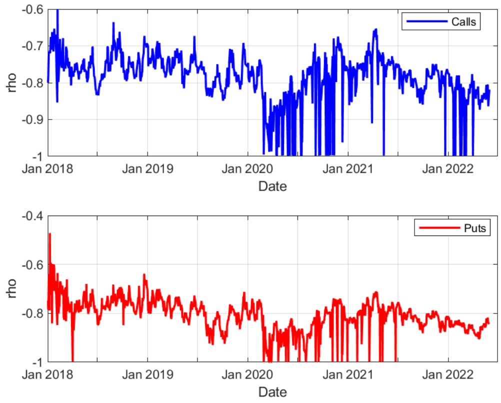

FIGURE B.5.10. RMSE FRFT

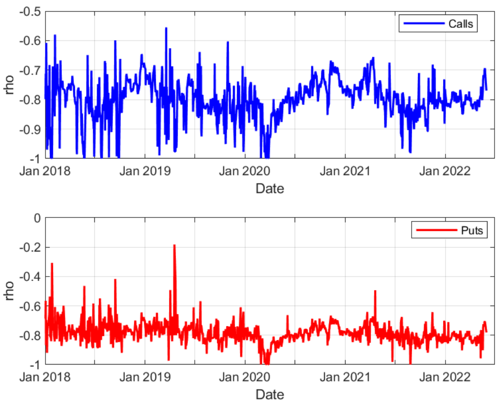

FIGURE B.5.11. IVRMSE Heston original

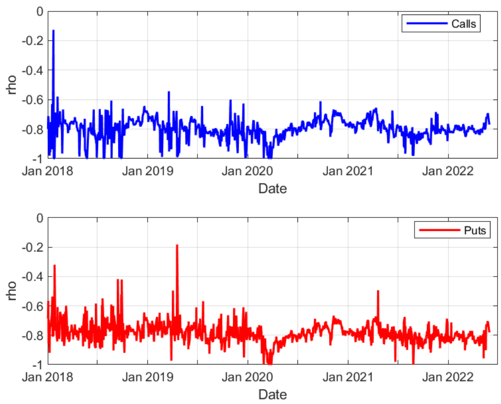

FIGURE B.5.12. IVRMSE Heston single integrand

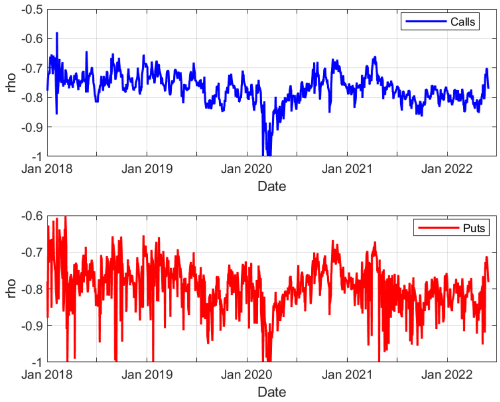

FIGURE B.5.13. IVRMSE Attari

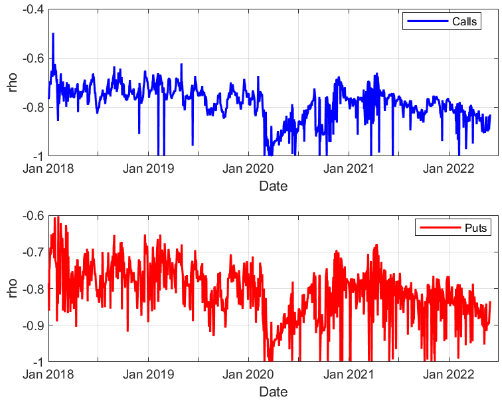

FIGURE B.5.14. IVRMSE FFT

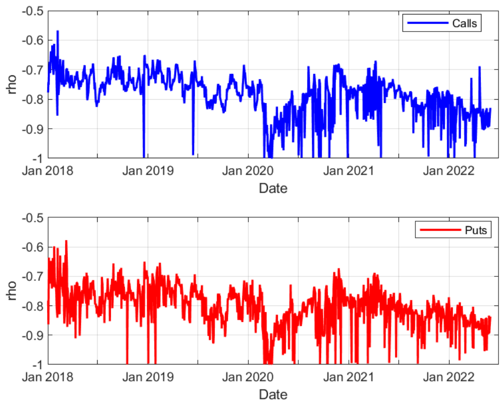

FIGURE B.5.15. IVRMSE FRFT

References

[1] Albrecher, H., Mayer, P., Schoutens, W., and Tistaert, J. (2007). "The Little Heston Trap." *Wilmott Magazine*, January 2007, 83–92.

[2] Attari, M. (2004). "Option Pricing Using Fourier Transforms: A Numerically Efficient Simplification." Working Paper, Charles River Associates, Boston, MA.

[3] Bakshi, G., Cao, C., and Chen. Z. (1997). "Empirical Performance of Alternative Option Pricing Models." *Journal of Finance*, 52(5):2003–2049.

[4] Bakshi, G., and Madan. D. (2000). "Spanning and Derivative-Security Valuation." *Journal of Financial Economics*, 55(2):205-238.

[5] Black, F., and Scholes, M. (1973). "The Pricing of Options and Corporate Liabilities." *Journal of Political Economy*, 81(3):637-654.

[6] Bollerslev, T., Gibson, M., and Zhou. H. (2011). "Dynamic Estimation of Volatility Risk Premia and Investor Risk Aversion From Option-Implied and Realized Volatilities." *Journal of Econometrics*, 160(1):235-245.

[7] Breeden, D.T. (1979). "An intertemporal asset pricing model with stochastic consumption and investment opportunities." *Journal of Financial Economics*, 7(3):265-296.

[8] Carr, P., and Madan. D. (1999). "Option Valuation Using the Fast Fourier Transform." *Journal of Computational Finance*, 2(4):61–73.

[9] Chensey, M., and Scott. L. (1989). "Pricing European Currency Options: a Comparison of the Modified Black-Scholes Model and a Random Variance Model." *Journal of Financial and Quantitative Analysis*, 24(3):267–284.

[10] Chourdakis, K. (2005). "Option Pricing Using the Fractional FFT." *Journal of Computational Finance*, 8(2):1–18.

[11] Christoffersen, P., Heston, S.L, and Jacobs. K. (2009). "The Shape and Term Structure of the Index Option Smirk: Why Multifactor Stochastic Volatility Models Work so Well." *Management Science*, 55(12):1914-1932.

[12] Cox, J.C., Ingersoll, J.E., and Ross. S.A. (1985). "A Theory of the Term Structure of Interest Rates." *Econometrica*, 53(2):385–407.

[13] Feller, W. (1951). "Two Singular Diffusion Problems." *Annals of Mathematics*, 54(1):173-182.

[14] Gil-Pelaez, J. (1951). "Note on the Inversion Theorem." *Biometrika*, 38(3-4):481-482

[15] Heston, S.L. (1993). "A Closed-Form Solution for Options with Stochastic Volatility with Applications to Bond and Currency Options." *Review of Financial Studies*, 6(2):327-343.

[16] Hull, J., and White. A. (1987). "The Pricing of Options on Assets with Stochastic Volatilities." *Journal of Finance*, 42(2):281–300.

[17] Lord, R., and Kahl. C. (2007). "Optimal Fourier Inversion in Semi-Analytical Option Pricing." Working Paper, Rabobank International and ABN AMRO.

[18] Marques, D.M. da C.D.A. (2023). "Empirical comparison of S&P 500 index options: Black-Scholes-Merton model and Heston model." [Dissertação de mestrado, Iscte - Instituto Universitário de Lisboa]. Repositório Iscte. http://hdl.handle.net/10071/30851.

[19] Merton, R.C (1993). "An Intertemporal Capital Asset Pricing Model." *Econometrica*, 41(5):867-887.

[20] Merton, R.C (1993). "Theory of Rational Option Pricing." *The Bell Journal of Economics and Management Science*, 4(1):141-183.

[21] NG, M. (2005). "Option Pricing via the FFT and its Application to Calibration." [Dissertação de mestrado, TU Delft - Delft University of Technology]. Repositório Uv. http://ta.twi.tudelft.nl/mf/users/oosterle/oosterlee/ng.

[22] Piedade, M.Â.V. da. (2020). "Pricing American-Style Options Under the Heston Model Using the Cos Approximation." [Dissertação de mestrado, Iscte - Instituto Universitário de Lisboa]. Repositório Iscte. http://hdl.handle.net/10451/48095.

[23] Rouah, F.D. (2013). "The Heston Model and Its Extensions in Matlab and C." Hoboken, NJ: John Wiley & Sons, Inc.

[24] Sáez, G.K.G. (2014). "Fourier transform methods for opcion pricing: An application to extended Heston-type models." [Dissertação de mestrado, Uv - Universitat de València]. Repositório Uv. https://www.uv.es/bfc/TFM2014/008-014.

[25] Scott, L.O. (1987). "Option Pricing When the Variance Changes Randomly: Theory, Estimation, and an Application." *Journal of Financial and Quantitative Analysis*, 22(4):419–438.

[26] Shreve, S.E (2004). "Stochastic Calculus for Finance II: Continuous-Time Models." New York, NY: Springer.

[27] Stein, E.M., and Stein. J.C. (1991). "Stock Price Distributions with Stochastic Volatility: An Analytic Approach." *Review of Financial Studies*, 4(4):727–752.

[28] Whaley, R.E. (2006). "Derivatives: Markets, Valuation, and Risk Management." Hoboken, NJ: John Wiley & Sons, Inc.

[29] Wiggins, J.B. (1987). "Option Values Under Stochastic Volatility: Theory and Empirical Estimates." *Journal of Financial Economics*, 19(2):351–372.